Boiler system modelling using Flownex®

Prepared by:

André Rossouw

RSSAND023

Department of Mechanical Engineering

University of Cape Town

Supervisor:

Dr. Wim Fuls

December 2015

Submitted to the Department of Mechanical Engineering at the University of Cape Town in partial fulfilment of the academic requirements for a Masters of Science degree in Mechanical Engineering.

Key Words: Heat transfer, cross flow heat exchanger, coal-fired station, boiler, radiation, convection, transient modelling.

Abstract

The objective of this project is to develop a boiler modelling methodology, specifically using Flownex, which is capable of running transient simulations for a large variety of coal-fired boiler designs typically used in Eskom. Flownex has been identified as the key software to accomplish the global objective of the Centre for Energy Efficiency under EPPEI at the University of Cape Town, which is to develop a software model of a complete coal-fired power station which includes all the main systems required for independent transient simulation.

The boiler model captures the true geometric layout and flow orientation with associated characteristics of a wide variety of boiler designs utilised by Eskom. In order to achieve this, boilers and heat exchangers are grouped according to common physical properties which simplify the modelling process and optimise results. This is preceded by an investigation into the types of boiler designs currently operational in Eskom including available associated geometrical and process characteristics.

A study into heat transfer mechanisms applicable to coal-fired boiler heat exchangers was done to ensure fundamental theoretical principles are adhered to during the development of the analytical models, the first step in the modelling process. The Flownex solving methodology is evaluated against the analytical models in a simplified heat exchanger before full detail modelling of heat exchangers are done. The component and method used in Flownex requires convection and radiation heat transfer to be accounted for separately and thus heat exchangers are classified sequentially according to their location in the boiler, this process relies heavily on data obtained in the boiler study. Heat exchangers and auxiliary systems are then integrated into a single system used to obtain steady-state results. The steady-state boiler model is evaluated against actual boiler design data for various loads to prove applicability to various boiler designs and operating conditions.

Steady-state results for two different boiler designs show that the model simulates the set of heat exchangers with suitable accuracy compared to plant data. The accuracy of results are compared are evaluated for the flue gas side, and the steam side for both individual heat exchangers and integrated heat exchanger sets. The average results of individual and integrated heat exchangers yields results with an error of less than 10%.

Transient simulations are done on various sections of the boiler model to prove simulating capabilities for different transient characteristics. Although this forms a small part of the total project, it is a crucial step in proving that the final product delivered will adhere to the necessary requirements for the final power station software model in which it will be used. The transient

capabilities are evaluated against expected trends rather than actual plant data due to the lack of an integrated control system which would manipulate multiple parameters during most transient scenarios. The result from the transient model indicates that the critical transient characteristics are captured adequately and that transient simulations with an integrated control system would be possible.

Declaration

I, *Andries Johannes Rossouw*, hereby declare the work contained in this dissertation to be my own. All information which has been gained from various journal articles, text books or other sources has been referenced accordingly. I have not allowed, and will not allow, anyone to copy my work with the intention of passing it off as their own work or part thereof.

Signed by candidate

Signature Removed

_____ 2016-07-25

Name Date

Acknowledgements

Most importantly I would like to thank my Heavenly Father for truly blessing me abundantly in all aspects of life. Everything I am is because of Him and I owe everything to Him.

Thank you to my wife Robyn-Lee for being on this journey with me and making it spectacular and one I would cherish forever.

I would like to thank my parents and family for their contribution to me as individual, without it I would never be who I am today and am truly thankful for my family.

Thank you to my academic mentor Dr. Wim Fuls, your guidance throughout my project is truly appreciated.

Thank you to Eskom and my direct management for supporting the EPPEI Project. I was granted a once in a lifetime opportunity, and one for which I am truly thankful.

Table of Contents

List of Figures

List of Tables

List of Nomenclature

General symbols

A	Area	m^2
a	Absorption coefficient	m^{-1}
C	Heat transfer capacity rate	MW/K
c,m,n	Constant values	-
c_p	Specific heat	kJ/kg
CV	Calorific Value of coal	MJ/kg
D	Diameter	m
d	Diameter	m
D_H	Hydraulic diameter	m
E	Emissive power	W/m^2
f	Friction factor	-
F	View factor	-
F_O	Opacity Factor	-
h	Heat transfer coefficient	W/m^2K
h_e	Enthalpy	kJ/kg
j_H	Colburn factor	-
k	Thermal conductivity	W/mK
L	Length	m
LMTD	Log Mean Temperature Difference	°C or K
$\dot{m}$	Mass flow	kg/s
NTU	Number of Transfer Units	-
Nu	Nusselt number	-
P	Perimeter	M
Pr	Prandtl number	-
q	Heat flux	W/m^2
Q	Heat transfer	W
r	Radius	m
Re	Reynolds number	-
s	Mean beam length	m
St	Stanton number	-
T	Temperature	°C or K
U	Overall heat transfer coefficient	W/m^2K
V	Volume	m^3

V_x	Velocity of fluid x	m/s
WT	Wall Thickness	mm

Greek symbols

β	Angle	°
ε	Effectiveness	-
ε_r	Emissivity	-
μ	Viscosity	kg/ms
ρ	Density	kg/m^3
σ	Stefan-Boltzmann constant	$5.67 \times 10^{-8} W/m^2K^4$
φ	Void fraction	-

Acronyms and Abbreviations

Att	Attemperator
BFP	Boiler Feedwater Pump
Eco	Economiser
EPPEI	Eskom Power Plant Engineering Institute
FD	Forced Draught
FGCP	Flue Gas Cleaning Plant
HP	High Pressure
HX	Heat Exchanger
ID	Induced Draught
IP	Intermediate Pressure
LP	Low Pressure
MCR	Maximum Continuous Rating
OEM	Original Equipment Manufacturer
P/S	Power Station
PA	Primary Air
PF	Pulverised Fuel
R	Resistance
R/H or RH	Reheater
S/H or SH	Superheater
SC	Supercritical
TMI	Thermal Mass Inertia
UCT	University of Cape Town

Subscripts

1,2…	Number of item (such as surface or location)
abs	Absolute
ci	Cold inlet
cond	Conduction
conv	Convection
eq	Equivalent
f	Flame
F	View Factor
fg	Flue gas
fgi	Flue gas inlet
fgo	Flue gas outlet
g	Gas
gp	Gas and particle
hi	Hot inlet
i	Inner (internal)
max	Maximum
min	Minimum
o	Outer (external)
r	Ratio
rad	Radiation
s	Surface
st	Steam
sti	Steam inlet
sto	Steam outlet
t	Tube
w	Wall

1. Introduction

The Centre for Energy Efficiency at the Mechanical Engineering Department of the University of Cape Town aims to develop a detailed software model of a complete coal-fired power station. The goal is to run high level system transients that include all the major systems and sub-systems of a typical coal-fired power station. Various systems have already been developed by students in the department and several systems require more work or are due to be developed in the future.

The software identified to be used in this project is Flownex, which is a one-dimensional thermo-hydraulic network solver. It contains a vast amount of low level elements that need to be linked together to create and simulate a desired system.

1.1 Purpose of project

The purpose of this project is to develop a boiler model for a coal-fired power station. The requirement is that the model should require minimal inputs, yet deliver accurate results comparable to that of an actual boiler at similar operating conditions. In addition, the model is required to accommodate the majority of the boiler designs commonly used by Eskom power stations, without significant adjustments.

The project requires that the methodology and software model developed must be well documented to assist any use by future students for more detailed studies. This is essential as it will eventually be integrated into the complete power station simulation model as discussed above.

Various built-in components in the Flownex library are capable of simulating heat transfer in a coal-fired boiler. An essential part of the project is thus to identify the best suited method, or combination of methods, of simulating heat transfer is the various heat exchangers of a coal-fired power station. This method needs to simplify the process as much as possible whilst still accurately representing all significant theoretical, geometrical and process properties. A systematic process needs to be followed which attempts to develop a heat exchanger utilising various tools and approaches in order to determine which method best satisfies this requirement.

1.2 Goals / Objectives

The goal of this project is to develop a generic boiler modelling methodology specifically for Flownex that can be used to simulate actual conditions in the majority of the boilers utilised in the Eskom fleet. Although generic, several geometrical and process properties need to be known for acceptable results to be achieved.

The following is a list of objectives planned to be addressed in the project:

- Identification of the main types of boilers currently in operation in the Eskom fleet.
    - Identifying characteristics that can be used to group boilers together, which will distinguish between physical properties which could impact the modelling methodology. This could potentially reduce the amount of inputs needed.
- Undertake a literature study on the different mechanisms of heat transfer in coal-fired power station boilers, where it is applicable and how to model them.
    - Identifying where specific mechanisms have to be modelled independently and where combinations can be incorporated.
    - Identification and studying other methods developed to calculate boiler heat transfer on a high level similar to this project.
- Identification of the best way to model boiler heat exchangers in Flownex and the development of a comprehensive model of a coal-fired boiler heat exchanger.
    - Identifying means of validating the accuracy of the model.
    - Integrating combinations of heat exchangers and sub-systems into a full detail boiler model.
- Evaluation of model steady-state results against design data from actual boilers.
- Running various sets of transient conditions to prove the model's capacity in capturing different transient characteristics required by a power station software model.
- Documentation of a modelling procedure, findings and recommendations for future work on this topic.

The focus of this study will be on the heat transfer taking place in the convective pass of coal-fired boilers. The main mechanisms facilitating heat transfer in this area of the boiler will be investigated thoroughly and modelled as accurately as possible within the scope of the project.

Heat transfer in the furnace has a large contribution to the total heat transfer, but is notoriously difficult to model and will thus be separately investigated and accurately modelled in another project. The radiation heat transfer in the furnace needs to be included and will be modelled with numerous simplifying assumptions to enable a full model to be developed.

2. Coal-fired power station overview

Coal-fired power stations are the most common commercial power producers in South Africa and produce around 80% of the electricity used in the country. Eskom produces approximately 95% of South Africa's energy and feeds about 42 000MW into the national grid. There are currently 13 operational coal-fired power stations in Eskom contributing around 85% of the total capacity. Additionally there are two power stations in the construction phase which are due to come on-load in the near future.

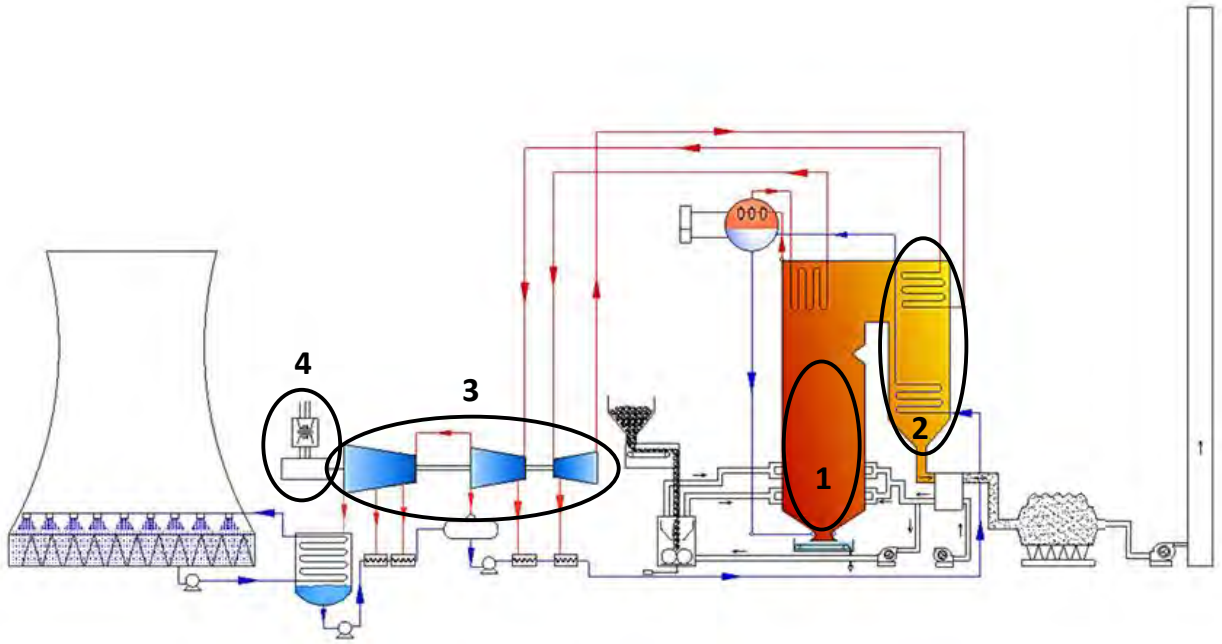

Figure 2-1: Typical layout of a coal-fired power station. [1]

A coal-fired power station produces electricity through a steam driven turbine-generator set. Steam for this process is produced by burning coal and heating water inside the boiler. The process works on the principle of converting or transferring energy sequentially from one form or fluid to another in a set of integrated systems. There are four main energy conversion processes that take place in a coal-fired power station which are indicated in the numbered ellipses in Figure 2-1 above and explained in Chapter 2.1 below.

2.1 Energy conversion processes

2.1.1 Chemical energy → Thermal energy

The process of a coal-fired power station is largely dependent on the chemical energy contained in the coal. This energy, contained in the various constituents of the coal, result in an exothermic reaction once heated or burned. The first energy process is a conversion of chemical energy into thermal energy and occurs during the combustion of coal that takes place in the furnace of the boiler.

2.1.2 Thermal energy transfer

The second energy process is a transfer of energy from one fluid to another. The thermal energy contained in the flue gas is transferred to the water or steam inside the tubes of the boiler. This results in an expansion of the fluid as high-pressure water is converted to steam. This energy transfer is the fundamental process on which the whole project was based.

2.1.3 Pressure & thermal energy → Mechanical energy

The third energy process occurs in the turbine where pressure and thermal energy is converted to mechanical energy. The high pressure and temperature steam is piped to the turbine where the combined pressure drop across the successive rows of turbine blades and the associated velocity increase facilitates rotation of the turbine blades and rotor. The set of turbines and the generator rotor are mounted on a common shaft and the rotation of the turbine thus facilitates and maintains rotation of the generator.

2.1.4 Mechanical energy → Electrical energy

The fourth energy process occurs in the generator where mechanical energy is converted to electrical energy. The electrical energy is generated by means of electromagnetic fields maintained inside the generator windings.

2.2 System fluid paths

In order to maintain production of electrical energy, a continuous transformation of energy must be maintained. This is maintained and controlled by separate systems or combinations of systems as a power station is essentially an integration of three different system fluid flow paths which continuously provide the material and fluids required to facilitate power production. Interaction between different fluid paths is the fundamental basis around which different systems are designed.

Other smaller systems are interconnected for various additional requirements such as safety, functionality, reliability, control and durability. Some of the relevant systems will be discussed later on in this document but those irrelevant to this project have been omitted.

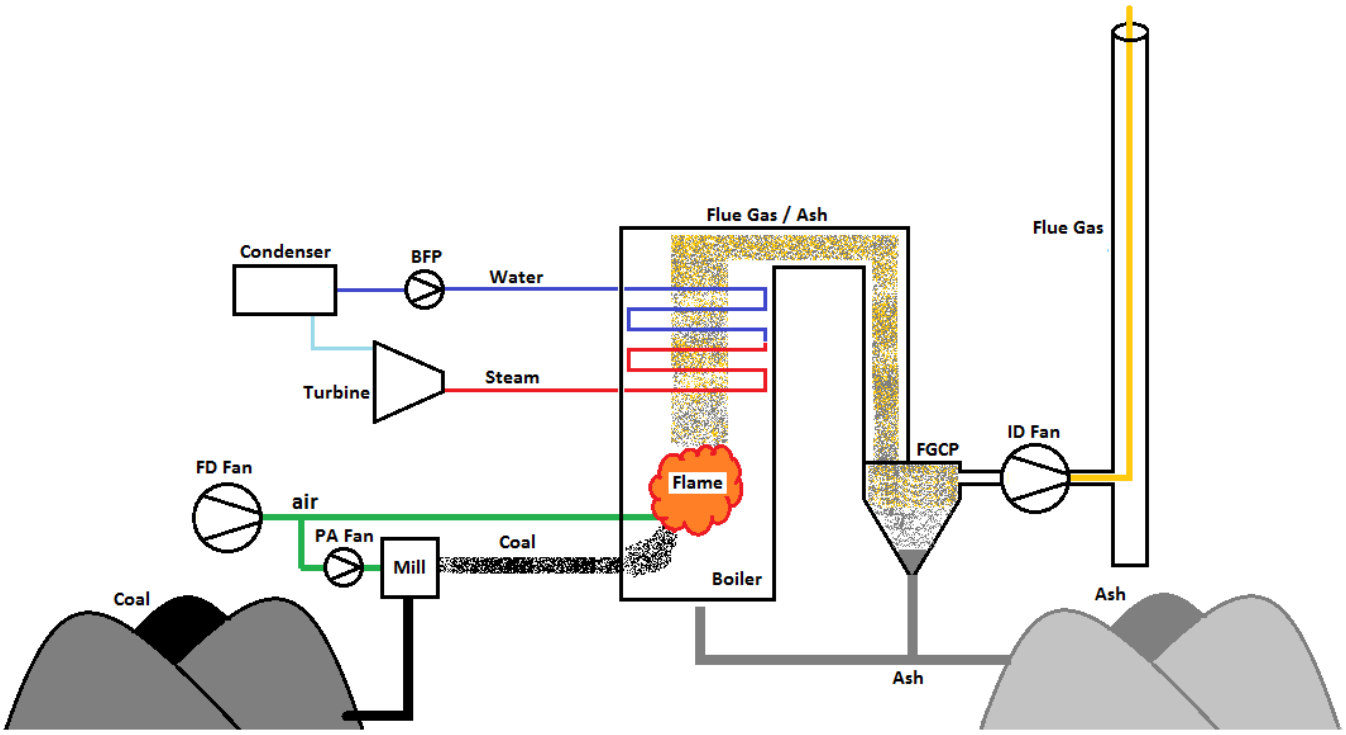

Figure 2-2: Illustration of system fluid paths in typical coal-fired power station.

2.2.1 The coal → ash cycle

Coal is fed into the power station from the coal stockyard or mine via various sets of conveyor belts, feeders and holding bunkers. It is pulverised into a fine powder in the milling system and transported by air to a set of burners which deposits the pulverised fuel (PF) into the boiler. Inside the boiler, the constant flow of coal powder is ignited by the high temperature maintained by the combustion process itself. The process is controlled by a flow of air through the boiler which supplies oxygen for combustion and also transports the coal particles, now partially or completely converted to ash, through the furnace.

Fly ash is the incombustible particles after combustion which are light enough to remain in suspension in the flue gas stream and will remain part of the gas through various sets of heat exchangers until it reaches the flue gas cleaning system at the back end of the boiler. Here it is removed from the gas and transported through different stages where it is mixed with coarse ash and dumped on an ash dump close to the power station. Flue gas is defined as the gas product after combustion.

Coarse ash is the incombustible particles of the coal which drop out of suspension to the bottom of the furnace. Here, it is removed by the bottom ash handling plant and mixed with fly ash before dumping.

2.2.2 The air → flue gas cycle

In order for combustion to take place, heat, fuel and oxygen are required. In a coal-fired power station, the fuel is the coal particles and once initial combustion is established by means of propane gas and fuel oil, this continuous combustion process also maintains and supplies the heat required. The oxygen required is the air that is supplied via the draught group. The draught group consists of forced draught (FD), primary air (PA) and induced draught (ID) fans. This group of fans ensure that sufficient air is admitted to the combustion process to facilitate complete combustion and that the required amount of flue gas is removed from the furnace.

FD fans supply air to the burners which is controlled in such a way that an excess percentage of oxygen is always present to avoid dangerous or explosive fuel-air mixtures. The FD fans supply inlet air to the PA fans, which force air through the mills to transport pulverised coal to the boiler. The ID fans are situated at the back end of the air-gas cycle and ensure the flue gas is effectively removed from the furnace and deposited through the chimney to the atmosphere. One of the main tasks of the ID fans is to control the furnace pressure, which is always kept below atmospheric pressure.

2.2.3 The water → steam cycle

The water–steam cycle was the key focus area of this project and is a closed cycle in which water is re-used repetitively in a cycle of evaporation and condensation through the various stages of the Rankine cycle. Water is pumped by two sets of pumps through feedwater heaters to the boiler. Here water is converted to steam and then superheated before it is piped to the turbine. After the final stage in the turbine, the steam is fed to the condenser where it is condensed to liquid water, which can then be pumped through the same process again. Cooling of the steam in the condenser is accomplished through a separate water cycle circulating cold cooling water through tubes, over which the condensing steam flows.

Some power stations make use of a reheat section in the steam cycle where outlet steam from the high pressure (HP) turbine flows back to the boiler to be reheated before flowing to the intermediate pressure (IP) and low pressure (LP) turbines. This significantly increases the efficiency of the cycle. A simplified layout of the water-steam cycle as well as a representation of the process on a T-s diagram is illustrated in Figure 2-3.

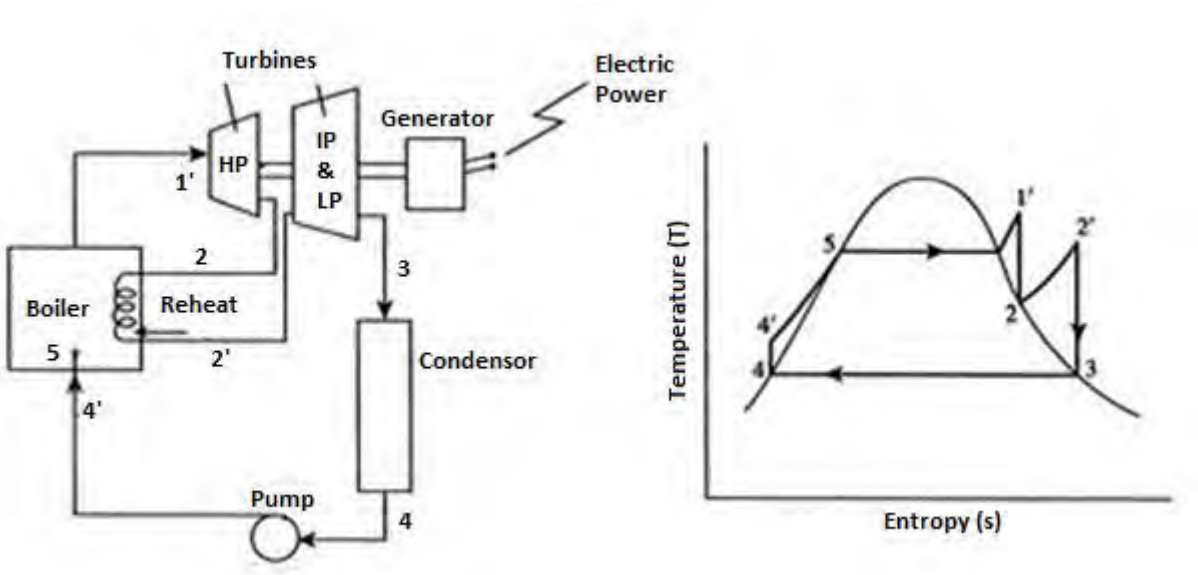

Figure 2-3: The layout of the water-steam cycle of a coal-fired PS and illustration of this cycle on a T-s diagram. (Edited form [2])

2.3 Applicable boiler designs

Boilers are equipment designed to boil water and create steam and thus are also often referred to as steam generators. Industrial boilers are generally split into one of two categories which are fire-tube and water-tube boilers, aptly named after the fluid flowing inside the tubes. All large industrial boilers, used in the power generation industry, make use of water-tube boilers as they can sustain the high volume flow required for large scale production of steam and electricity. Water-tube boilers were thus the only type of boiler investigated in this project.

Boiler feedwater pumps supply the system with high-pressure water which is heated through various sets of feedwater heaters in order to supply the boiler with high-temperature and high-pressure water. Boilers consist of several different heat exchangers installed in a complex flow orientation in series to achieve specified outlet temperature and pressure steam as required by the turbine. The different types of heat exchangers are designed to optimise reliable heat transfer at the specific conditions in which they operate in the system. These operating conditions change throughout the process, and ensuring that the components utilised sustain optimal heat transfer throughout the complete predicted plant life is essential. The different types of heat exchangers are discussed in Chapter 2.4.

The two types of water tube boilers commonly utilised in the power industry are the drum-type and once-through boilers.

2.3.1 Drum-type boiler

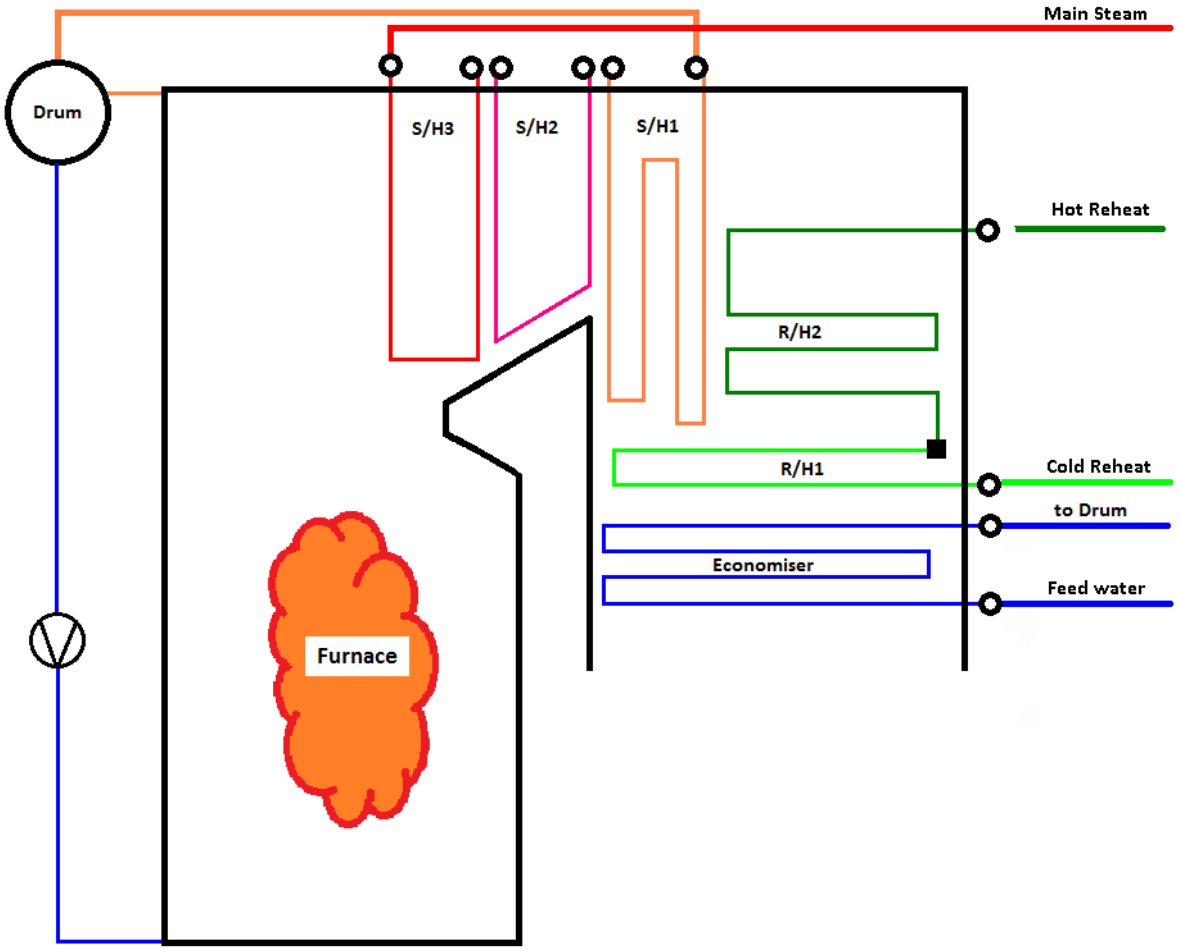

Figure 2-4: General layout of typical drum-type boiler with reheat and assisted circulation.

Drum-type boilers comprise the majority of boilers used in Eskom. They depend on a constant circulation of water through some of the heating components of the boiler to ensure that operating temperatures remain within specification. A large vessel, called a drum, is installed at the top end of the boiler in which a constant water level is maintained to supply the downcomer and water-wall tubes with saturated water. The circulation of water through these components is maintained in one of two ways:

Natural circulation

Natural circulation is achieved on the basis of density differences in the fluid, induced by temperatures differences in the various water columns. Fluid flow is facilitated by the natural rising of the lower density water-steam mixture inside the water-wall tubes in the furnace, while saturated water flows down from the drum into the downcomer and enters the boiler water-wall tubes at the bottom.

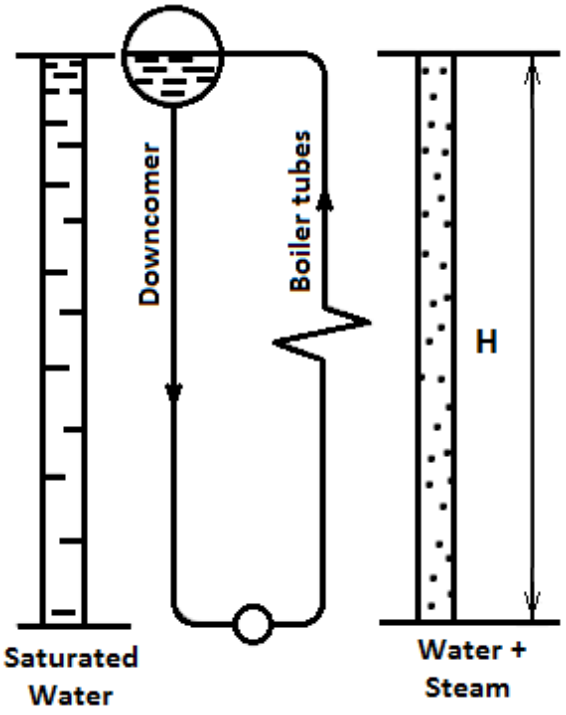

Figure 2-5: Typical natural circulation system layout. Edited from: [2]

Assisted circulation

Assisted circulation drum-type boilers make use of a boiler water circulating pump to assist flow through the water-steam path. This system remains in operation to ensure a constant flow of water to the water-wall tubes.

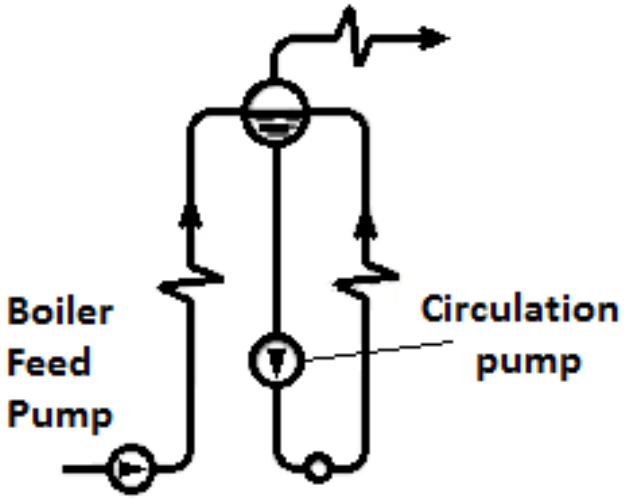

Figure 2-6: Layout of assisted circulation drum. Edited from: [2]

Drum

The drum is a large vessel that fulfils a two-fold role: the need for constant water supply to the water-wall tubes and steam separation for the water-steam mixture that exits the water-wall tubes. The drum, illustrated in Figure 2-7, has four main lines feeding into and out of it, namely:

- The feedwater inlet from the economiser outlet
- The outlet from the drum to the down-comer pipe to feed the water-wall tubes
- The inlet from the water-wall outlet back to the drum
- The steam outlet from the drum to the first stage superheater (S/H)

The water-steam mixture is fed into the drum where the water droplets are removed and mixed with water in the vessel. The saturated steam which remains then flows to the first stage superheater.

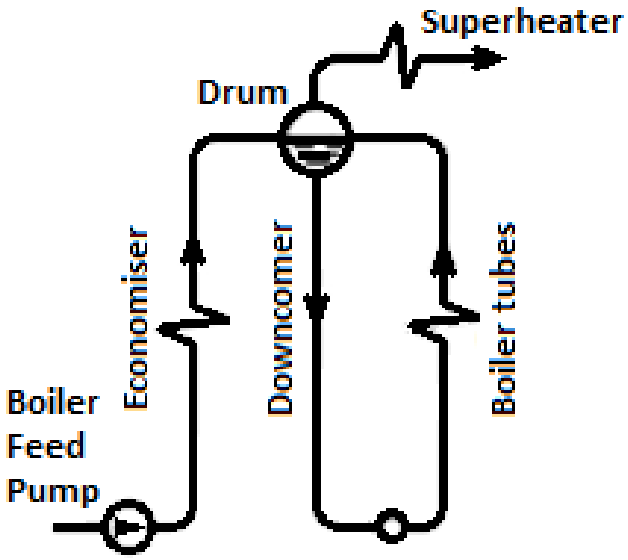

Figure 2-7: Layout of drum with main inlets and outlets shown. Edited from: [2]

General

Drum-type boilers are typically lower in height due to the lower evaporation load required in the water-wall tubes. Therefore, most drum-type boilers consist of two flue gas passes with some heat exchangers installed in the back pass of the boiler. High temperature heat exchangers are typically installed as pendant or vertical heat exchanger banks partially above the furnace.

It can be assumed that the general flue gas flow direction across the vertical tubes is still considered to be cross-flow because of the direction change at the top of the boiler. See Figure 2-4. [3]

2.3.2 Once-through boilers

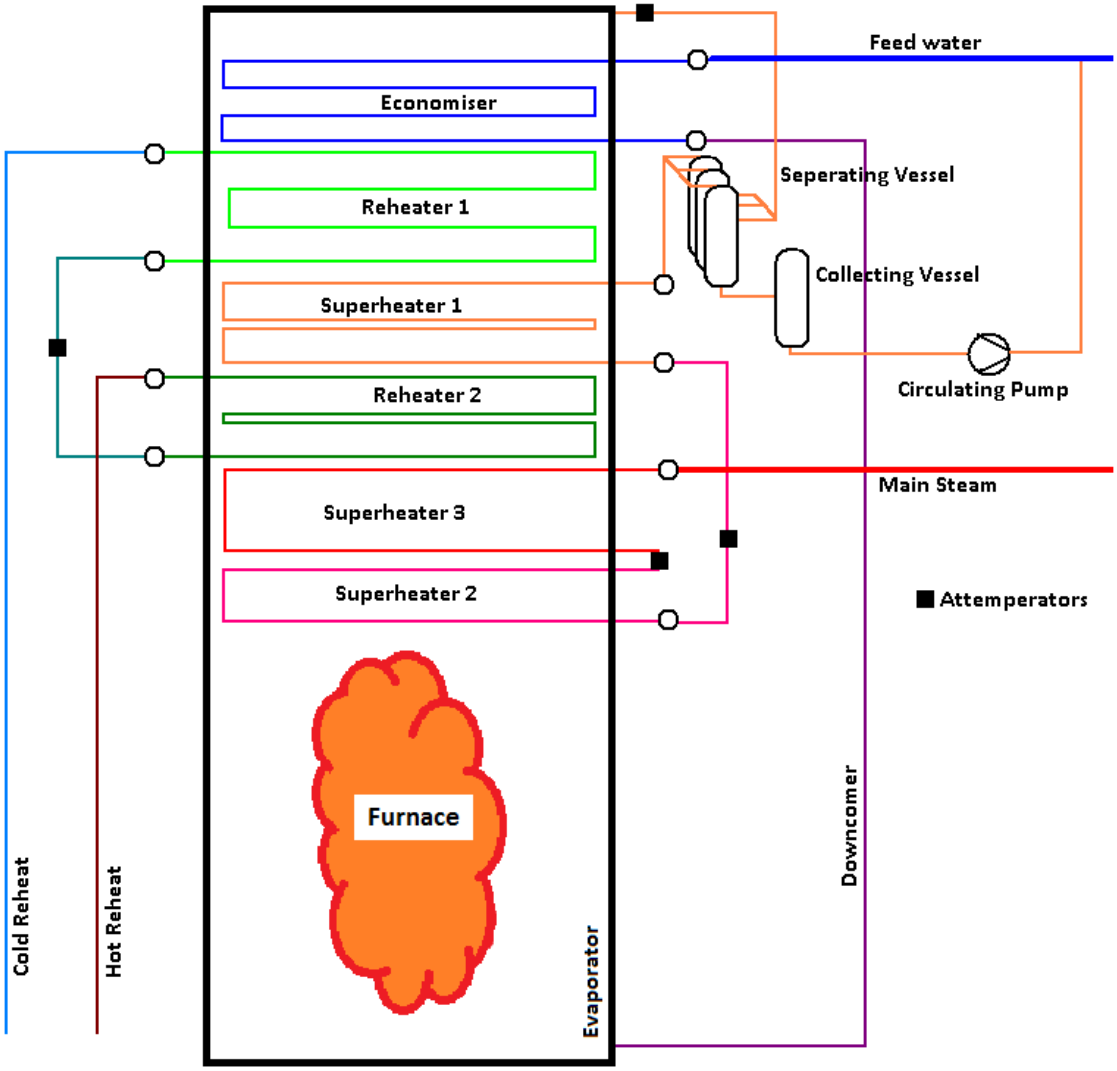

Figure 2-8: General layout of typical once-through boiler.

Once-through boilers, also known as Benson boilers, named after Mark Benson who designed the first commercial once-through boiler in 1923. The name stems from the fact that the water-steam mixture will make only a single pass through the boiler at high loads, which is one of the fundamental differences between the two designs and is a result of complete evaporation in the evaporator. The other key characteristic is that once-through boilers typically sustain, and are associated with higher operating pressures and some designs can reach the supercritical range.

At low loads, typically below 40%, once-through boilers operate similar to a drum-type boiler as insufficient heat is present in the furnace for complete evaporation of feedwater. As loads approach 40%, feedwater in the evaporator is heated to boiling point and a two-phase fluid exits from the evaporator to the separating vessels, where separation of steam and water takes place similar to in

a drum. At higher loads, typically greater than 40%, complete evaporation of feedwater takes place inside the evaporator tubes and slightly superheated steam exits the evaporator which is fed directly to the superheater.

All of the applicable once-through boilers for the purpose of this project are single pass vertical boilers and thus all heat exchanger banks are installed horizontally. No direction change of flue gas is experienced inside the convective pass and thus all heat exchangers are modelled as cross-flow. Two-pass once-through boilers do exist outside of Eskom and they typically have a similar physical flow orientation and layout as that of the drum boiler explained above with lower temperature heat exchangers installed in the back-pass.

Circulating system

At high loads, full evaporation of water take place within the evaporator, thus once-through boilers do not require a vessel to cope with the constant water level. This is however not the case at low loads and therefore the need for a circulating system. The circulating system is designed to recirculate the water from the evaporator outlet back to the economiser at lower loads. It typically consists of multiple separating vessels, where the water-steam mixture is separated, and a collecting vessel. The water flows via the separating vessels to the collecting vessel before being pumped back into the system. This system is illustrated in Figure 2-8.

Once the load increases and more evaporation takes place in the evaporator, the loading on this system will decrease until eventually, typically around 40% of Maximum Continuous Rating [MCR], the system will no longer need to be required.

Supercritical boilers

Once-through boilers can be designed to operate in the supercritical range, which results in a considerable efficiency increase. The operating pressure of a supercritical boiler is above the critical pressure of water. This results in the water-steam cycle bypassing the two-phase zone altogether and can be seen in the comparison of T-s diagrams of subcritical and supercritical cycles in Figure 2-9. The two-phase zone is represented by the area underneath the curves in Figure 2-9. The two new Eskom power stations currently under construction will both utilise boilers that operate in the supercritical range.

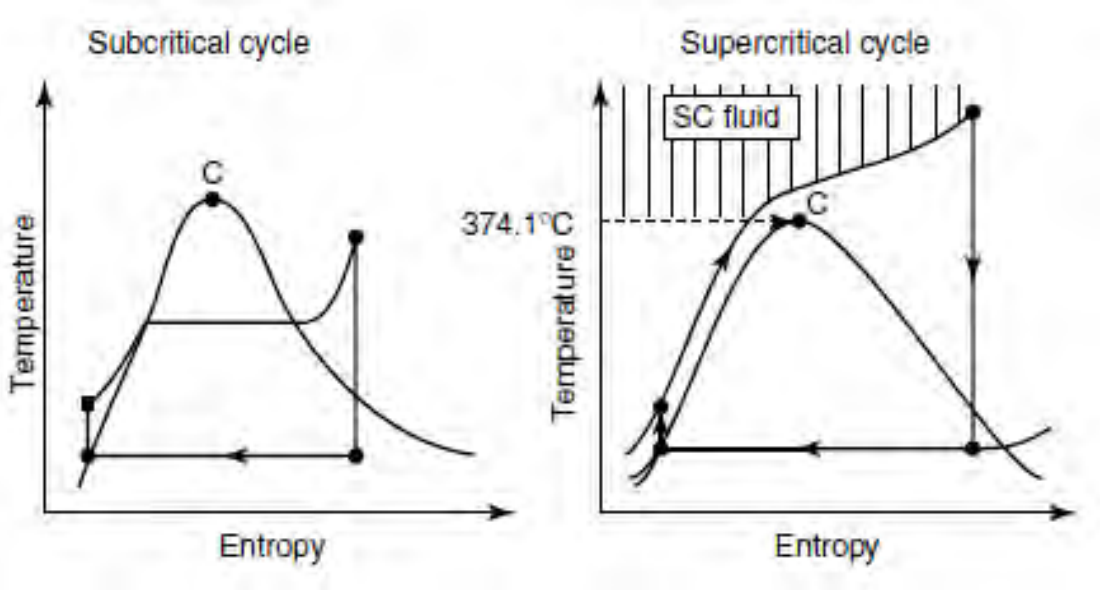

Figure 2-9: T-s diagram comparison of a subcritical and a supercritical cycle. [2]

2.4 Boiler pressure parts

The term 'boiler pressure parts' is given to all heat exchanger tubing that collectively form the complete steam generating system of a boiler. The pressure parts system is responsible for the total amount of heat transfer from the flame and flue gas to the water-steam cycle. Boilers in the power plant industry typically consist of a combination of the following components.

2.4.1 Economiser

The economiser is the first heat exchanger in the water-steam path and the final heat exchanger with regards to the flue gas path. It is used to heat up the feedwater, before it enters the water-wall tubes, with the remaining heat energy in the flue gas at the back end of the boiler. It is designed to operate at lower differential temperatures between flue gas and water as the majority of the heat in the flue gas has been absorbed by other heat exchangers. The tubes of the economiser are typically finned to maximise the heat transfer surface area. An example of a typical finned tube is illustrated in Figure 2-10.

Figure 2-10: Typical geometry of fins on economiser tubes. [4]

2.4.2 Evaporator / Water-walls

Boiler furnace walls are constructed of tubes which are known as evaporator or water-wall tubes. Tubes are connected by strips of metal plate called membranes in order to form a solid surface to enclose the furnace. A typical arrangement of furnace wall tubes is shown in Figure 2-11 with varying sizes of both tubes and membranes being utilised in boilers.

Figure 2-11: Section view of typical furnace wall tubes with connecting membranes. [5]

The furnace section of the boiler is referred to as the radiative heating zone as combustion takes place within this enclosure and heat transfer by other mechanisms are negligibly low. Burners are located in the walls of the boiler and tubes are manipulated around the burners to allow coal and air flow to the furnace. The evaporator typically initiates at the bottom and extends all the way to the top of the boiler structure, enclosing the convective pass heat exchangers as well as furnace section. The top portion, however, does not contribute significantly to the total heat transfer and is excluded from the illustration of an evaporator in Figure 2-12 .

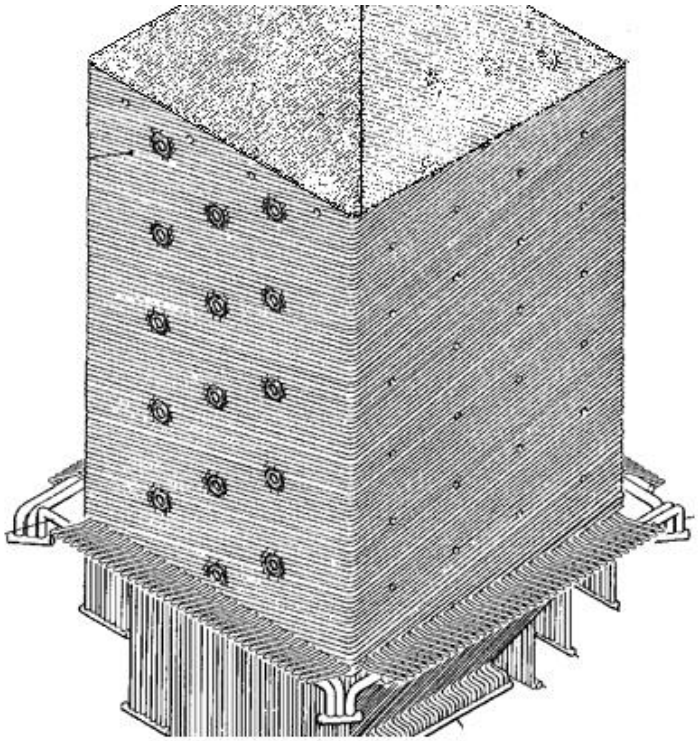

Figure 2-12: Typical furnace section of boiler with water-wall tubes and burners. Edited from: [7]

Some boilers make use of a division wall in the centre of the furnace that effectively splits the furnace into two parts. This is mainly done in larger boilers when a mismatch between tube surface area and volume in the furnace can sometimes exist. [2] The furnace exit is defined as the last point in the furnace before flue gas enters any convective heat exchanger banks and is located at the top level of the drawing in Figure 2-12.

Once-through boilers typically utilise helical wall tubes in the furnace section, whereas drum-type boilers often make use of vertical water-wall tubes. Helical tubes reinforce better mixing of the fluid to ensure a homogeneous mixture which optimise heat transfer and minimise losses during boiling. Drum-type boilers don't require this as full evaporation does not take place inside these tubes.

2.4.3 Superheaters

The term superheater, theoretically, is given to any heat exchanger that heats steam to a certain degree of superheat. In this project, the term superheater refers to a specific collection of heat exchangers that superheat the high pressure steam feeding the HP turbine. The term reheater is given to the set of heat exchangers that superheat lower pressure steam downstream of the HP turbine before it enters the IP and LP turbines. Reheaters are theoretically also superheaters and are used on larger power stations due to the efficiency improvement that is achieved by installing them.

Superheaters and reheaters in coal-fired power stations typically consist of two or more heat exchanger banks installed in series in a complex arrangement. The term complex is used as heat exchangers can comprise overall parallel or overall counter flow orientations and are typically not installed sequentially in terms of either the steam flow or the flue gas flow.

The optimisation of arrangement, sequence and material is a complex cost and performance exercise where theoretical knowledge goes hand in hand with practical and economical experience of boilers. The final superheater is thus usually not the first heat exchanger when viewed along the flue gas flow direction. A typical example of a superheater and reheater layout is given in Figure 2-13.

Within this complex layout, individual heat exchanger banks are designed for specific properties of both flue gas and steam where many operating variables influence the final design. The typical physical characteristics that will vary are the tube material, tube dimensions and number of tubes, passes and horizontal number of elements that together form the heat exchanger. This is done to maintain internal and external fluid velocities in order to optimise heat transfer within specified requirements to ensure reliable operation.

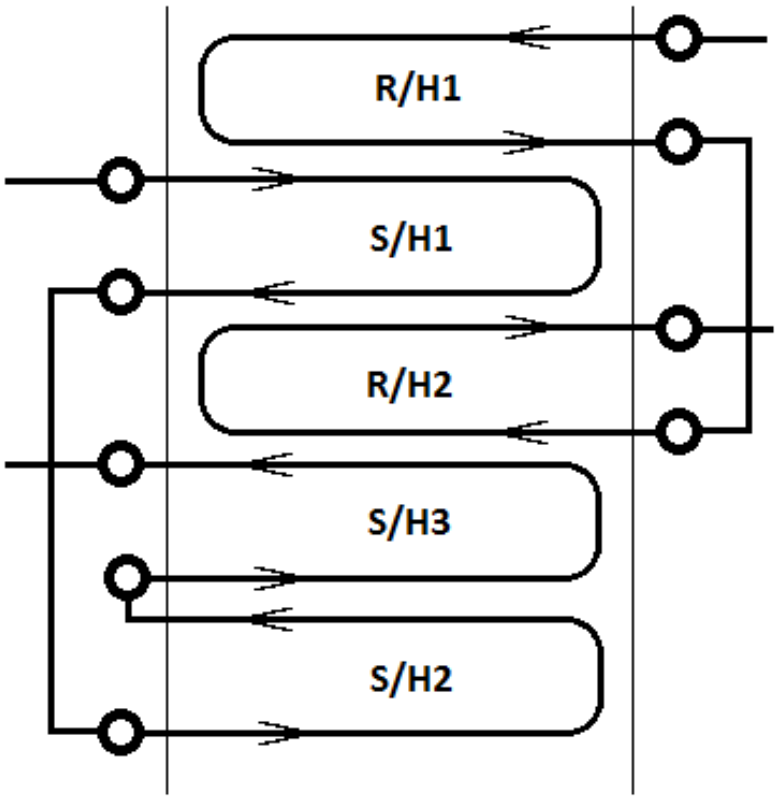

Figure 2-13: Typical layout and flow orientation of heat exchanger set.

Fly-ash erosion

As described in Chapter 2.2.1, once the combustion process of the coal is completed, the incombustible material that remains in suspension in the flue gas is known as fly-ash. This flue gas mixture is an extremely abrasive fluid, especially at high velocities. Fly-ash erosion is a damage mechanism where tube material is eroded away due to impingement of high velocity particles on the material surface. Severe cases of fly-ash erosion will lead to tube failure with associated repair and production loss costs. Fly-ash erosion is the most common cause for tube failures in conventional coal-fired boilers and thus flue gas velocity is an essential parameter when designing boiler heat exchangers. [7]

As the flue gas cools, the density changes significantly thereby enabling designers to decrease the horizontal tube spacing between tubes in the superheaters and reheaters progressively as they move further down the flue gas path. This allows for more heat transfer surface per furnace cross section. This is illustrated in Figure 2-14.

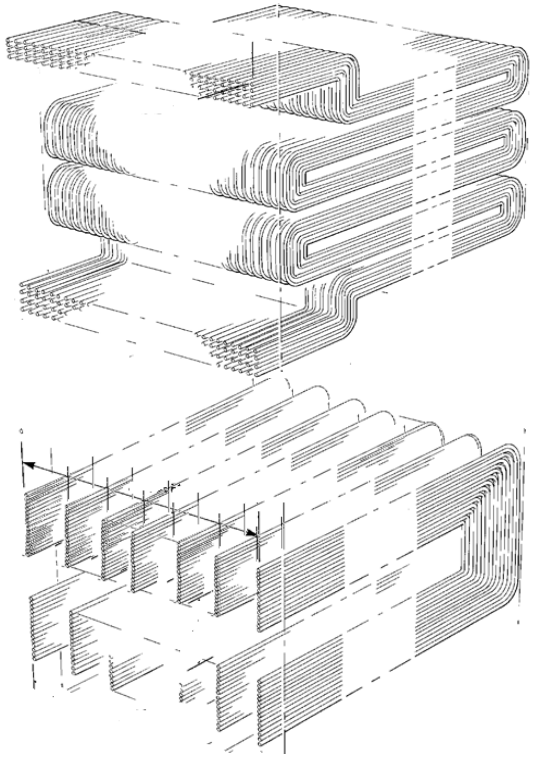

Figure 2-14: Layouts of different heat exchanger banks. Edited from: [7]

2.4.4 Sling Tubes

Sling tubes are used in conjunction with horizontal heat exchangers. They form part of either the evaporator or are classified as the first stage superheater. The sling tubes are suspended from the top of the boiler and their primary purpose is to support the weight of horizontal tubes that are suspended on attachments to the sling tubes. The wall thickness of the sling tubes is thus significantly thicker than that of heating tubes as they need to carry significantly more weight. The flow of water or steam in the sling tubes is primarily to cool the tubes and ensure that the mechanical properties of the material remain sound.

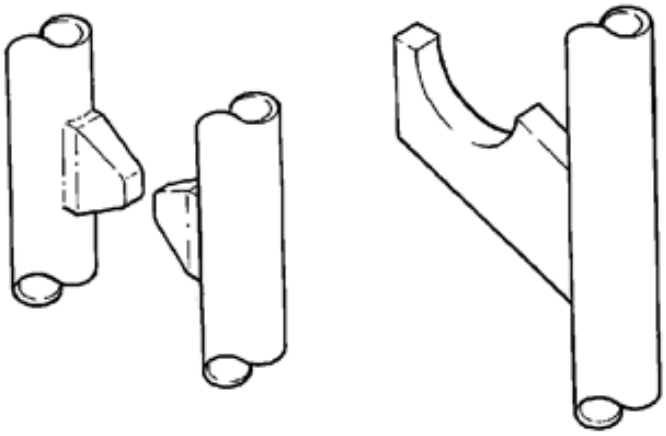

Figure 2-15: Common types of sling tube attachments. [7]

2.5 Boiler auxiliaries

2.5.1 Attemperators / Spraywater System

Large portions of the boiler, main steam piping and turbines are constructed of high temperature resistant materials. These materials are designed to remain mechanically sound for the design life of a power station at high temperatures and are extremely expensive. These materials are also developed to withstand a specific maximum operating temperature for the required projected life of the plant to which strict adherence is required. Operating above the maximum design temperatures will greatly accelerate a metallurgical failure mechanism known as creep.

Any metal exposed to a combination of high temperatures and tensile load will experience creep and deform over time. The migration of carbon atoms in creep-aged materials to common locations inside the material to form voids is an indication of the onset of creep. Creep occurs naturally in all materials, but becomes detrimental at temperatures above specified maximum temperatures, where it occurs exponentially more rapidly. Prolonged exposure to creep range temperatures will result in premature component failure if not identified and rectified timeously. Due to the enormous scale of utility plants and the lack of finer high level flue gas temperature control ability, some form of local steam temperature control must be employed.

Local control is achieved by introducing variable flow rates of colder water at strategic locations along the steam path to sustain acceptable steam temperatures throughout all the heat exchangers. This function or sub-system is commonly known as spray-water or attemperation.

The spray-water introduced is tapped off from the feedwater piping before the economiser at higher pressure to avoid reverse flow. Spray-water for the reheat section of the steam cycle is normally tapped off at an intermediate stage of the boiler feed pump to ensure that the appropriate water pressure is utilised. Flow rates are controlled by upstream control valves and this in turn is controlled by temperature measurements at strategic locations along the steam path.

2.5.2 Milling plant and burners

Coal is burnt in modern boilers in the form of a fine power and this is done to optimise both combustion and control of the combustion process. Control of the combustion process is critical as poorly controlled combustion can lead to plant damage, unsafe operating conditions and efficiency losses.

Coal is pulverised to the appropriate size in the milling system, transported by air to the boiler through PF pipes and is deposited into the furnace through a set of burners installed in the boiler wall. A set of burners are commonly associated with a specific mill and are located at different positions in the furnace, see Figure 2-12. The milling plant is typically designed as a redundant system and a boiler will operate with various mill combinations to achieve the required heat generation for any desired load. Mindful of different burner layouts, there exist numerous different combustion heat transfer profiles in the radiative heating zone. A typical burner set will have very little flexibility in terms of controllability on-line as most adjustable settings are done once-off during the commissioning of a plant.

The two common burner layout types are:

- Front and rear wall fired
- Corner fired

2.5.3 Draught Group

The draught group on a power station normally consists of three sets of fans, as described briefly in Chapter 2.2.2. They are split into two categories namely, supply and extraction. Combustion air is supplied to the boiler by FD fans, which also feed the intake of the PA fans. The PA fans are responsible for transporting the coal particles to the boiler. Extraction of flue gas is facilitated by the ID fans, which are also responsible for furnace pressure control. See Figure 2-2.

Several sets of air-heaters are normally installed in the draught group. The main air-heater is located in the back pass of the boiler, where hot flue gas exits. This regenerative air-heater uses hot flue gas to heat up cold air by rotating a large metal mesh with extremely large surface area between the two streams. The hot flue gas heats up the mesh and when exposed to the air side, transfers this heat to the cold air. Two sets of air pre-heaters are used to heat air prior to the FD fan to ensure a specific temperature is maintained on the cold side of the regenerative air-heater. Air below the dew-point temperature leads to condensation on the air-heater mesh which results in corrosion as the flue gas and water reacts.

2.6 Summary of boiler properties in the Eskom fleet

Extensive research was done to find as much information as possible on the boilers currently used in the Eskom fleet. The following chapter will provide some of the summarised data obtained. The data was obtained from sources which are not publicly available as this is classified information to Eskom and the original equipment manufacturers (OEM's). Much of the data was gained from design specification documentation supplied by the OEM's to Eskom upon completion of projects. Many of these documents are quite old and some of the actual plants might not currently match the documents. It is assumed that the majority of the documentation was accurate and small changes not updated will become negligible once values are averaged out across groups of boilers.

2.6.1 Total Eskom fleet

Eskom has 13 operational coal-fired power stations feeding into the national grid. A number of the older power stations utilise different boiler designs on a single plant, but the newer stations mainly use a single design. A study was undertaken on the available information and the following criteria were investigated to identify commonalities amongst boilers, or groups of boilers:

- General:
    - Type of boiler
    - Commission date
    - Size
- Plant geometries:
    - Reheater or no reheater
    - Number of heat exchangers in series
    - Typical tube dimensions - heat transfer surface area
    - Tube pitches or spacing
- Process conditions:
    - Mass flow of steam and flue gas
    - Mass flow and calorific value (CV) of coal
    - Predicted or tested steam and flue gas temperatures throughout

There are a total of 87 boilers and 18 different boiler design types used in the Eskom fleet and the figure below shows the boiler types at various power stations. The approximate age of the boilers is indicated with the black dots showing the approximate year of commissioning with the date provided on the secondary axis. There is also a distinction drawn between boilers without a

reheater, marked in blue, and boilers with a reheater, marked in red. It must be noted that the size indicated on the primary axis is the generating capacity of the unit. The boiler thermal size is typically in the range of three times more than unit's generating capacity as the efficiency of coal-fired power stations range between 30% - 35%.

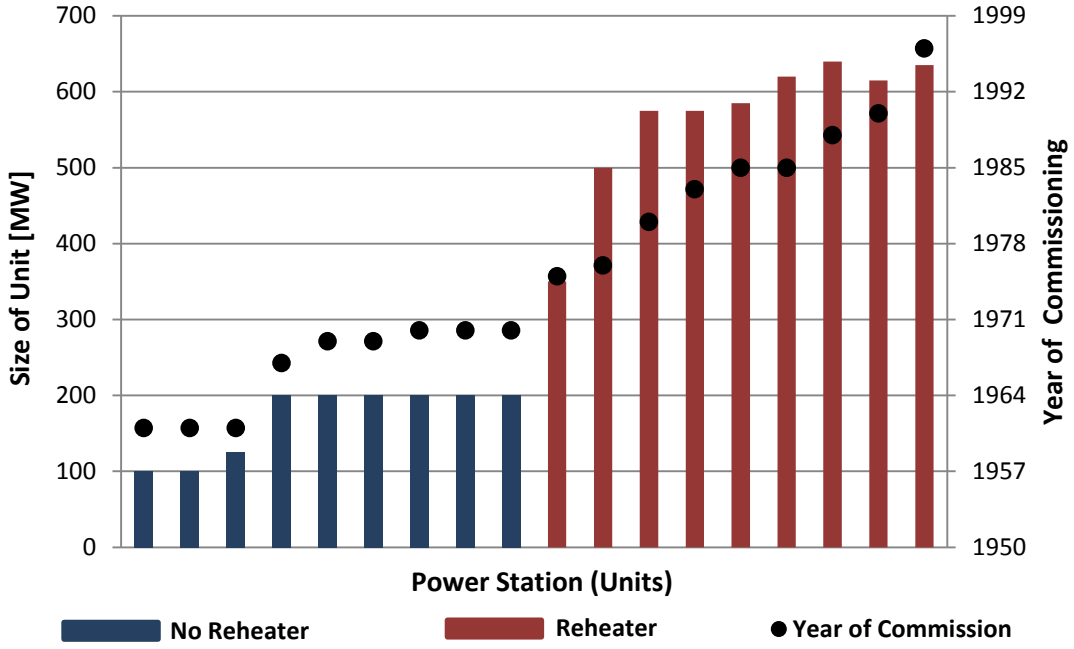

Figure 2-16: Boiler designs and their corresponding unit size.

The types of boilers was also analysed and the results are given below. It can clearly be seen that the dominant boiler design type is the drum-type boiler. The majority of the drum-type boilers are the older boilers which are due to be decommissioned within the next 10 – 15 years.

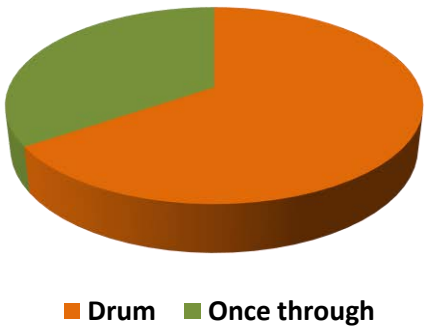

Figure 2-17: Drum-type to once-through type boiler ratio for individual boilers.

2.6.2 Grouping boilers

One of the objectives of this project was to identify ways of grouping the boilers that would possibly require different modelling approaches in order to simplify modelling and increase accuracy. The summary of boilers in Figure 2-16 gives much information as to an obvious criterion possibility that would capture two very important characteristics namely size and whether a boiler is equipped with a reheat section or not. It can be seen that a split of boilers larger and smaller than 300MW will encapsulate the big step change in size as well as the split between reheaters and no reheaters. Further investigation showed that this grouping of boilers also includes other important variables that are shown below.

Table 2-1: Breakdown of criteria for boiler grouping.

Boiler Size	**> 300 MW**	**< 300 MW**
Reheater	Yes	No
Average # of heat exchangers	6	5
Superheaters **Reheaters** **Economiser**	3 2 1	4 0 1
Tube Outer Diameter: **Superheater** **Reheater**	 45 mm 60 mm	 57 mm -

The available data proved that boilers in the Eskom fleet, although completely unique in many aspects with individualised characteristics, have somewhat of a generic nature in that a typical physical size will result in similar layout of boiler with similar plant conditions during operation. There had also globally not been major changes to utility boiler designs in the era that all of the Eskom power stations were designed and built.

The following paragraphs will look at, group and illustrate some of the above mentioned characteristics.

Flue gas temperature

The combustion process in most boilers will yield flame temperatures that are in the range of 1 600°C – 1 800°C. The furnace exit temperature in the Eskom boilers are typically controlled to range between 1 100°C and 1 200°C. The main driving mechanism for this temperature is ash fusion temperature. The ash fusion temperature is a function of the ash composition and this is done to

avoid slagging formation and is discussed in Chapter 3.1.1. The design of the evaporator or water-wall is thus done in such a way that sufficient heat is absorbed to cool the flue gas down to ensure adherence to these specifications.

The lower temperature boundary of the flue gas side is typically determined by the equipment specifications of the plant installed downstream of the boiler and air-heater, which is sensitive to high temperatures. The inlet temperature of feedwater to the economiser also contributes as flue gas needs to be hotter than that.

The flue gas temperature profile from furnace exit temperature to boiler exit temperature is comparative across all boiler designs and thus emphasises the importance of the number of heat exchangers as it will influence the average flue gas temperature across a specific bank which will impact how radiation heat transfer is modelled later on.

Boiler heat exchangers are analysed sequentially with regards to flue gas flow, numbering them effectively from the heat exchanger experiencing hottest to coolest flue gas. This best matches up similar heat exchangers to each other in order to determine whether significant trends exist which could be utilised in the modelling process.

Flue gas temperatures

Design documentation was analysed from six of the nine boilers larger than 300 MW and average flue gas temperatures per heat exchanger are illustrated in Figure 2-18.

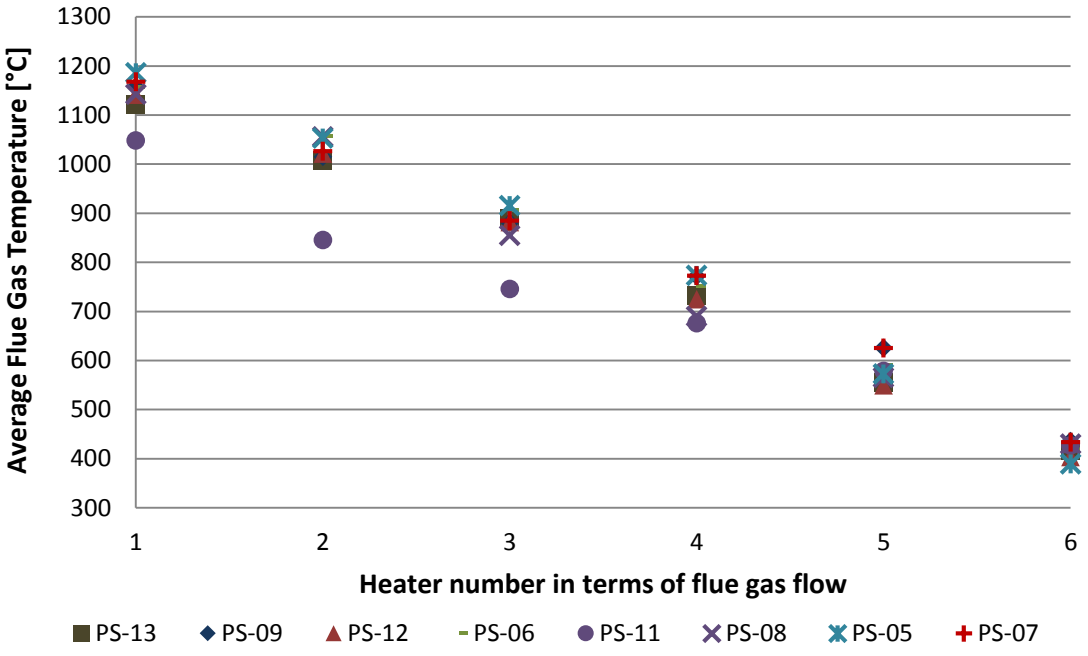

Figure 2-18: Average flue gas temperatures per heater bank for boilers > 300 MW.

PS-11 flue gas temperatures, marked by the purple dots and line, are clearly lower across the first few heat exchangers. It is not shown, but PS-11 utilises seven heat exchangers which is the root cause of the discrepancy. It was excluded from average value calculations in order to obtain better accuracy for the remainder of the boilers.

Design documentation from seven out of ten boilers smaller than 300 MW were analysed and average flue gas temperatures per heat exchanger are illustrated in Figure 2-19.

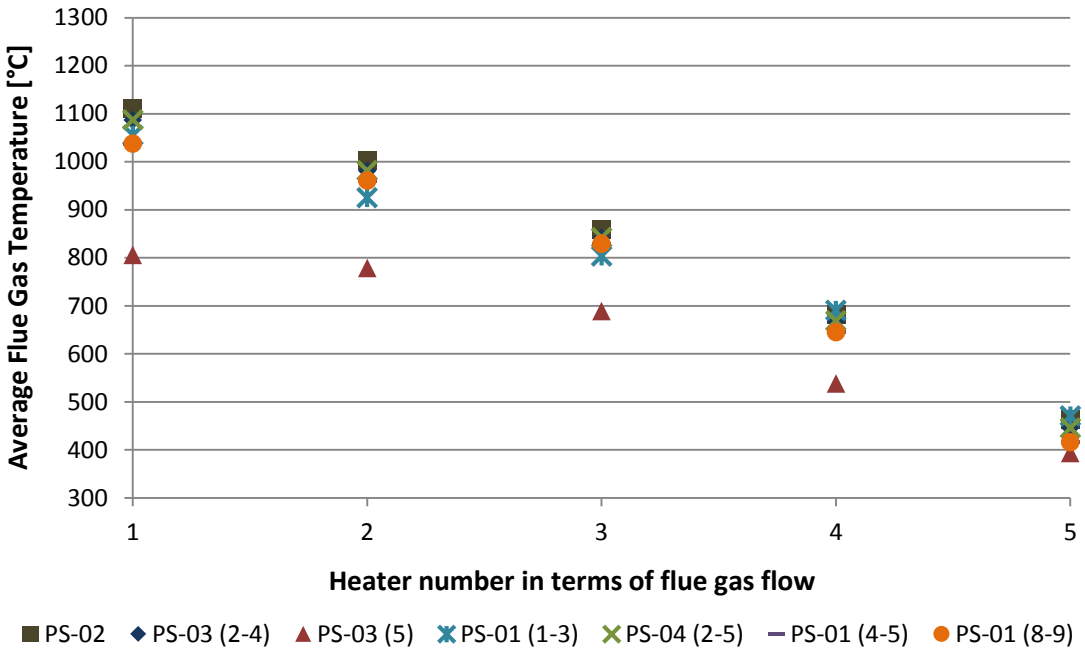

Figure 2-19: Average flue gas temperatures per heater bank, boilers < 300 MW.

PS-03 unit 5 boiler data, marked by the red triangles, falls well outside the average temperatures. It has a unique first stage superheater that is part of the boiler wall so its data was thus ignored for all calculations of this project.

Water–steam temperature

Water-steam properties play a big role in determining the inlet conditions of water to the boiler. Due to the high pressure operation of power plants, feedwater downstream of the feed pumps can be significantly heated using bled-off steam from the turbine, which increases the efficiency of power plants. Boiler feedwater typically falls in the temperature range of 200°C - 250°C and is closely related to the size of the plant. The increase in boiler size and subsequent increase in operating pressures enable modern boilers to be supplied with higher temperature water. This is clearly illustrated in Figure 2-20.

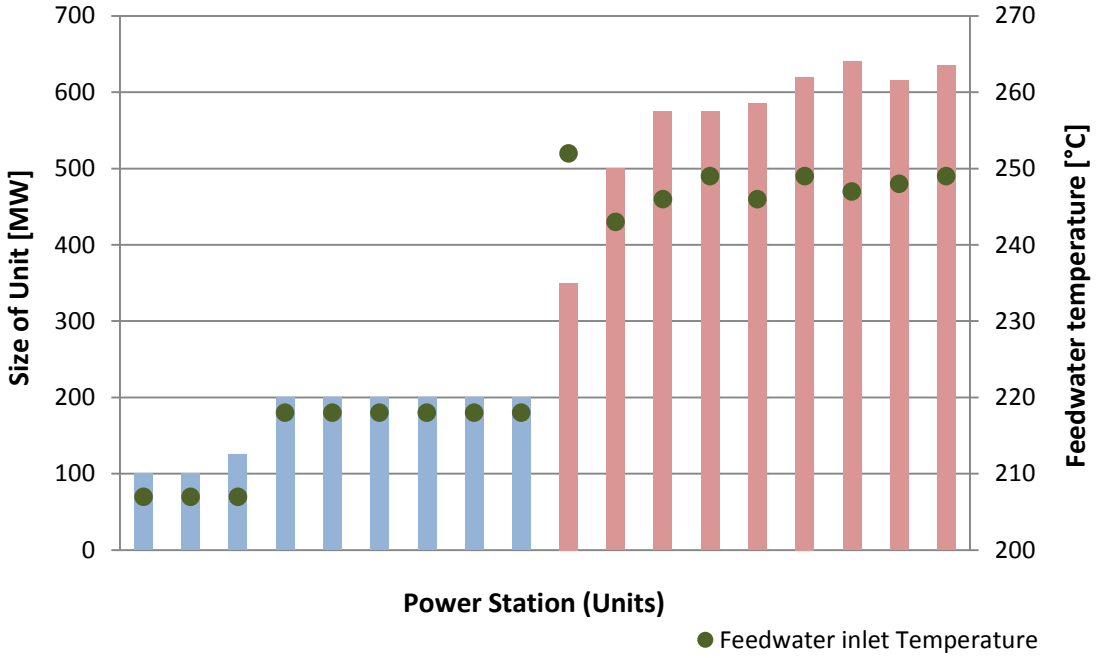

Figure 2-20: Boiler feedwater inlet temperatures.

Due to the generic nature of power stations and turbine sets, the required inlet temperature of HP turbines generally has not changed much from older power stations still in service. This is greatly influenced by the material grades and proves that no significant improvement in reliable and economic high temperature materials have been made and implemented in the period from the 1960's to the 1990's. The superheater outlet temperature for most Eskom boilers typically varies between 510°C and 550°C.

Steam temperatures

No trend lines are added to the data sets in Figure 2-21 and Figure 2-22 because of the complex layout of the steam flow path. It will not make logical sense as heat exchangers are numbered in terms of flue gas flow. The same boilers, as mentioned above, for boilers larger than 300 MW were analysed and average steam temperatures per heat exchanger are illustrated in Figure 2-21.

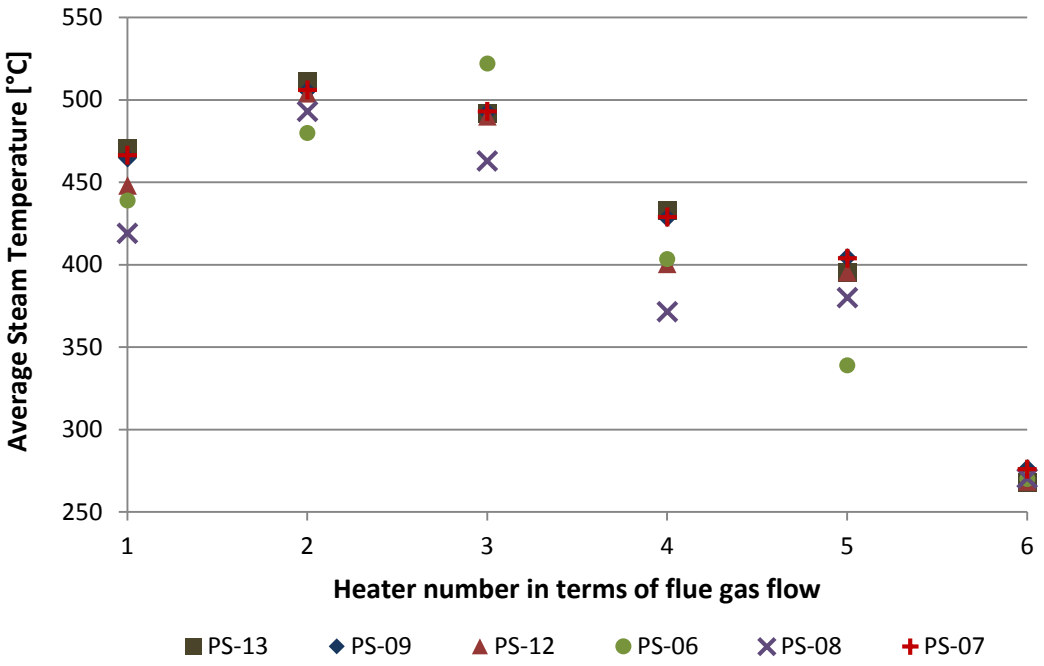

Figure 2-21: Average steam temperatures per heat exchanger bank for boilers > 300MW.

The same boilers, as mentioned above, for boilers smaller than 300 MW were analysed and average steam temperatures per heat exchanger are illustrated in Figure 2-22.

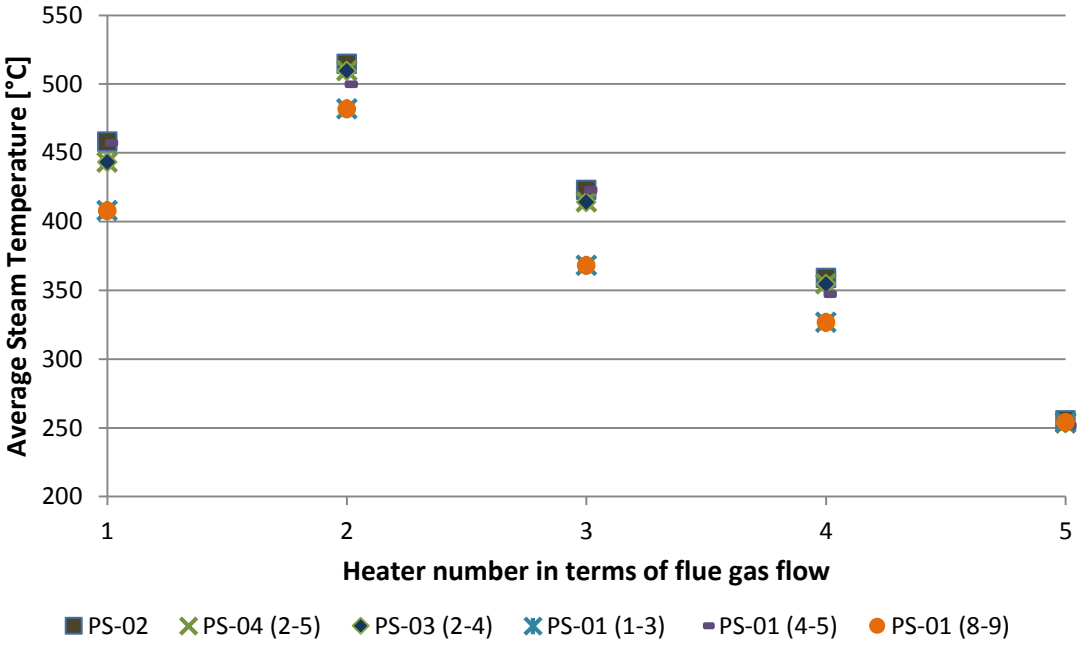

Figure 2-22: Average steam temperatures per heat exchanger bank for boilers < 300MW.

Tube pitches

The flue gas velocity is controlled to a certain maximum value to limit the effect of fly-ash erosion damage on the tubes. This results in an increase in tube density as the flue gas density decreases with a drop in temperature. This is illustrated in Figure 2-23 and Figure 2-24.

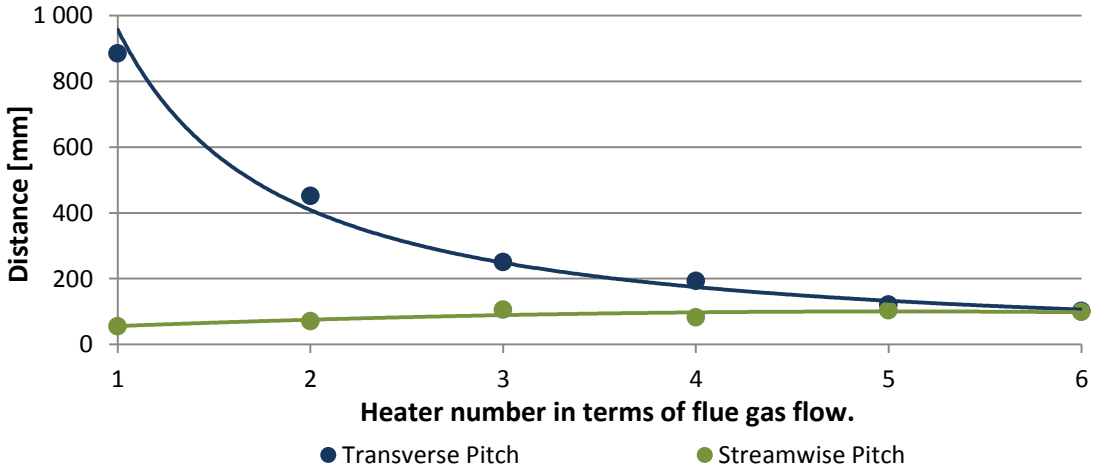

Figure 2-23: Average tube pitches per heat exchanger for boilers > 300MW.

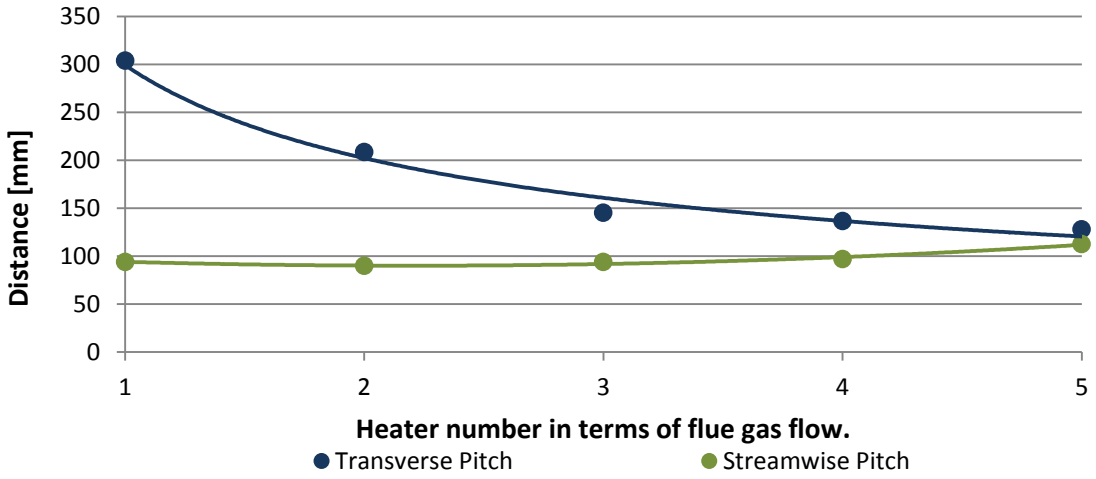

Figure 2-24: Average tube pitches per heat exchanger for boilers < 300MW.

2.6.3 Conclusion

This chapter shows that there are certain characteristics to boilers, and power stations in general, which are similar across specific sizes and types. The characteristics that were identified highlight that similar type boilers typically follow similar trends for many of the important variables, especially for heat transfer calculations. These trends will be used in the next chapters to develop the generic boiler model that represents a large percentage of the boilers in the Eskom fleet.

3. Heat transfer theory in boilers

This chapter covers of the theory of heat transfer, focussing primarily on the mechanisms of heat transfer and their applications in typical coal-fired power station boilers. A summary of what is found in literature on the various solving methodologies for heat transfer will be discussed concentrating on the application thereof in coal-fired power stations specifically.

The main focus of this project was to understand, calculate and model the heat transfer from the flue gas or flame to the water or steam inside the tubes in a typical coal-fired boiler heat exchanger. The general heat transfer phenomenon typically looks as follows:

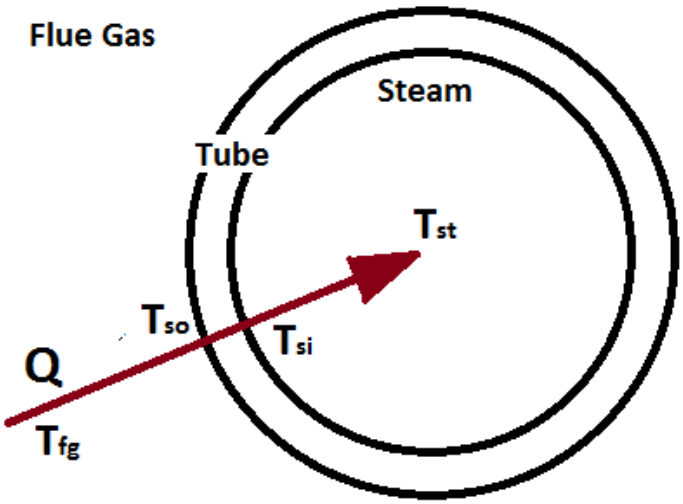

Figure 3-1: General heat transfer situation found in coal-fired boilers.

The general heat transfer calculation is a combination of all three heat transfer mechanisms and can typically be split up into three separate sections:

1. Total heat transfer [***Q***] from flue gas [***fg***] to external tube surface [***so***].
    - Convective heat transfer
    - Radiative heat transfer
2. Conduction from external tube surface [***so***] through tube to internal tube surface [***si***].
    - Including any layers of fouling on the external or internal surface of the tube.
3. Convection from internal tube surface [***si***] to steam [***st***].

3.1 Conduction

Conduction heat transfer in boiler applications mainly occurs in the tube wall material. Heat is conducted from the external surface through the tube wall to the internal surface of the tube as shown in Figure 3-2. The amount and rate of heat transfer is dependent on the thermal conductivity of the material ***k***, the distance or length of material ***x*** and the difference in temperature of the two surfaces. Heat transfer due to conduction is given by **Fourier's Law**:

$$q_x = -kA\frac{dT}{dx} = -kA\frac{T_o - T_i}{x} \tag{3-1}$$

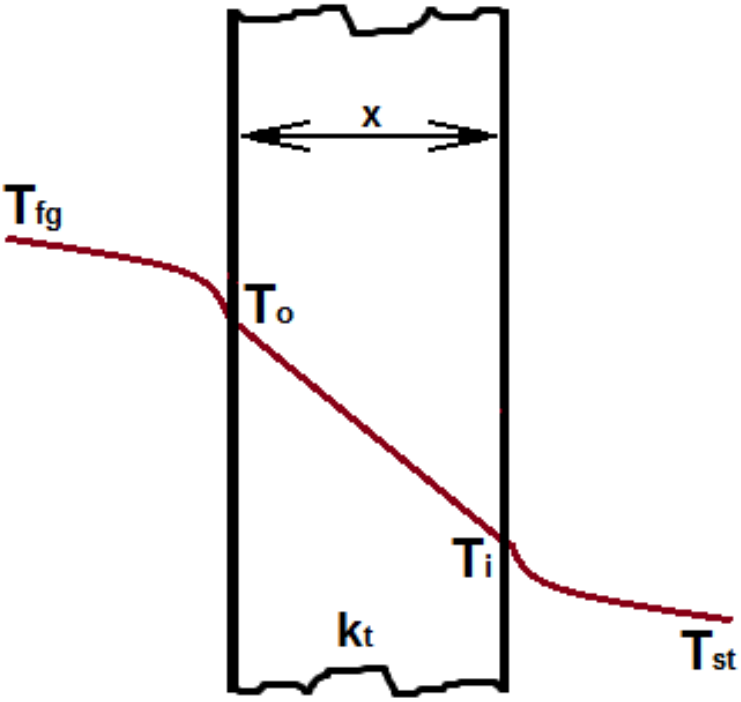

Figure 3-2: Conduction heat transfer through plate.

3.1.1 Fouling

Fouling is defined as any deposits of foreign material onto either the external or internal surface of the tube. This additional material has its own thermal conductivity and contributes, generally negatively, to the effective thermal conductivity of the tube. The common types of fouling experienced in coal-fired boiler heat exchanger tubes are the following:

- Ash build-up on external surface

  This is common amongst all types of boilers and occurs when ash settles on horizontal surfaces of the tube, or at locations of stagnant flow. This is controlled or managed by soot-blowing.

- Slagging – External surface

  Slagging occurs when gas temperatures amongst tubes are above the melting temperature of ash, or the ash fusion temperature. Molten ash attaches to the cooler tube, cools down and solidifies. Slagging in the convective pass is caused by excessively high temperatures which is typically a result of delayed or prolonged combustion.

- Scaling – Internal surface

  Chemical reaction between tube metal and the steam inside tube leads to the formation of thin oxide layers inside the tube. This layer is normally associated with and occurs exponentially quicker at operating temperatures above the maximum allowable design temperature and is directly related to creep damage.

Internal and external tube surface fouling has a negative impact on plant safety, reliability and efficiency, but effects thereof occurs in slightly different forms. External fouling leads to efficiency losses as higher external gas temperatures are required due to increased resistance to heat transfer from the gas to the external tube surface. This phenomenon is illustrated in Figure 3-3.

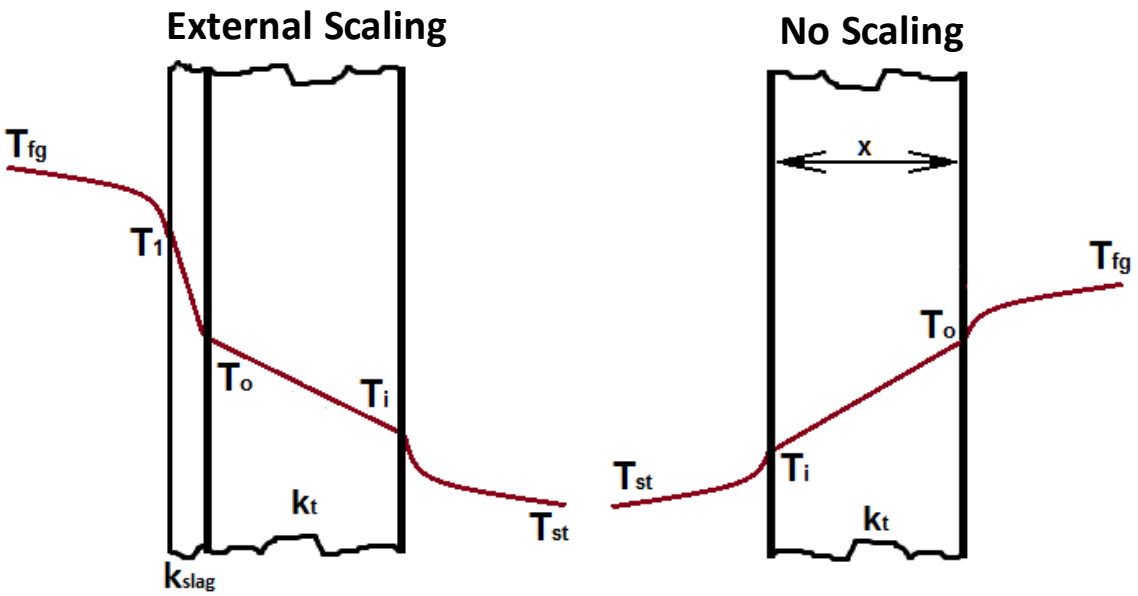

Figure 3-3: Effect of external tube fouling illustrated.

Internal fouling leads to both a higher mid-wall tube temperatures and an efficiency loss due to higher gas temperature requirements. The higher tube metal temperature often leads to tube failures and it is thus essential to manage all forms of fouling as far as possible. This phenomenon is illustrated in Figure 3-4.

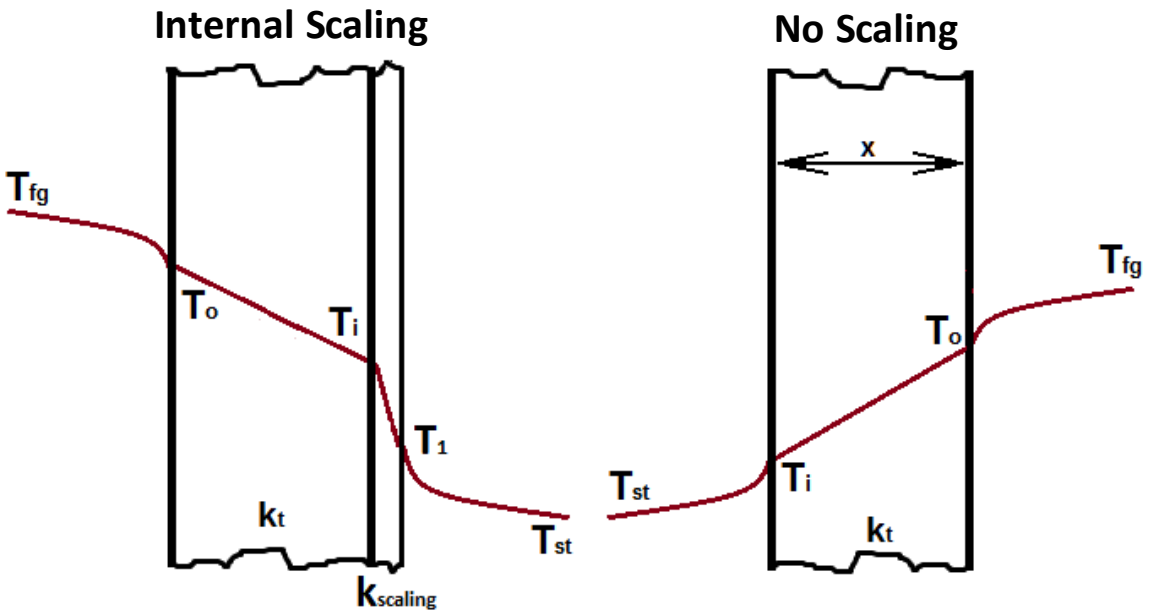

Figure 3-4: Effect of internal surface fouling illustrated.

The temperature in both the fluids as well as the tube material is represented by the line and the thermal conductivity of each material is represented by the gradient of the line. It is clear that fouling has a significantly higher resistance to conductive heat transfer. Typical values are given in Table 3-1.

Table 3-1: Material conductivity of typical materials applicable in boiler heat exchangers.

Material	**Thermal conductivity $\left[\frac{W}{mK}\right]$ in typical temperature range**
High temperature alloy - 13CrMo44	38 – 42 [8]
High temperature alloy - X20CrMoV121	23 – 26 [8]
Coal slagging	0.6 – 1.7 [9]
Tube oxides - Magnetite	0.03 – 1.06 [7]

3.2 Convection

Convective heat transfer in coal-fired boilers occurs when a fluid flows across a stationary solid body at a different temperature. It is the dominant heat transfer mechanism in the convective pass of the boiler where the superheater, reheaters and economisers are located. The transfer of heat is driven by the convective heat transfer coefficient, the surface area exposed and the temperature difference of the fluid and solid body involved and is calculated by the following correlation:

$$Q = h_{conv} A \cdot \left(T_{hot} - T_{cold} \right) \tag{3-2}$$

For the purpose of this project, convective heat transfer is split into two separate sections namely external and internal convection. External convection takes place due to a temperature difference and interaction between the flue gas and the external tube surface and can be modelled as a cross-flow type heat exchanger. Internal convection takes place due to a temperature difference and interaction between internal tube surface and steam and can be modelled as heat transfer to fluid flowing inside a tube. The flow orientation of a typical heat exchanger is illustrated in Figure 3-5 below with blue arrows indicating internal steam flow and red arrows indicating external flue gas flow:

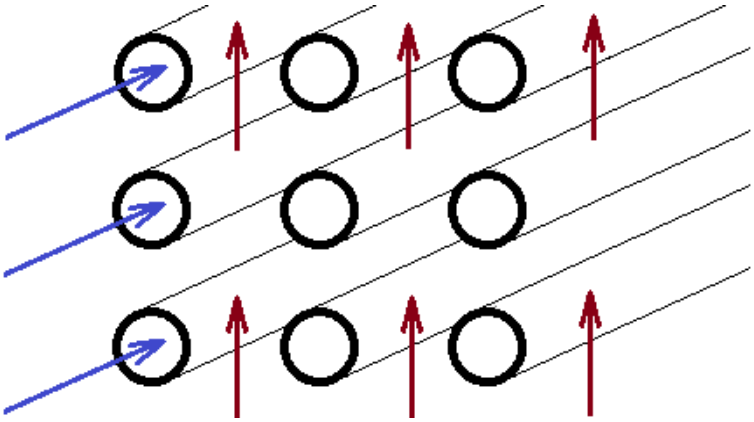

Figure 3-5: Diagram showing fluid flow and orientation of typical heat exchangers in boilers.

The defining property when calculating convective heat transfer is the convection heat transfer coefficient [$\boldsymbol{h_{convection}}$]. It is a function of the Nusselt number [$\boldsymbol{Nu}$], the thermal conductivity of the fluid [$\boldsymbol{k_{fluid}}$] and the hydraulic diameter [$\boldsymbol{D_H}$]. It can be calculated using the following correlation:

$$h_{conv} = \frac{Nu \cdot k_{fluid}}{D_H} \tag{3-3}$$

The Nusselt number is the only variable in the above correlation that is not a fluid or geometrical property and cannot be calculated in a single step. It is thus important to establish from literature which correlations will yield accurate results for the specific application in which it will be used. The following sections looks mainly at Nusselt number correlations that were developed specifically for the applications at hand. Some geometrical properties that are outside of the norm will also be discussed. In order to calculate the Nusselt number, other key dimensionless numbers need to be calculated first.

The Reynolds number is a dimensionless number that describes the type of flow experienced by a fluid. This ranges from an orderly type of flow, which is known as laminar flow, to the more chaotic type of flow known as turbulent flow as described in [10]. It is an important variable as a strong correlation exists between the Reynolds number of a fluid, and heat transfer to or from this fluid. This is clearly evident as the Reynolds number is typically used in most of the Nusselt number correlations. It is typically defined by the following correlation:

$$Re = \frac{\rho V_x D_H}{\mu} \tag{3-4}$$

For general heat exchangers, it is calculated using the hydraulic diameter, which is a function of surface area [***A***] and wetted perimeter [***P***]. This essentially is the total heat transfer surface area and the flow area for any given shape and is defined by:

$$D_H = 4\frac{A}{P} \tag{3-5}$$

The Prandtl number is another important dimensionless number which gives some indication of what heat transfer mechanism will be dominant in any specific fluid. It is determined as a ratio of the product of viscosity and specific heat to thermal conductivity of a fluid and is represented as follows:

$$Pr = \frac{\mu \cdot c_p}{k} \tag{3-6}$$

3.2.1 External forced convection

In calculating the external heat transfer coefficient, the geometrical set-up for a cross-flow heat exchanger is not as straight forward because the surfaces are not uniform and adding a third dimension is required to accommodate the layout. The hydraulic diameter is thus defined in [11] by the fluid flow length [$\boldsymbol{L_{flow}}$] which is the distance from the leading tube to the last tube as indicated

in Figure 3-6, the total free flow area of the flue gas [A_{fg}] which is a product of A as indicated in Figure 3-6 and the length of the tubes, and the total external tube surface area [A_{TS_Ex}]:

$$D_H = \frac{4 \cdot L_{flow} \cdot A_{FG}}{A_{TS\_Ex}} \tag{3-7}$$

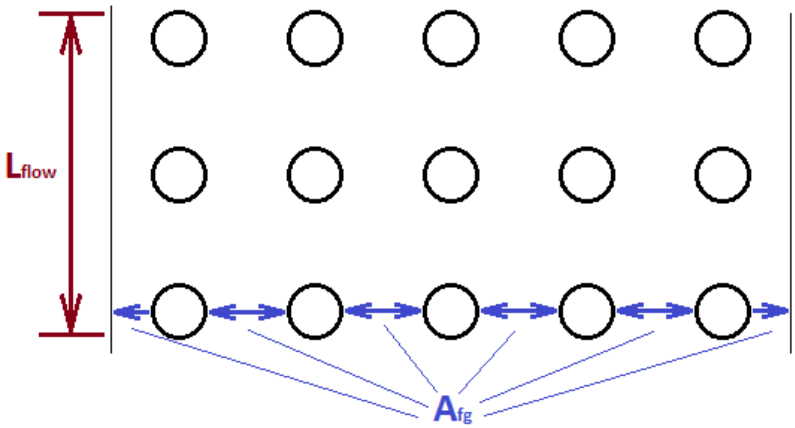

Figure 3-6: Illustration of hydraulic diameter parameters.

Nusselt number correlations:

The first three correlations are developed for single tubes in cross-flow. Not specifically for bundles of tubes.

- **Hilpert Correlation** [12]

$$Nu_s = c \cdot Re^n \cdot Pr^{0.33} \tag{3-8}$$

Table 3-2: Hilpert Nusselt number correlation variables defined.

Reynolds Number	*C*	*n*
0.4 – 4	0.989	0.33
4 – 40	0.911	0.385
40 – 4000	0.683	0.466
4000 – 40 000	0.193	0.618
40 000 – 400 000	0.027	0.805

- **Churchill & Bernstein** [13]

All properties are evaluated at film temperature and for Pr > 0.2.

For Re > 400 000:

$$Nu = 0.3 + \frac{0.62 \cdot Re^{1/2} \cdot Pr^{1/3}}{\left[1 + \left(\frac{0.4}{Pr}\right)^{2/3}\right]^{1/4}} \cdot \left[1 + \left(\frac{Re}{282000}\right)^{5/8}\right]^{4/5} \quad (3\text{-}9)$$

For 10 000 < Re < 400 000:

$$Nu = 0.3 + \frac{0.62 \cdot Re^{1/2} \cdot Pr^{1/3}}{\left[1 + \left(\frac{0.4}{Pr}\right)^{2/3}\right]^{1/4}} \cdot \left[1 + \left(\frac{Re}{282000}\right)^{1/2}\right] \quad (3\text{-}10)$$

For Re < 10 000:

$$Nu = 0.3 + \frac{0.62 \cdot Re^{1/2} \cdot Pr^{1/3}}{\left[1 + \left(\frac{0.4}{Pr}\right)^{2/3}\right]^{1/4}} \quad (3\text{-}11)$$

- **Zukauskus Correlation** [12]

$$Nu = c \cdot Re^{m} \cdot Pr^{n} \cdot \left(\frac{Pr}{Pr_s}\right)^{1/4} \quad (3\text{-}12)$$

Table 3-3: Zukauskus Nusselt number correlation variables defined.

Reynolds Number	***c***	***m***
1 – 40	0.75	0.4
40 - 1000	0.51	0.5
1000 – $2x10^5$	0.26	0.6
$2x10^5$ – 10^6	0.076	0.7
Prandtl Number	**n**	
$Pr \leq 10$	0.37	
$Pr \geq 10$	0.36	

The subscript ***s*** indicates that the specific property is evaluated at the surface temperature, not the free stream temperature as the other properties, which makes this correlation troublesome to use. This correlation is valid for Pr > 0.2.

- **Gnielinski Correlation** [14]

In order to obtain correlations for bundles of tubes in cross-flow, one needs to first look at the correlations for a single tube in cross-flow:

$$Nu_{single} = 0.3 + \left(Nu^2_{laminar} + Nu^2_{turbulent} \right)^{1/2} \tag{3-13}$$

$$Nu_{laminar} = 0.664 \cdot Re^{1/2} \cdot Pr^{1/3} \tag{3-14}$$

$$Nu_{turbulent} = \frac{0.037 \cdot Re^{0.8} \cdot Pr}{1 + 2.443 \cdot Re^{-0.1} \cdot \left(Pr^{2/3} - 1 \right)} \tag{3-15}$$

The Nusselt number for a bank of in-line tubes is then calculated, as discussed in [15]:

$$Nu_{bundle} = f_b Nu_{single} \tag{3-16}$$

The same correlations are used, as mentioned above, for a single tube in cross-flow with some additions. The geometrical layout of the heater bank is an important factor and both the transverse and stream-wise pitch of the tubes needs to be known to calculate the void fraction and the bundle-factor. Tube pitches are illustrated in Figure 3-7.

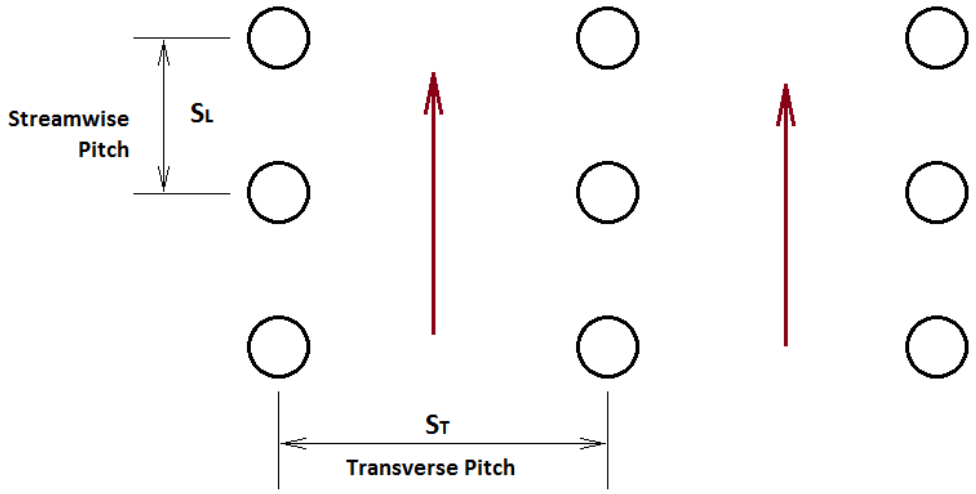

Figure 3-7: Figure illustrating in-line tubes pitches.

Geometrical variables are defined:

$$a = \frac{s_1}{d_0} \tag{3-17}$$

$$b = \frac{s_2}{d_0} \tag{3-18}$$

The void fraction can then be calculated by:

$$\varphi = 1 - \frac{\pi}{4a} \quad \text{for} \quad b \geq 1 \tag{3-19}$$

$$\varphi = 1 - \frac{\pi}{4ab} \quad \text{for} \quad b < 1 \tag{3-20}$$

The bundle-factor for in-line tubes is given by:

$$f_b = 1 + \frac{0.7\left(b/a - 0.3\right)}{\varphi^{1.5}\left(b/a + 0.7\right)^2} \tag{3-21}$$

** The bundle factor for staggered tubes is not discussed as it is not commonly found in coal-fired boilers.*

3.2.2 Internal forced convection

All equations below are for fully developed turbulent flows. The flow rate required for laminar flow inside any of the boiler tubes would typically be out of range for any operating conditions considered in this project.

- **Ditus-Boelter Equation** [12]

$$Nu_s = 0.023 \cdot Re^{0.8} \cdot Pr^n \tag{3-22}$$

Table 3-4: Variable description for Dittus-Boelter equation.

	n
Cooling fluid	0.3
Heating fluid	0.4

- **Gnielinski Equation** [16]

$$Nu = \frac{\left(f/8\right)\cdot \mathrm{Re}\cdot Pr}{1+12.7\cdot\left(f/8\right)^{1/2}\cdot\left(Pr^{2/3}-1\right)}\cdot\left[1+\left(d_i/l\right)^{2/3}\right] \tag{3-23}$$

With associated friction factor:

$$f = \left(1.8\cdot log_{10}\left(Re\right)-1.5\right)^{-2} \tag{3-24}$$

Another form of friction factor that is representative for a large range of Reynolds numbers was developed by Petukhov: [12]

$$f = \left(0.79\cdot ln\left(Re\right)-1.64\right)^{-2} \tag{3-25}$$

- **Sieder-Tate Equation** [12]

$$Nu = 0.027\cdot Re^{4/5}\cdot Pr^{1/3}\cdot\left(\frac{\mu}{\mu_s}\right)^{0.14} \tag{3-26}$$

The subscript ***s*** indicates that the property is evaluated at the boundary surface temperature and not the free stream temperature as for the other properties.

Table 3-5: Summary of applicable ranges for internal pipe flow correlations. [17]

Correlation	**Range – Reynolds**	**Range - Prandtl**	**Other limitations**	**Accuracy**
Ditus-Boelter	Rey > 10^4	0.7 ≤ Pr ≤ 160	L/D > 10	25%
Gnielinski	3000 ≤ Re ≤ 5x10^6	0.5 ≤ Pr ≤ 2000	None	10%
Sieder-Tate	Re ≥ 10 000	0.7 ≤ Pr ≤ 16700	none	25%

3.2.3 Summary

The external fluid Nusselt number was calculated using the Hilpert correlation. This was as a result of the external heat transfer coefficient calculation method within the modelling software Flownex. The software utilised a method where the layout of the Nusselt number correlation was important as it was used to calculate the Colburn factor. This process is later described in more detail.

The internal fluid Nusselt number correlation was also dictated by the modelling software calculation methods. The modelling software utilises the Ditus-Boelter correlation without an option to change any of the variables as is sometimes done.

3.3 Radiation

Radiation is the transfer of energy from one body or volume to another across a boundary due to a differential temperature and is facilitated by photon emission. All material surfaces and substances with a temperature above absolute zero emit and absorb radiation energy and no media is required for heat transfer to take place.

The black body in radiation terms is used as a baseline for all calculations and is the only body that has direct correlations known for heat transfer due to radiation. The property given to a black body is that all radiation emitted towards it will be absorbed without any transmission or reflection. No other body at similar temperature will emit or absorb more radiation. A black body is an idealistic substance and does not exist in reality.

Emissive power is defined as the gross energy emitted from an ideal surface per unit area time. This is known as the Stefan-Boltzman Law. The radiation heat flux between two black bodies is the difference between the emissive power of the two surfaces.

$$E = \sigma \cdot T_{abs}^{\ 4} \tag{3-27}$$

$$q'' = E_1 - E_2 = \sigma T_1^{\ 4} - \sigma T_2^{\ 4} \tag{3-28}$$

Any real or grey body does not emit the same power as a black body and will emit only a certain percentage of what a black body does at the same temperature. This phenomenon is defined as emissivity. Emissivity is entirely dependent on the properties and temperature of the surface of the body.

$$\varepsilon_r = \frac{Real\ radiative\ heat\ transfer}{Black\ body\ radiative\ heat\ transfer} \tag{3-29}$$

The general equation for radiation heat transfer between two grey bodies in full view of each other can thus be defined as:

$$Q_{12} = \sigma \varepsilon_r A(T_1^{\ 4} - T_2^{\ 4}) \tag{3-30}$$

Radiation in coal-fired boilers contributes a large percentage of total heat transfer due to the extremely high temperatures produced by the combustion process. It is, however, split into two separate sections for the purpose of modelling different sections of the boiler, namely the furnace and convective pass.

3.3.1 Radiation in the furnace

The furnace is defined as the portion of the boiler where the combustion process occurs. The radiation heat transfer referred to in this section is between the flame or gas in the furnace and the boiler evaporator or water-wall tubes.

View Factor [F_{12}]

The view factor is a percentage that takes into account how much of the specific surface is exposed to the radiating surface. The shape of both the radiating bodies is taken into account when calculating the view factor.

$$F_{12} = \frac{1}{\pi A_1} \int_0^{A_1} \int_0^{A_2} \frac{\cos\beta_1 \cos\beta_2}{s^2} dA_1 dA_2 \tag{3-31}$$

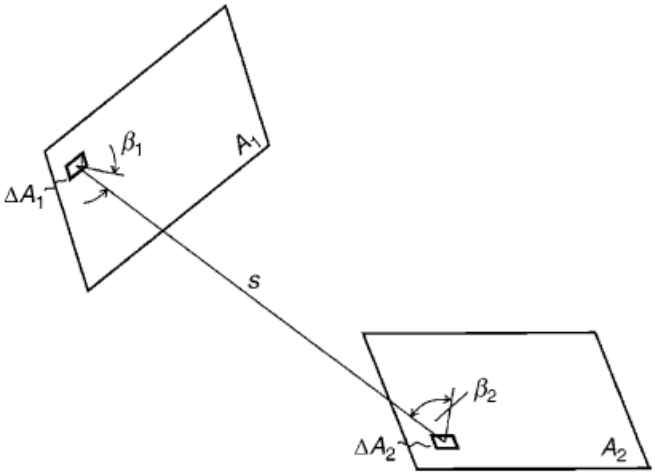

Figure 3-8: Two arbitrary surfaces radiating heat towards each other. [18]

The net energy exchange between two grey bodies with equal emissivity and the view factor included is given by the following equation:

$$Q_{12} = \varepsilon_r F_{12} A_1 \sigma T_1^4 - \varepsilon_r F_{21} A_2 \sigma T_2^4 \tag{3-32}$$

When thermal equilibrium is reached ($T_1 = T_2$), and the net energy transfer must be equal to zero, we have:

$$F_{21} = \frac{A_1}{A_2} F_{12} \tag{3-33}$$

Including the view factor, equation (3-30) can thus be rewritten as:

$$Q_{12} = \varepsilon_r \sigma A_1 F_{12} \left(T_1^4 - T_2^4 \right) \tag{3-34}$$

3.3.2 Radiation in the convective pass

Radiation needs to be taken into account not only in the furnace, but also in the convective pass where heat transfer takes place between the flue gas and the tubes. Most gases at a temperature above absolute zero emit radiation. The various constituents of the flue gas however, have different contributions to the total radiative heat transfer. Some gases such as oxygen and nitrogen are transparent to radiation, meaning they do not contribute to the heat total transfer. Other gasses such as nitrogen oxide and sulphides (NO_x's & SO_x's) do contribute to heat transfer but it is present in such small quantities that these have been ignored through the calculations of this project. The two gasses that were analysed in the flue gas are water vapour [$\boldsymbol{H_2O}$] and carbon dioxide [$\boldsymbol{CO_2}$]. Ash particles also have a significant impact on radiative heat transfer and its presence in the flue gas will be discussed later.

For simplicity, the radiation heat transfer was calculated differently in the convective pass than in the furnace. The contribution of radiation was accounted for by calculating a radiation heat transfer coefficient similar to that of convection, which was added to the convective heat transfer coefficient to form the total heat transfer coefficient for the external fluid:

$$h_{total} = h_{conv} + h_{rad} \tag{3-35}$$

The first step in this process was to define a control volume around the tube which accurately represents the area filled with gas and ash which contributes to the radiation heat transfer to that specific tube.

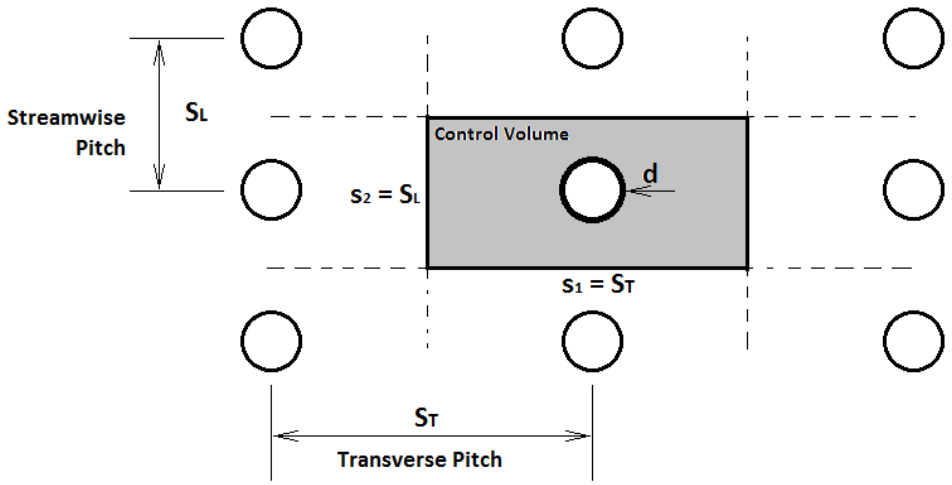

Figure 3-9: Control volume for radiation heat transfer coefficient calculation. Edited from: [19]

Radiation from gasses only

Taler and Taler developed the following simplified approach to calculate the radiation heat transfer coefficient in the convective pass of boilers. [19]

The radiation heat transfer coefficient is given by:

$$h_{rad} = \frac{\sigma_{SB}\varepsilon_{eq} as}{as + \varepsilon_{eq}} \frac{\left(\bar{T}_g^{\,4} - T_w^{\,4}\right)}{\left(\bar{T}_g - T_w\right)} \tag{3-36}$$

Where the equivalent emissivity is defined by some combination of the tube wall emissivity [ε_w]:

$$\varepsilon_{eq} = \frac{2\varepsilon_w}{2 - \varepsilon_w} \tag{3-37}$$

The mean beam length in plain tube bundles is calculated from the control volume geometry and is given by:

$$s = c\frac{d}{4}\left(\frac{4}{\pi}\frac{s_1 s_2}{d^2} - 1\right) \tag{3-38}$$

The absorption coefficient of the gas can be calculated with the basic composition of the flue gas known:

$$a = \left(0.78 + 1.6 r_{H_2O} - 0.1\sqrt{p_{sum} s}\right) \times \left(1 - 0.37\frac{T_g}{1000}\right)\sqrt{p_{sum} s} \tag{3-39}$$

Other literature recommends the following correlation for radiative heat transfer and is suggested in [20]:

$$q_{r,g} = \frac{\varepsilon_w + 1}{2} \cdot \varepsilon_g \cdot \sigma \cdot A_g \cdot \left(T_g^4 - T_w^4 \right) \tag{3-40}$$

Hausen [21] states that the arithmetic mean temperature between inlet and outlet of the heat exchanger bank is not sufficient, as the temperature is utilised to the power of four. He recommends that the average of the following temperatures be used in radiation calculations:

$$T_{g,20} = T_{g,i} - 0.2 \cdot \left(T_{g,i} - T_{g,o} \right) \tag{3-41}$$

$$T_{g,80} = T_{g,i} - 0.8 \cdot \left(T_{g,i} - T_{g,o} \right) \tag{3-42}$$

A significant limitation on this method is the exclusion of the contribution that ash particles entrained in the flue gas stream have on the total radiation.

Radiation from gas-particle mixtures

Brummel and Vortmeyer suggest that the main contribution of radiation heat transfer is as a result of particles in the flue gas at similar temperature as the gas itself. [18] [22]

The correlation presented is the following:

$$h_{rad} = \frac{\varepsilon_w \sigma}{\left(\alpha_{gp} + \varepsilon_w - \alpha_{gp} \varepsilon_w \right)} \cdot \frac{\varepsilon_{gp} T_g^4 - \alpha_{gp} T_w^4}{T_g - T_w} \tag{3-43}$$

With:

$$\alpha_{gp} = \alpha_g + \varepsilon_p - \alpha_g \varepsilon_p \tag{3-44}$$

$$\varepsilon_{gp} = \varepsilon_g + \varepsilon_p - \varepsilon_g \varepsilon_p \tag{3-45}$$

$$\varepsilon_g = \varepsilon_{H_2O} + \varepsilon_{CO_2} - \Delta\varepsilon_g \tag{3-46}$$

$$\alpha_g = \alpha_{H_2O} + \alpha_{CO_2} - \Delta\alpha_g \tag{3-47}$$

For pressure p = 1 bar:

$$\alpha_{H_2O} = \varepsilon_{H_2O} \left(\frac{T_g}{T_w} \right)^{0.45} \tag{3-48}$$

$$\alpha_{CO_2} = \varepsilon_{CO_2} \left(\frac{T_g}{T_w} \right)^{0.65} \tag{3-49}$$

The emissivity for various gasses in the flue gas stream was calculated from a graph given by Vortmeyer. The graph requires three variables to be known in order to predict the emissivity which are: the mean beam length [s_{mb}], the partial pressure of gas [p_x] and the temperature of gas [T]. For more detail and additional gas constituents, see Appendix C.

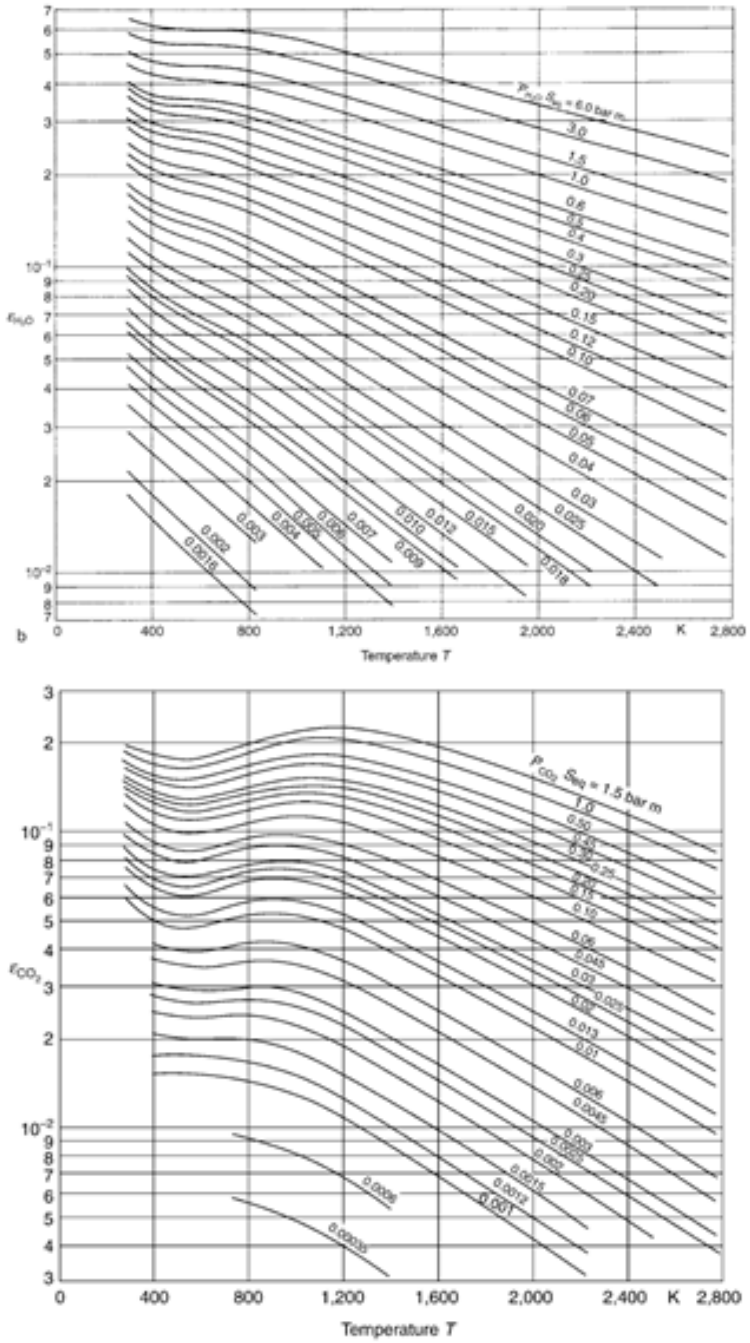

Figure 3-10 (a) & (b): Graphs for calculating emissivity of CO_2 and H_2O. [18]

Particle emissivity calculation [ε_p]:

The method developed by Brummel [22] for calculating the particle emissivity of the ash is briefly illustrated below. A substantial amount of ash properties are required to be known in order to calculate the emissivity which are: the particle substance constant [$\boldsymbol{k}$ in $m^{-1/3}$], the effective absorption projection area [$\boldsymbol{Q_{abs}A}$ in m^2/kg], the material density [$\boldsymbol{\rho}$ in kg/m^3], the particle load [$\boldsymbol{L_p}$ in kg/m^3] and the mean beam length [$\boldsymbol{l_{mb}}$ in m].

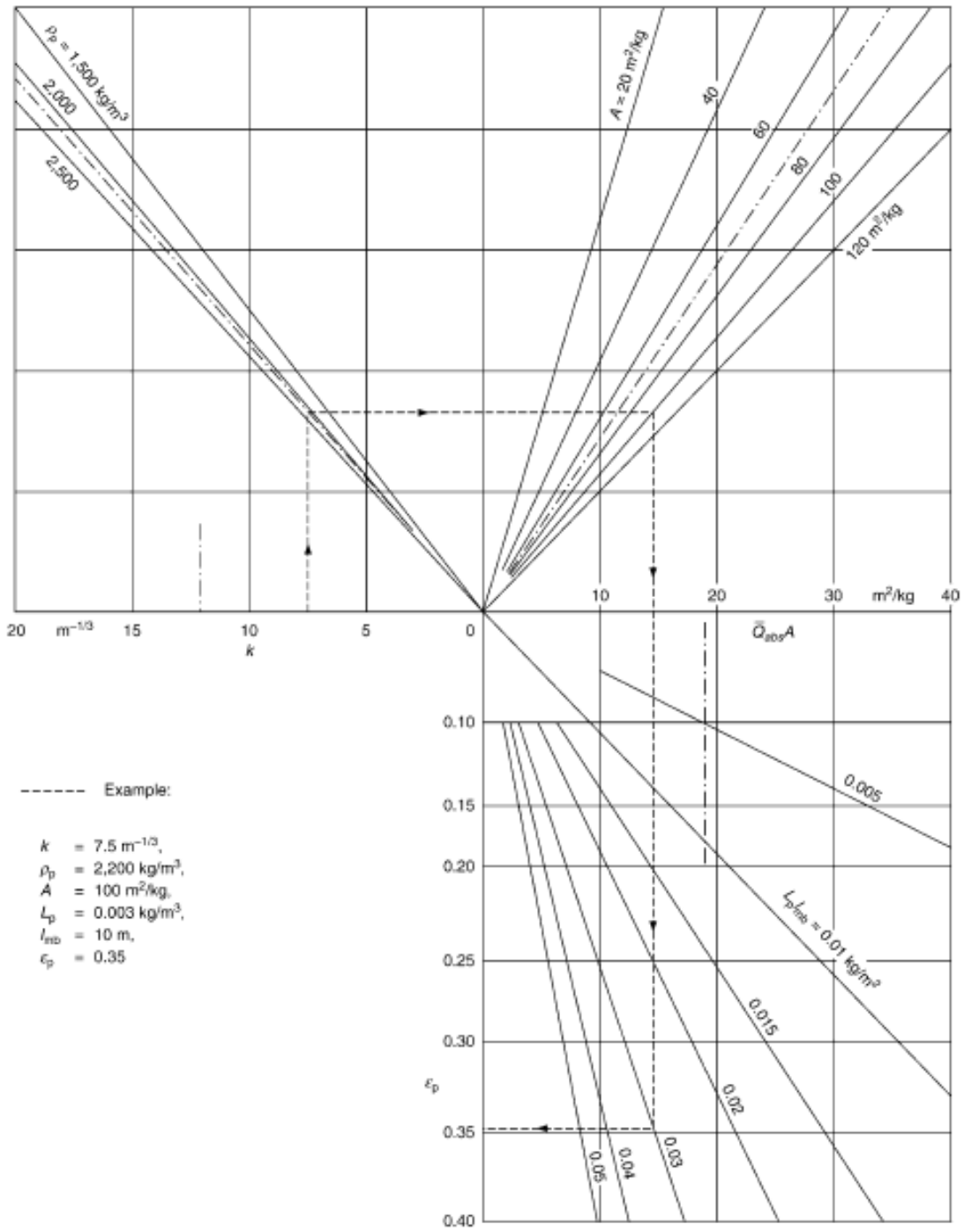

Figure 3-11: Nomogram for determining ash particle emissivity. [22]

This depth of investigation into ash particle emissivity calculation will not form part of the project and thus this method falls outside the scope of this project. An assumed ash emissivity value will be used throughout the project.

Radiation between "flame" and first row of tubes in the lowest superheater:

The contribution of radiative heat transfer between the heat source and the first rows of visible tubes can be calculated similarly to that of radiation in the furnace. It incorporates parameters such as a three-dimensional view factor, beam length and actual gas temperatures. This is excluded from this project as it will require a row-by-row model of the superheater. This could be considered for incorporation in future radiation research work.

3.3.3 Conclusion

The correlations as described by Brummel in [22] and Vortmeyer in [18] will be used to calculate radiative heat transfer from the gas and ash-particles respectively in the convective zone. Some of the detail, however, will be excluded in order to simplify the calculation process to adhere to specific objectives of this project. The flue gas composition will not be analysed accurately as it falls outside the scope of this project and thus a simple gas composition will be used to calculate radiative heat transfer.

It is suggested that the method developed for gas-particle mixtures could perhaps over-estimate the radiation heat transfer coefficient as a result of scattering which is not included in the model. Additional research could be done in the radiative heat transfer in the convective pass to determine whether the inaccuracies resulting from not including scattering into the model is significant enough to motivate a revision and update of this model.

3.4 Heat exchanger calculation methods

3.4.1 Log Mean Temperature Difference (LMTD) Method

The LMTD method is most often used to calculate heat transfer when the inlet and outlet temperatures of both streams in a heat exchanger are known. This method is commonly used in heat exchanger design when physical properties such as size, arrangement and material that will be required to deliver specific performance characteristics for the given flow conditions and temperatures need to be determined. The subscript *x* can either refer to internal or external reference point which calculations are based on. The heat transfer correlation for the common concentric tube heat exchanger is given by:

$$Q = U_x A_x \Delta T_{LMTD} \tag{3-50}$$

The overall heat transfer coefficient is a function of the total effective resistance and is given by:

$$U_x = \frac{1}{R_{total,x}} \tag{3-51}$$

The total resistance corresponding with the either the external or the internal surface area is given by:

$$R_{total,o} = \left[\frac{r_o}{k} \cdot ln\frac{r_o}{r_i} + \frac{1}{h_{fg}} + \frac{r_o}{h_{st} \cdot r_i} \right] \tag{3-52}$$

$$R_{total,i} = \left[\frac{r_i}{k} \cdot ln\frac{r_o}{r_i} + \frac{r_i}{h_{fg} \cdot r_o} + \frac{1}{h_{st}} \right] \tag{3-53}$$

The temperature difference is a function of the flow orientation of the heat exchanger and is given by:

$$\Delta T_{LMTD} = \frac{\Delta T_2 - \Delta T_1}{ln\left(\Delta T_2 / \Delta T_1 \right)} \tag{3-54}$$

The two common types of flow orientations are the parallel flow and counter flow orientations. Basic layouts are indicated in Figure 3-12 and Figure 3-13 and the temperature differences are subsequently explained.

Parallel flow layout:

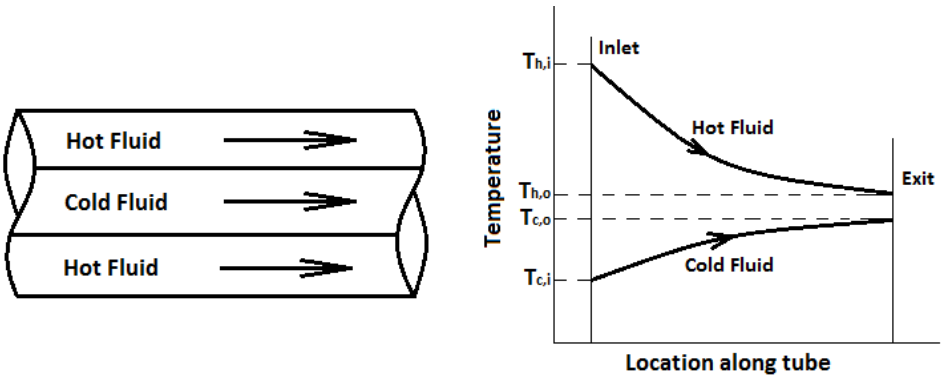

Figure 3-12: Parallel flow orientation with subsequent temperature differences.

$$\Delta T_1 = T_{hi} - T_{ci} \tag{3-55}$$

$$\Delta T_2 = T_{ho} - T_{co} \tag{3-56}$$

Counter-flow layout:

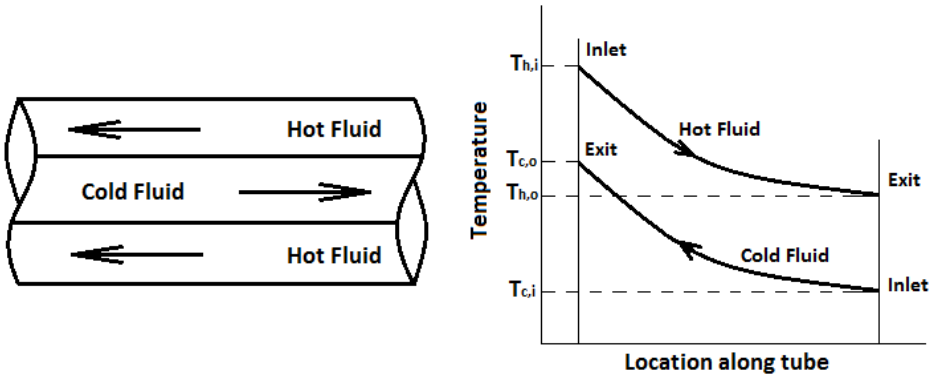

Figure 3-13: Counter flow orientation with subsequent temperature differences.

$$\Delta T_1 = T_{hi} - T_{co} \tag{3-57}$$

$$\Delta T_2 = T_{ho} - T_{ci} \tag{3-58}$$

An important fact to note is that with a parallel flow heat exchanger it is not possible for the cold stream outlet temperature to be heated above that of the hot fluid outlet temperature. It is however possible to accomplish that with a counter-flow layout.

Multi-pass and Cross-flow heat exchangers:

In order to solve for multi-pass and cross-flow heat exchangers using the LMTD method, a correction factor F is utilised to calculate an adjusted log mean temperature difference as follows:

$$\Delta T_{LM\_F} = F \cdot \Delta T_{LMTD,CF} \tag{3-59}$$

The differential temperature to be adjusted is assumed to be that of a counter-flow heat exchanger which is represented by Equations (3-54), (3-57) and (3-58).

The log mean temperature difference equation for multi-pass or cross-flow heat exchangers thus becomes:

$$Q = U \cdot A \cdot \Delta T_{LM\_F} \tag{3-60}$$

The correction factor ***F*** is determined from graphs that were developed for specific layouts of heat exchangers. The two most applicable types of layouts expected in a typical coal-fired boiler are the single-pass cross-flow heat exchanger with both fluids unmixed and a similar layout with a single fluid mixed and the other unmixed. The graphs for both layouts are illustrated in Figure 3-14 and Figure 3-15.

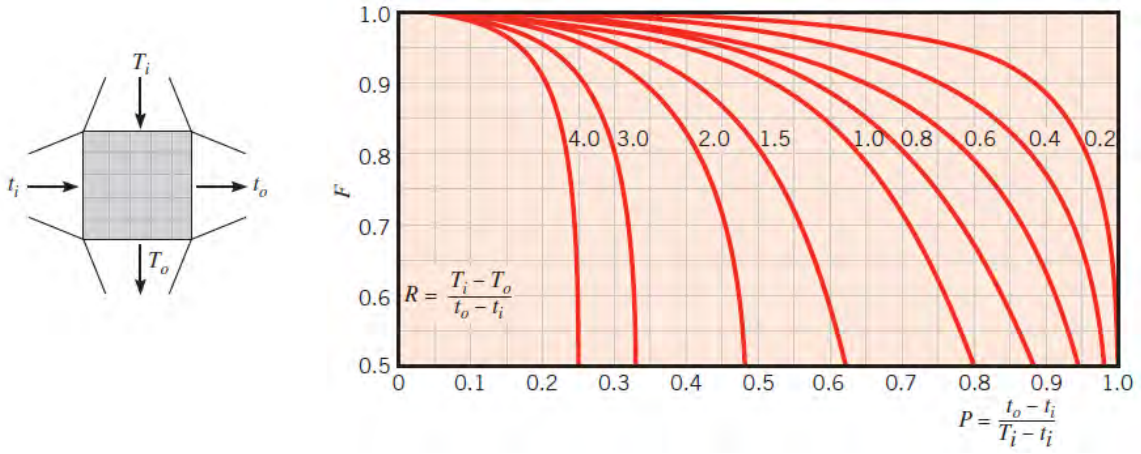

Figure 3-14: Correction factor for single-pass cross-flow heat exchanger with both fluids unmixed. [23]

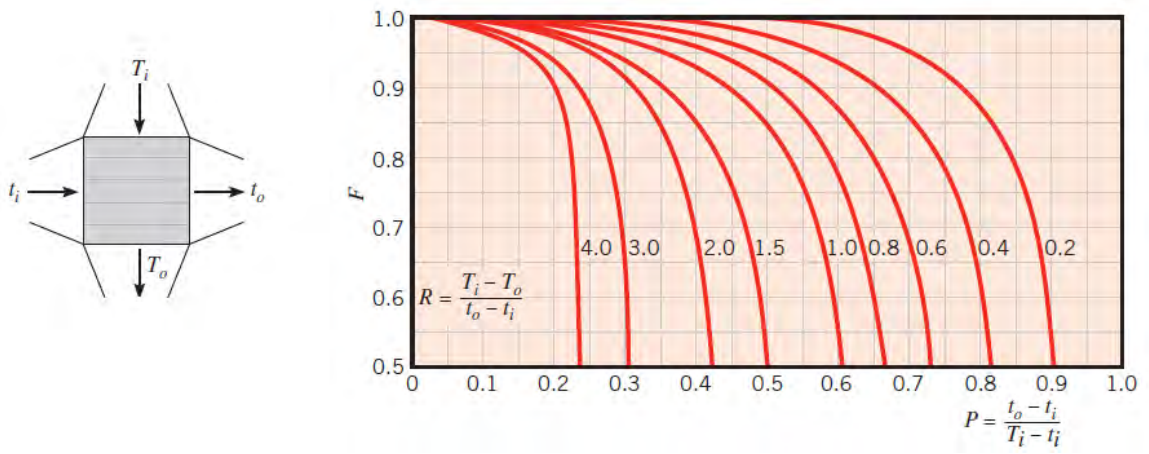

Figure 3-15: Correction factor for single-pass cross-flow heat exchanger with a single fluid mixed and the other fluid unmixed. [23]

3.4.2 ε-NTU Method

The effectiveness-number of transfer units (ε-NTU) method is most commonly used to calculate outlet temperatures of a heat exchanger for which the physical properties are known. Some of the parameters which must be known include common geometrical properties such as size and arrangement and fluid properties such as inlet temperatures and mass flows of both streams. The method uses the philosophy that specific size and flow orientation heat exchangers typically transfer a specific percentage of the maximum possible heat available, also known as the effectiveness, and is defined by the following correlation:

$$Q = \varepsilon \cdot Q_{max} \tag{3-61}$$

The maximum possible heat transfer is determined by manipulating the correlation for heat transfer for a single fluid stream and is given by the following equation:

$$Q_{max} = C_{min}\left(T_{hi} - T_{ci}\right) \tag{3-62}$$

The fluid with lower heat transfer capacity will be the limiting fluid in terms of heat transfer and is thus the one that will be used for any calculations. The minimum heat transfer capacity is defined as:

$$C_{min} = minimum\ of \begin{vmatrix} C_h = \dot{m}_h . c_{ph} \\ C_c = \dot{m}_c . c_{pc} \end{vmatrix} \tag{3-63}$$

The highest possible temperature change in any fluid would be represented by the difference between the hot fluid inlet and cold fluid inlet temperatures.

The effectiveness is defined as the ratio of the actual heat transferred by a specific heat exchanger to the maximum possible heat transfer for the given set of operating conditions.

$$\varepsilon = \frac{Q}{Q_{max}} \tag{3-64}$$

The heat transfer correlation for a typical heat exchanger in a coal-fired power station is thus given by:

$$Q = \varepsilon C_{min}\left(T_{fgi} - T_{sti}\right) \tag{3-65}$$

Effectiveness correlations of various flow layouts

The following are correlations for calculating the effectiveness of various layouts and flow arrangement of heat exchangers given by [24]. In typical coal-fired boiler heat exchangers, the steam is accepted to be an un-mixed fluid, while the flue gas is assumed to be a completely mixed fluid. Additionally, the number of transfer units and heat transfer capacity ratio is defined as:

$$NTU = \frac{UA}{C_{min}} \tag{3-66}$$

$$C_r = \frac{C_{min}}{C_{max}} \tag{3-67}$$

- All heat exchangers with:
  - $C_r = 0$
  - A typical heat exchanger that would be represented by this heat transfer capacity ratio is a single tube, or single row of tubes, in cross flow with an insignificant change in temperature of the external flow around the tube.

$$\varepsilon = 1 - exp\left(-NTU\right) \tag{3-68}$$

- Single pass cross-flow heat exchanger with:
  - C_{max} – mixed and C_{min} – unmixed
  - This scenario is not typically encountered in coal-fired boiler heat exchangers as fluids do not match specified heat transfer capacity rates. This is illustrated in the graph in Figure 4-10.

$$\varepsilon = \left(\frac{1}{C_r}\right)\left(1 - exp\left(-C_r\left(1 - exp\left(-NTU\right)\right)\right)\right) \tag{3-69}$$

- C_{min} – mixed and C_{max} – unmixed
- This is the typical scenario encountered in coal-fired boiler heat exchangers. The flue gas represents the minimum heat transfer capacity fluid, and is mixed. The steam represents the maximum heat transfer capacity rate and is accepted as unmixed. This is illustrated in the graph in Figure 4-10.

$$\varepsilon = 1 - exp\left(-C_r^{-1}\left(1 - exp\left(-C_r\left(NTU\right)\right)\right)\right) \tag{3-70}$$

- C_{min} – unmixed and C_{max} – unmixed
- This scenario could be encountered in finned tube heat exchangers where the fins prohibit the external fluid from mixing.

$$\varepsilon = 1 - exp\left(\left(\frac{1}{C_r}\right)\left(NTU\right)^{0.22} \cdot \left(exp\left(-C_r\left(NTU\right)^{0.78}\right) - 1\right)\right) \tag{3-71}$$

3.4.3 Dimbo – Dimensioning of Boilers

DimBo is an existing software tool developed by coal-fired boiler designers. It is a steady-state mass and energy balance tool capable of simulating the outputs of typical boiler heat exchangers. It uses geometrical properties of heat exchangers to integrate a collection of heat exchangers into a complete boiler. The geometrical properties represent all the important physical aspects of a heat exchanger, which include the heat transfer surface area, which is a key property in heat transfer calculations. Process properties include all the required fluid inlet conditions of both fluid streams.

Due to the large variety of boiler designs used in the industry with many individual geometrical and process properties, individual models need to be developed for different boiler designs. Process property inputs are required for both fluid streams and it could be defined at various locations. For example, the flue gas stream can be defined either by the coal and air mass flows along with CV to calculate flame temperature, or alternatively, the FET can be directly defined depending on the requirement of analysis. Another input is an effectiveness factor which is included in the modelling methodology to account for aging of boiler with associated fouling or slagging. Once all inputs are completed the software model solves iteratively to calculate inlet and outlet temperatures of all the heat exchangers in the boiler.

An important parameter in the set-up and solving process to DimBo is the effectiveness factor. This factor needs to be manually adjusted until the appropriate temperature profiles for both fluids are achieved. This is a systematic process in which heat exchanger effectiveness factors are adjusted sequentially. An example of the software model set-up is shown in Figure 3-16.

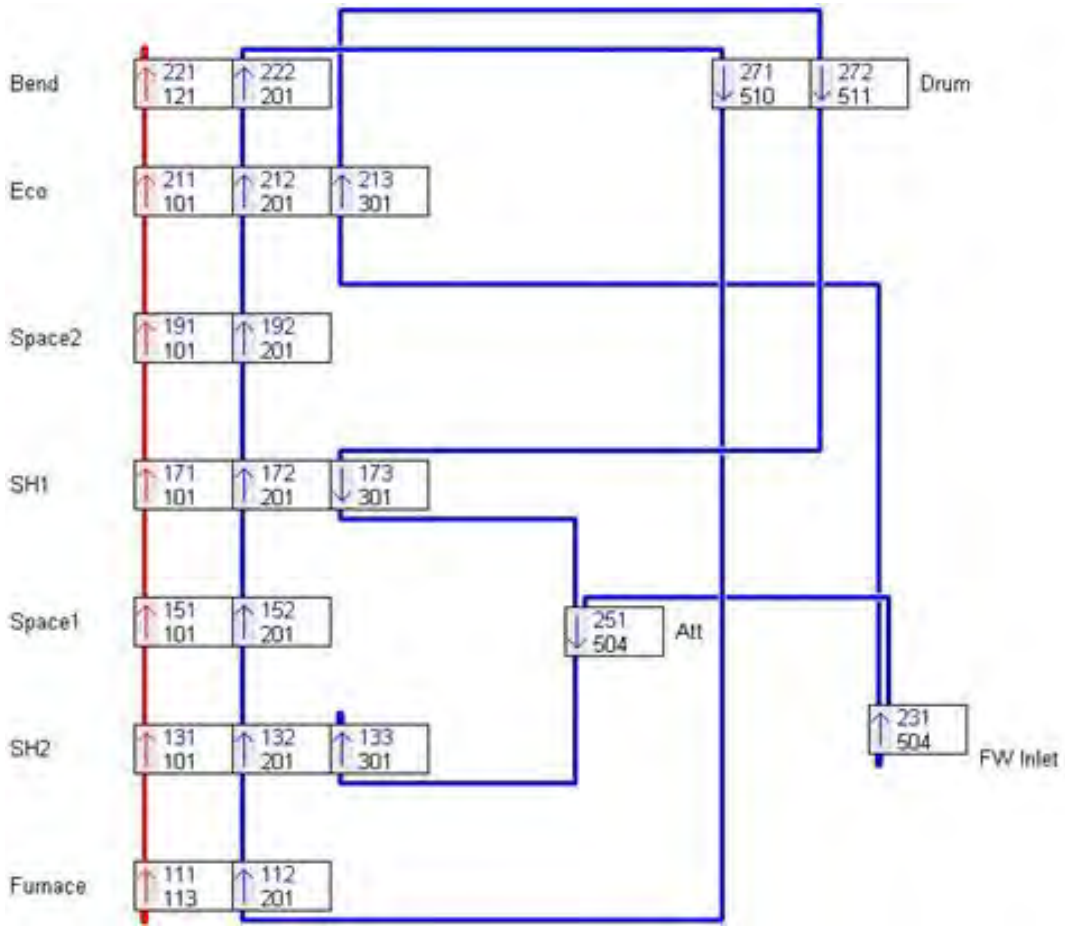

Figure 3-16: Basic drum-type boiler set up in DimBo. [17]

The integral correlations used by DimBo to calculate heat transfer and thus simulate heat exchanger performance, is intellectual property of the developers and thus unknown. Govindsamy [17] attempted to evaluate results from the software against known correlations, solving techniques and actual plant design data and it proved to be quite successful.

DimBo is often used in the industry to do performance analyses of heat exchangers. A major draw-back of the DimBo model however, is that it solves for steady-state conditions and thus key transient characteristics are omitted.

4. Modelling methodology

4.1 Evaporator

The evaporator model developed in this project might not be used in the final power station simulation model being developed by the Energy Efficiency Centre as it uses numerous assumptions and is an approximation of heat transfer to simulate the evaporator and give acceptable results. Other projects are specifically focussing research into the radiative heat transfer in the coal-fired boiler furnaces and will calculate the heat transfer accurately. It is, however, essential that some form of a model is developed in order to simulate a complete boiler as it is used to calculate the steam inlet conditions to the superheater. The model will only be used on once-through boilers as the inlet conditions to the superheater for drum-type boilers are known to be at saturation from the drum, thus making the evaporator wall heat transfer analysis redundant. The calculation process for this section of the boiler is explained below.

4.1.1 Assumptions

Multiple tubes

The model assumed that all evaporator tubes are exposed to identical conditions such as an even distribution of temperature across a section of furnace, internal fluid inlet temperature and flow rate. The heat transfer contribution is thus evenly spread across to the total number of tubes. The model was developed to calculate heat transfer to a single tube and results were extrapolated to the complete assembly of tubes.

In order to simplify the geometrical inputs required, all heat transfer was assumed to take place in the helical section of the boiler. Heat transfer to tubes below and above that was ignored.

Heat sources

The firing system of the boiler was assumed to create multiple point heat sources that are at specific locations inside and at the centre of the furnace corresponding to each mill that is in operation. This was done to ensure that the firing effect of various mill combinations can be adequately accounted for. This position of the different heat sources are illustrated in Figure 4-1.

View factor

It was assumed that all increments of the tube were directly opposing each heat source. This simplified the view factor equation to a one-dimensional problem consisting of a single angle, instead of a three-dimensional problem consisting of multiple angles as described in Chapter 3.3.

These view factor angles were calculated using basic geometry of the furnace and the location of the current tube increment as is illustrated in Figure 4-1.

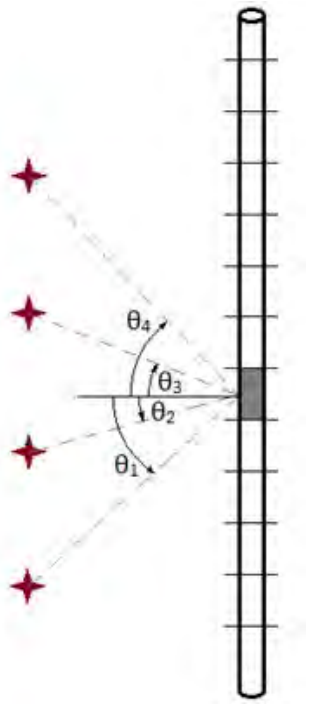

Figure 4-1: One-dimensional view factor angles to various heat sources.

The view factor angle was included in the heat transfer correlation by adjusting the surface area for heat transfer as follows:

$$A_F = cos\theta \cdot A_{normal} \tag{4-1}$$

The total heat transfer equation thus became:

$$Q = \varepsilon A_F \sigma \left(T_f^{\,4} - T_t^{\,4} \right) \tag{4-2}$$

Opacity factor [F_O]

Localised radiation takes place between the flue gas and the tube and not between the flame and the tube as was assumed in this model. Temperature losses from the actual flame to the localised gas around the tube due to scattering and reflection for example need to be accounted for. These losses were not investigated in this project but were accounted for by what is termed the opacity

factor. The opacity factor was adjusted in such a way that the calculated evaporator outlet temperatures were similar to the desired temperatures from plant and design data at various loads.

$$Q = \varepsilon A_{VF} \sigma F_O \left(T_f^{\,4} - T_t^{\,4} \right) \tag{4-3}$$

Tube surface temperature

It was assumed that the external tube surface temperature T_t was consistently 5°C higher than that of the water, steam or mixture flowing inside the tube.

Flue gas composition

Air was used in all calculations as supposed to actual flue gas. Calculating the composition and subsequent gas properties of flue gas was excluded from the scope of this project.

4.1.2 Methodology

Flame temperature

The flame temperature was a crucial variable in the model as it was responsible for driving heat transfer. It was calculated by doing a simple energy balance around the combustion process itself. The inputs to the calculation were the primary air and secondary air process conditions along with flow rate and CV of the coal. The resultant energy output was used to calculate the flame temperature by using the resultant enthalpy and flow rate of the flue gas. The simplified process is illustrated in the diagram in Figure 4-2.

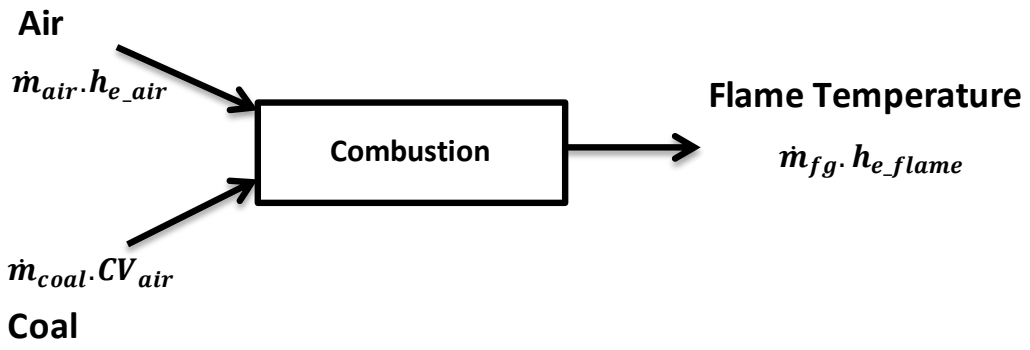

Figure 4-2: Basic flame temperature calculation.

$$h_{e\_flame} = \frac{\dot{m}_{coal} \cdot CV_{coal} + \dot{m}_{sec\_air} \cdot h_{e\_sec\_air} + \dot{m}_{prim\_air} \cdot h_{e\_prim\_air}}{\dot{m}_{total} + \dot{m}_{coal}} \tag{4-4}$$

$$T_{flame} = f(h_{e\_flame}) \quad (4\text{-}5)$$

Process:

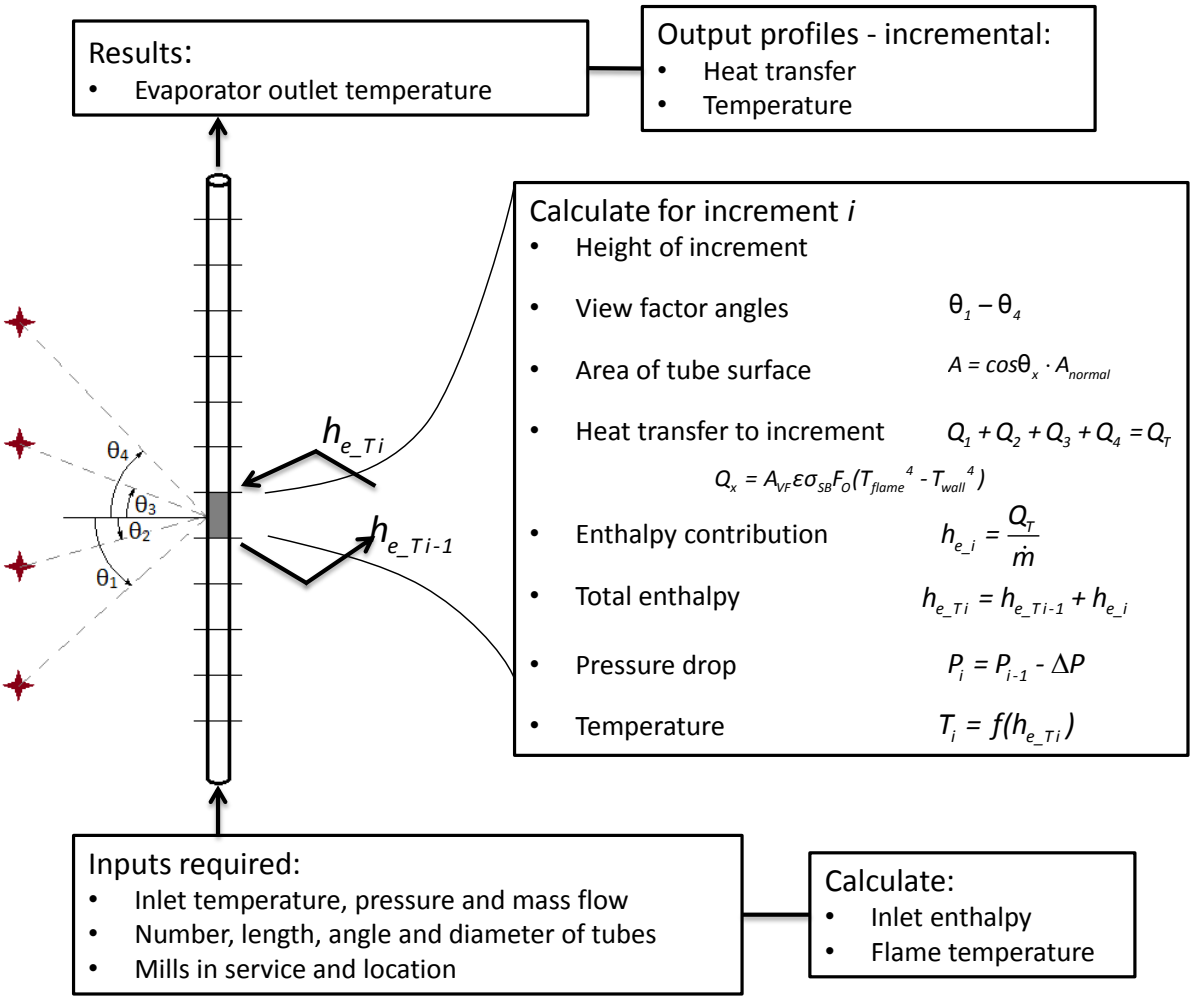

Figure 4-3: Flow diagram of evaporator methodology.

A single tube was divided into a finite number of increments and heat transfer was calculated individually to each. The total heat transfer to the tube increment from all the heat sources was calculated along with the subsequent enthalpy change. The outlet conditions of one increment defined the inlet conditions and thus fluid properties for the next, and the process was sequentially repeated until the outlet conditions of the tube were known. The pressure drop in the tubes was accounted for by defining the known inlet and approximate outlet pressures at various loads. The total pressure drop was evenly distributed across the total number of increments and included per increment as the solver sequentially moved through the tube. This pressure drop was assumed to represent the total pressure drop sufficiently and thus effect of elevation due to the water column in the height of tube was ignored. This process is illustrated in a flow diagram in Figure 4-3 above.

The expected outcome of this methodology will yield results per increment of tube that can be represented as the heat flux profile across the total length of tube. The expected profile is illustrated in Figure 4-4.

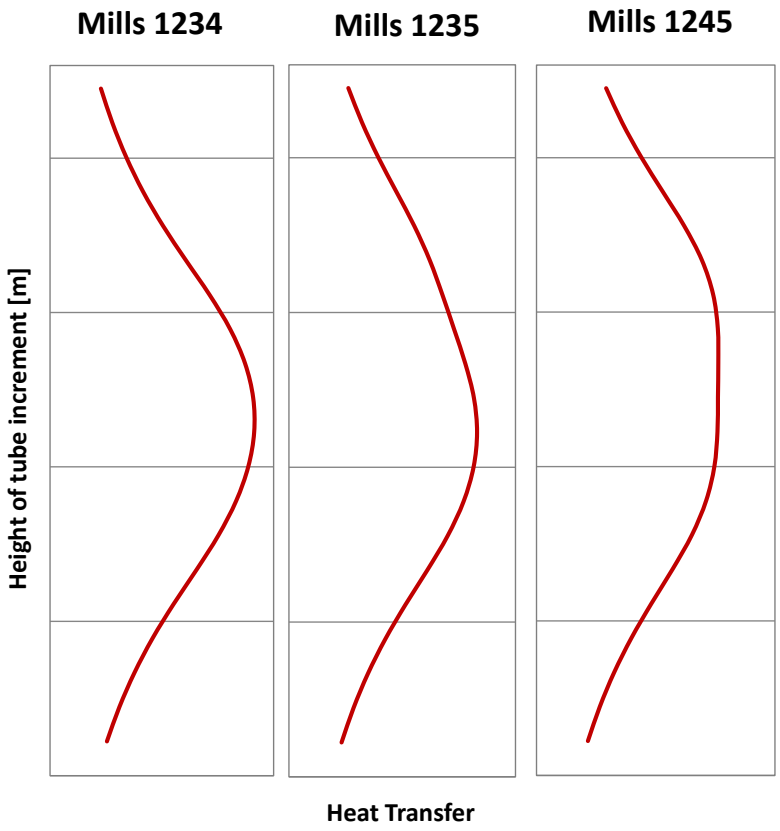

Figure 4-4: Expected heat flux profile for evaporator model for various mill combinations.

The model was repeatedly run with an updated opacity factor until appropriate outlet steam temperatures were achieved. This process was repeated for all load cases in which design data for operating conditions were available.

4.1.3 Conclusion

It is clear that there were numerous assumptions made in order to develop a working solving model that was not excessively complex but still yielded usable information. The main outcome identified, which was used later in this project, was the total heat transferred to the evaporator. Secondary outcomes from this model that could be useful for future use was the heat transfer profile generated for various mill combinations and the opacity factors for boilers at various loads.

4.2 Superheater

The overall superheater modelling process was sequentially followed from a fundamental basis and increases in complexity until all required physics, geometries and sub-systems were included. The analytical model was developed from theoretical fundamentals and included the basic layout and theoretical principles that was encountered throughout the project. It utilised some assumptions that simplified the modelling process yet ensured that all theoretical principles were adhered to and captured in the fundamental basis of the model.

The analytical model was used to validate the solving methodology of the thermo-fluid modelling software Flownex, before any detail modelling commenced. A model with similar layout and constant property fluids was developed in Flownex and results were evaluated to ensure acceptable solving methodology was used throughout the rest of the project.

Only after the Flownex modelling methodology yielded acceptable results, did development of the full model commence. This model captured the full detail of a typical coal-fired boiler heat exchanger and was validated using operational plant process data from actual boilers used in the Eskom fleet.

The process is explained in the flow diagram in Figure 4-5:

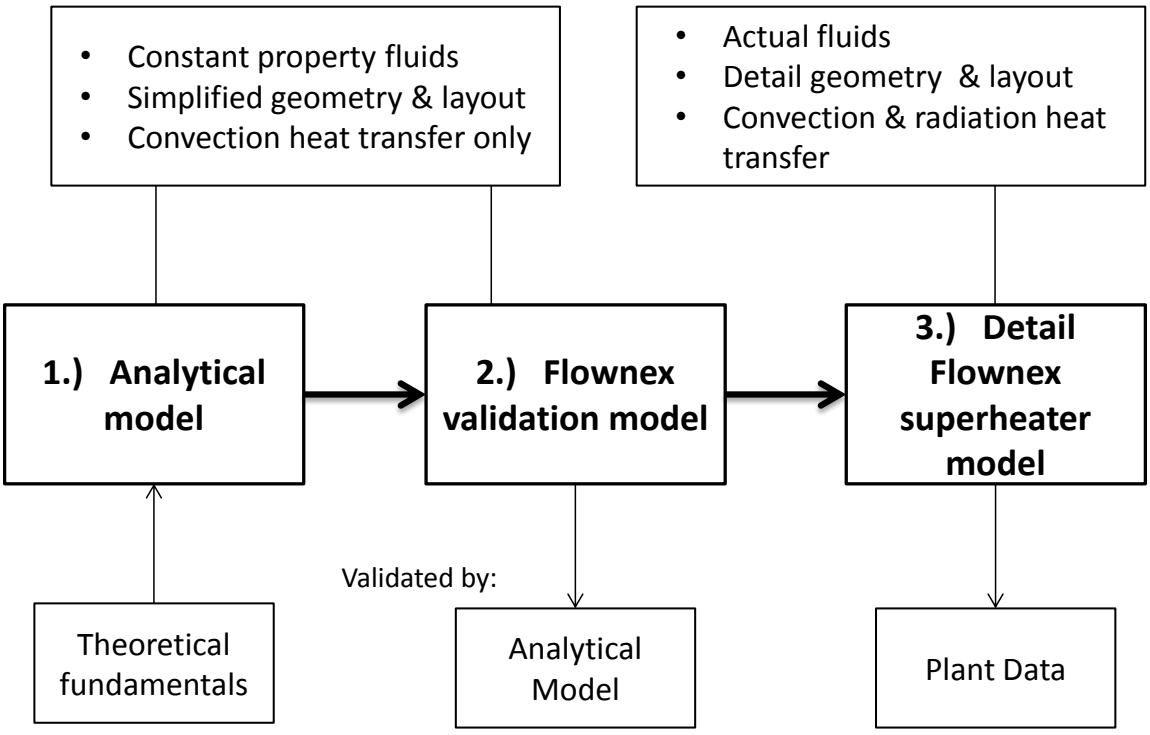

Figure 4-5: Flow diagram of superheater modelling process.

4.2.1 Analytical model

An analytical model of a simplified fictitious two pass heat exchanger was developed as is commonly found in final stage superheaters. It was developed using theoretical fundamentals discussed in Chapter 3. The flow orientation of the heat exchanger was defined as cross-flow with overall counter-flow layout and is illustrated in Figure 4-6:

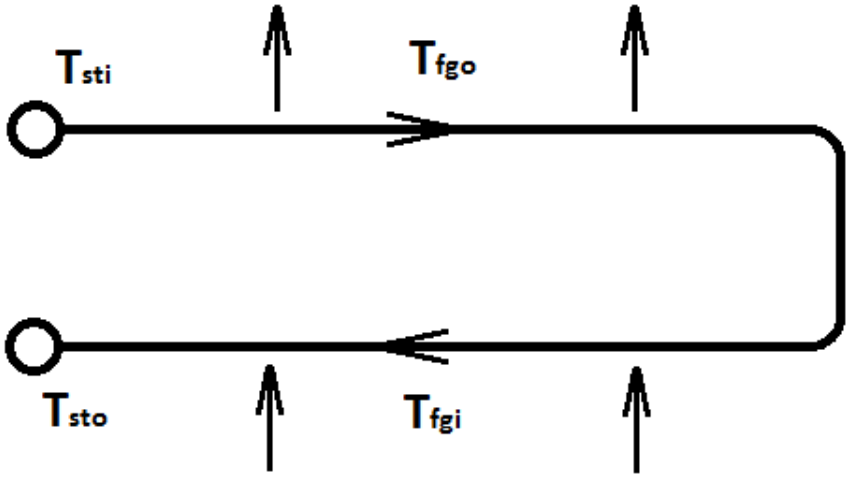

Figure 4-6: Layout and flow orientation of simple heat exchanger.

In typical boiler heat exchanger modelling, the majority of the geometrical properties are known. A single set of flow conditions of both fluid streams thus needed to be known in order to calculate other heat exchanger properties using the ε-NTU method.

This set-up resulted in three unknown variables which were the flue gas outlet temperature [$\boldsymbol{T_{fgo}}$], the steam outlet temperature [$\boldsymbol{T_{sto}}$] and the total heat transfer [$\boldsymbol{Q}$]. In order to solve all three variables simultaneously, three different equations were defined. To do this, heat transfer correlations for the hot fluid, the cold fluid and the combined heat exchanger was derived using steady-flow thermal energy equations and the ε-NTU method respectively.

$$Q = \dot{m}_{fg} c_{pfg} (T_{fgi} - T_{fgo}) \tag{4-6}$$

$$Q = \dot{m}_{st} c_{pst} (T_{sto} - T_{sti}) \tag{4-7}$$

$$Q = \varepsilon C_{min} \left(T_{fgi} - T_{sti} \right) \tag{4-8}$$

Fluid properties for both streams were calculated at the inlet conditions and were assumed to remain constant throughout the heater. This was done for simplicity of calculation, as the change in some fluid properties with temperature can become troublesome to calculate analytically, but would be accounted for in the numerical model in Flownex at a later stage. Heat transfer coefficients

for internal and external fluids were calculated using Nusselt number correlations described in Equations (3-22), (3-8). It was accepted that the external fluid, or flue gas, completely mixed between heat exchangers and between passes and that the internal fluid, or steam, was completely unmixed. The conduction heat transfer coefficient was calculated by the following correlation:

$$h_{conduction} = \left(\frac{r_o}{k} \cdot ln \frac{r_o}{r_i} \right)^{-1} \tag{4-9}$$

All variables in equations (4-6) and (4-7) were relatively straight-forward to obtain and the calculation procedure for variables in equation (4-8) is explained in the diagrams in Figure 4-7 and Figure 4-8:

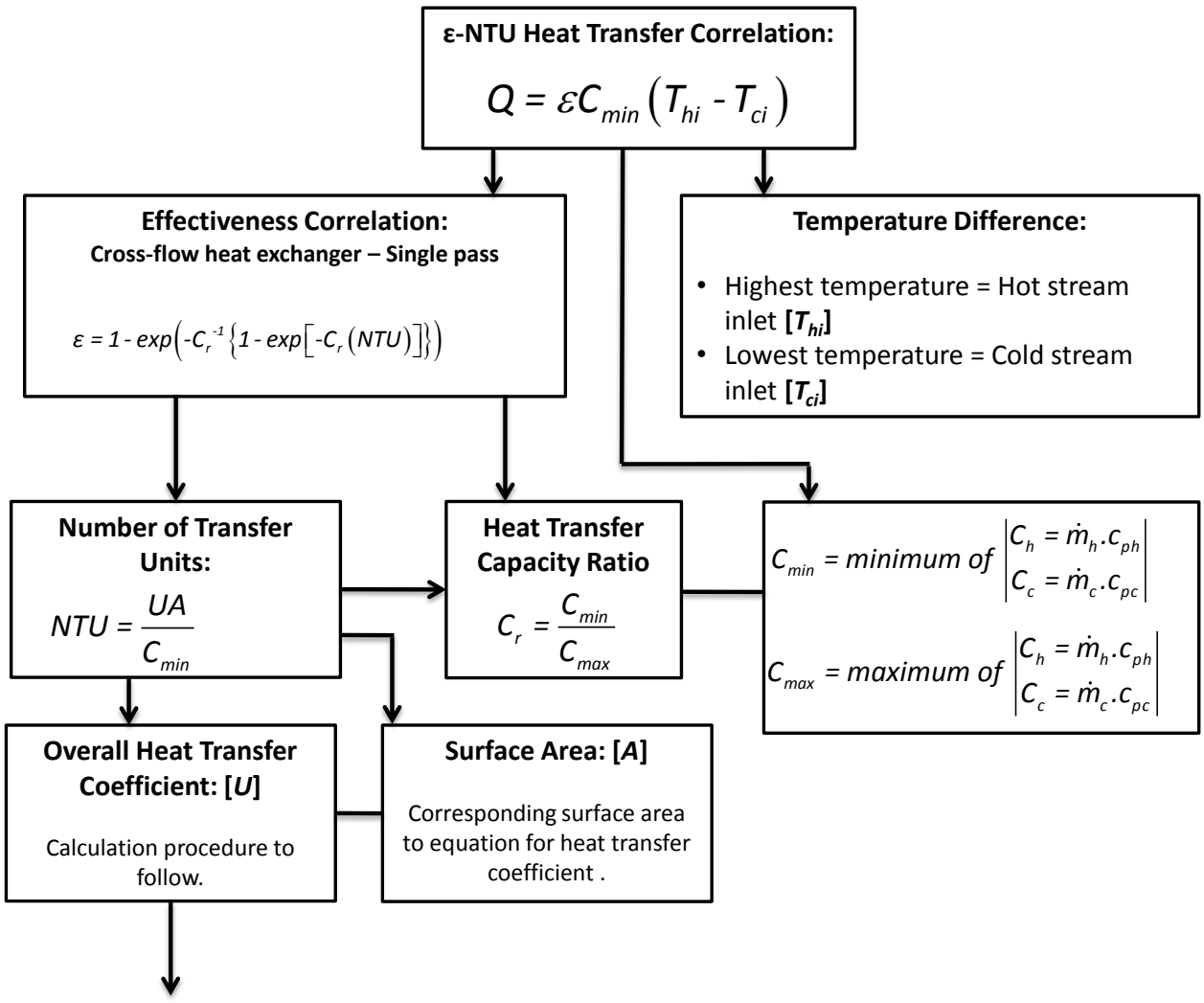

Figure 4-7: Flow diagram of ε-NTU methodology.

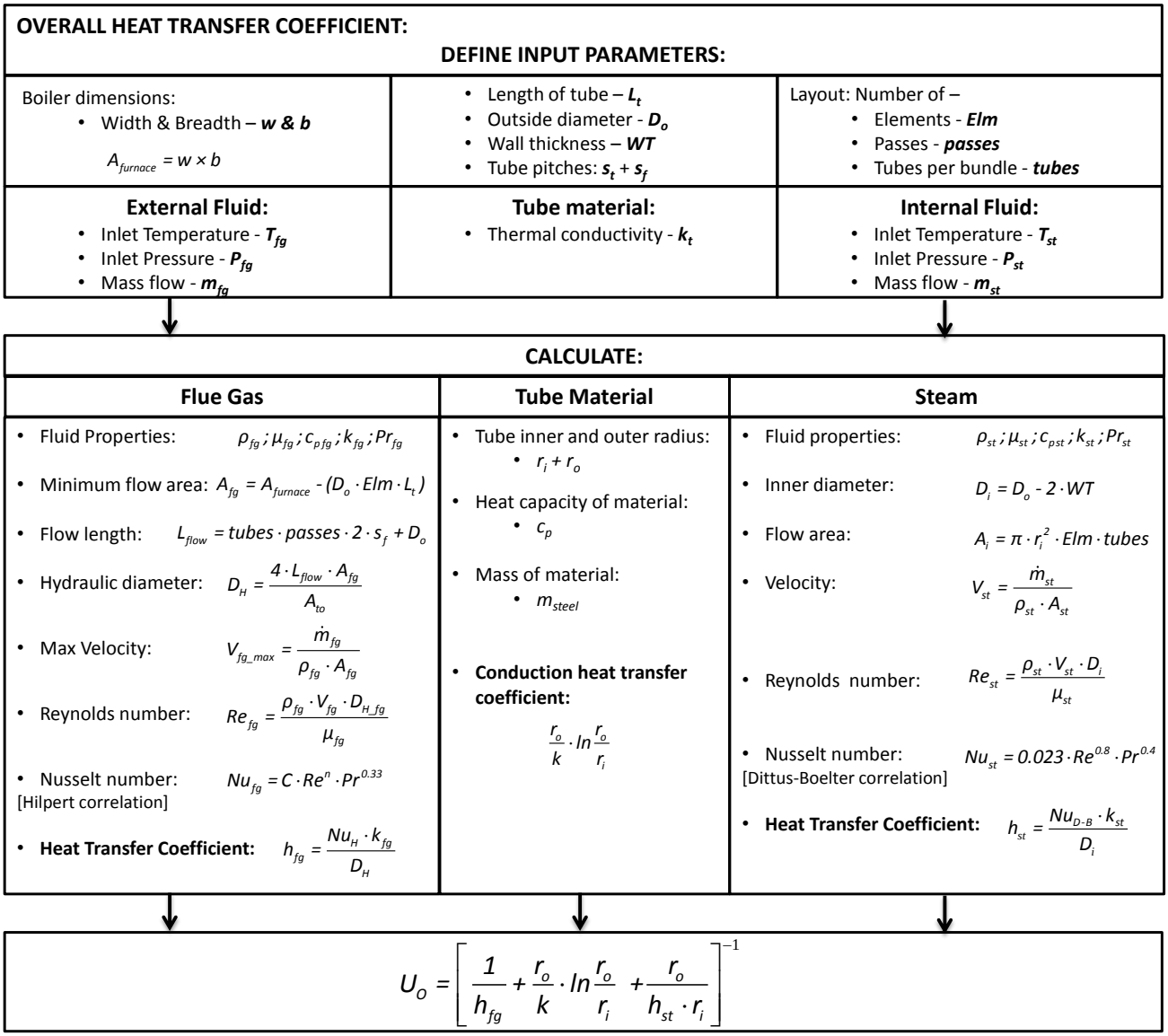

Figure 4-8: Methodology for calculating overall heat transfer coefficient.

Once all the known variables were calculated, matrix algebra was used to solve all three unknown variables simultaneously. Separating the known from unknown variables in all three equations and rewriting yielded the following:

$$\begin{bmatrix} \dot{m}_{fg} c_{pfg} T_{fg\_i} \\ -\dot{m}_{st} c_{pst} T_{st\_i} \\ \varepsilon C_{min} \left(T_{fg\_i} - T_{st\_i} \right) \end{bmatrix} = \begin{bmatrix} 1 & \dot{m}_{fg} c_{pfg} & 0 \\ 1 & 0 & -\dot{m}_{st} c_{pst} \\ 1 & 0 & 0 \end{bmatrix} \cdot \begin{bmatrix} Q \\ T_{fg\_o} \\ T_{st\_o} \end{bmatrix} \tag{4-10}$$

$$\begin{bmatrix} Q \\ T_{fg\_o} \\ T_{st\_o} \end{bmatrix} = \begin{bmatrix} 1 & \dot{m}_{fg} c_{pfg} & 0 \\ 1 & 0 & -\dot{m}_{st} c_{pst} \\ 1 & 0 & 0 \end{bmatrix}^{-1} \cdot \begin{bmatrix} \dot{m}_{fg} c_{pfg} T_{fg\_i} \\ -\dot{m}_{st} c_{pst} T_{st\_i} \\ \varepsilon C_{min} \left(T_{fg\_i} - T_{st\_i} \right) \end{bmatrix} \tag{4-11}$$

This methodology can also be expanded to accommodate larger sets of series heat exchangers. The superheater in a common boiler, for example, will have two or more banks installed in a complex layout. A third fluid heat exchanger such as a reheater can also be included if fluid conditions are known.

Similar equations are defined for each of the three heat exchangers as can be seen in Figure 4-9 and a matrix is developed using nine equations to solve for the nine unknown variables.

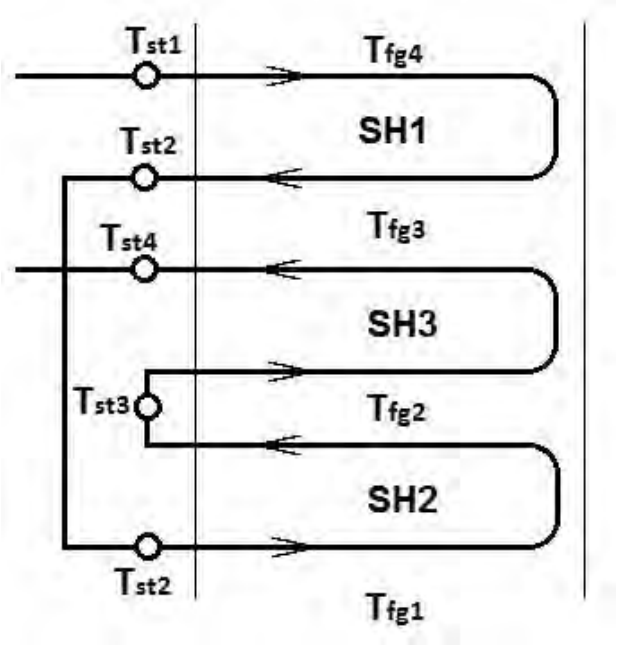

$$\begin{cases} Q_1 = C_{fg}(T_{fg3} - T_{fg4}) \\ Q_1 = C_{st}(T_{st2} - T_{st1}) \\ Q_1 = \varepsilon_A C_{min}(T_{fg3} - T_{st1}) \end{cases}$$

$$\begin{cases} Q_2 = C_{fg}(T_{fg2} - T_{fg3}) \\ Q_2 = C_{st}(T_{st4} - T_{st3}) \\ Q_2 = \varepsilon_A C_{min}(T_{fg2} - T_{st3}) \end{cases}$$

$$\begin{cases} Q_3 = C_{fg}(T_{fg1} - T_{fg2}) \\ Q_3 = C_{st}(T_{st3} - T_{st2}) \\ Q_3 = \varepsilon_A C_{min}(T_{fg1} - T_{st2}) \end{cases}$$

Figure 4-9: Complex layout of three heat exchangers in series with associated equations.

Splitting known from unknown variables yield the following matrix that can simply be solved:

$$\begin{bmatrix} Q_1 \\ T_{st2} \\ T_{fg4} \\ Q_2 \\ T_{st4} \\ T_{fg3} \\ Q_3 \\ T_{st3} \\ T_{fg2} \end{bmatrix} = \begin{bmatrix} -1 & C_{st} & 0 & 0 & 0 & 0 & 0 & 0 & 0 \\ -1 & 0 & -C_{fg} & 0 & 0 & C_{fg} & 0 & 0 & 0 \\ -1 & 0 & 0 & 0 & 0 & E_c & 0 & 0 & 0 \\ 0 & 0 & 0 & -1 & C_{st} & 0 & 0 & -C_{st} & 0 \\ 0 & 0 & 0 & -1 & 0 & -C_{fg} & 0 & 0 & C_{fg} \\ 0 & 0 & 0 & -1 & 0 & 0 & 0 & -E_c & E_c \\ 0 & -C_{st} & 0 & 0 & 0 & 0 & -1 & C_{st} & 0 \\ 0 & 0 & 0 & 0 & 0 & 0 & -1 & 0 & -C_{fg} \\ 0 & -E_c & 0 & 0 & 0 & 0 & -1 & 0 & 0 \end{bmatrix}^{-1} \cdot \begin{bmatrix} C_{st} \cdot T_{st\_in} \\ 0 \\ E_c \cdot T_{st\_in} \\ 0 \\ 0 \\ 0 \\ 0 \\ -C_{fg} \cdot T_{fg\_in} \\ -E_c \cdot T_{fg\_in} \end{bmatrix} \quad (4\text{-}12)$$

The heat capacity rates for typical flue gas and steam conditions are compared in Figure 4-10. It can be seen that the minimum heat capacity rate is typically that of the flue gas which is what was stated by Cantrell [3]. The same average values were used as will be discussed later for radiative heat transfer calculations.

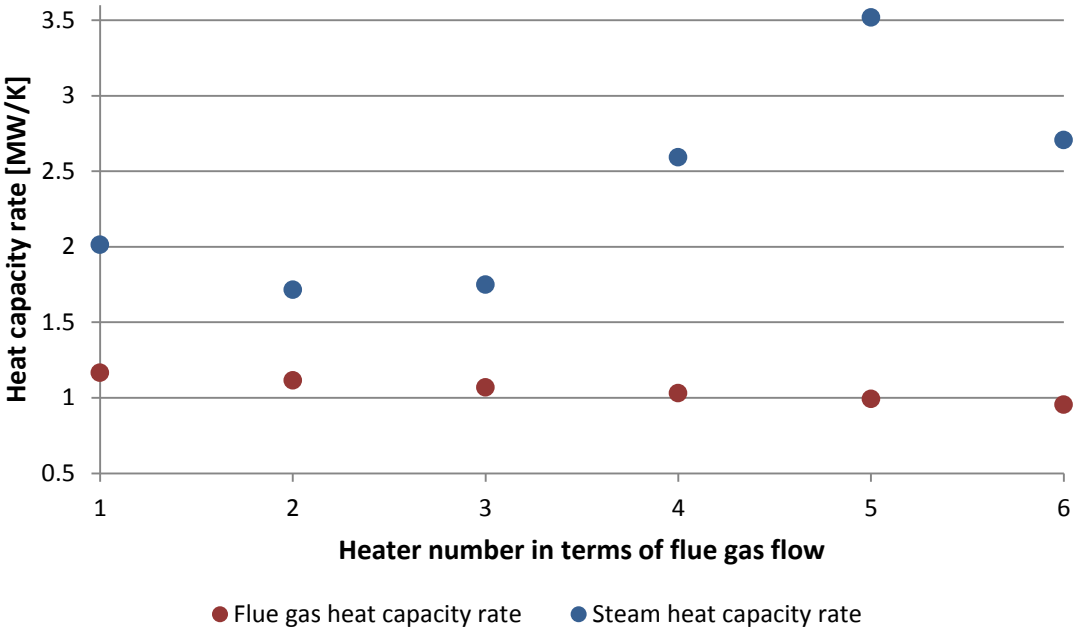

Figure 4-10: Heat capacity rates for both fluids compared for typical boiler heat exchanger conditions.

Conclusion

There are some limitations to this method such as its inability to accurately solve on a high level for actual fluids as the influence of property changes along the length of the heater becomes very difficult to capture. The model is developed as a generic overview solver to a heat exchanger and does not give insight into more detailed analysis of specific tubes or locations within the heater itself. Although it can be used for basic high level calculations, the purpose of the model in this project is purely to validate the solving methodology of the numerical modelling software. It is thus of great importance that the software model to be validated is set up identically to that of the analytical model. This procedure is further explained below.

4.2.2 Validation model methodology

Various modelling approaches using different Flownex components was investigated to identify the best way to model the cross-flow heat exchangers as found in typical coal-fired boilers. Components were also set up using different approaches in terms of detail of plant layout. Some of the criteria used for evaluating which method best achieves the objectives of this project are:

- Applicability to range of boilers in the Eskom fleet
- Difficulty / ease of modelling
- Solving time
- Accuracy of output

The modelling process was planned to follow a high detail down approach in which the highest detail model is developed first to determine the highest accuracy results. The following models would remove some detail and simplify the model to improve on user friendliness and ease of modelling. Then other components would be tested with the known knowledge to evaluate the best option for modelling. These approaches with graphical illustrations of models are listed below:

4.2.2.1 Multiple steam flow and gas flow paths

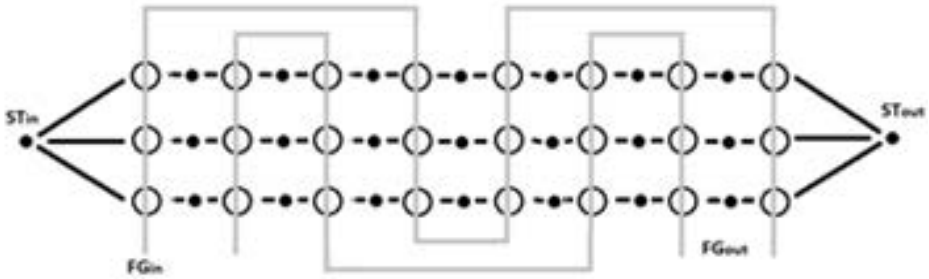

Figure 4-11: High detail model with multiple flow paths for steam and flue gas.

The heat exchanger is designed using basic pipe components for both steam and flue gas with heat transfer links in between, it requires a high level of detail. It utilises individual flow paths representing each tube and the flue gas side is divided into multiple flows. It also simulates slight differences in tube lengths and pressure due to layout of the tubes. This approach yields very accurate results, but is not practical for further modelling as it is extremely modelling intensive with a slow solving time.

4.2.2.2 Multiple steam flow paths, single flue gas flow path

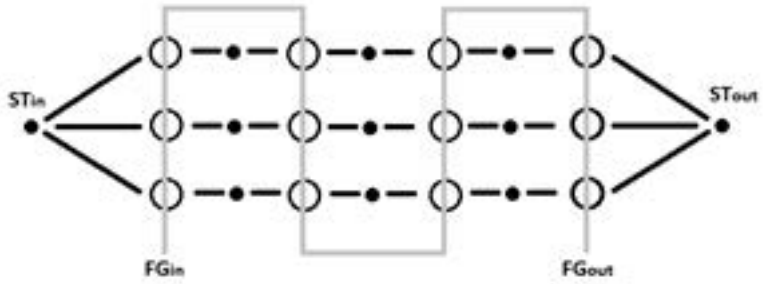

A similar heat exchanger was developed as above, but the detail were integrated into fewer components. Only a single flue gas flow path was simulated and the steam tubes were thus represented by fewer components in series. This model yields were accurate results, but similarly to the high detail one, it is quite modelling intensive and slow to solve. It is thus also not suitable for the purposes of this project.

4.2.2.3 Simplified model, single flue gas & single steam tube

A similar model was developed with both the steam and flue gas streams being simulated by a single flow path. It was the most simplified version of a basic pipe component model with heat transfer links in between. The model performs well in terms of modelling intensity but lacks terms of accuracy of results yielded.

4.2.2.4 Built-in component - Simplified Heat Exchanger

A built in component in the Flownex library was also evaluated for a possible modelling approach. It yielded suitable results for steady-state simulations, but was not quite suitable in terms of transient solutions. The flow orientation and limitations on variability of heat transfer was also two drawbacks.

4.2.2.5 Built-in component - Finned Tube Heat Exchanger

The finned tube heat exchanger is a built-in component in the Flownex library. It was not originally designed to model heat exchangers with similar geometrical properties as is commonly found in coal-fired boiler heat exchangers. It does however represent heat exchangers with a similar flow orientation as is commonly found in coal-fired power station boilers in that tubes are exposed to a fluid in cross-flow. The built-in component defines two fluid streams in separate components, which represents the internal and external fluids. With sufficient discretisation, it develops a heat exchanger similar to that of the high detail heat exchanger above, but with a significantly easier set-up. This component is suitable for various transient modelling simulations and heat transfer between the sub-components can be manually changed. The flow orientation, transient capabilities and high level of heat transfer variability made this component the most suitable for the purposes of this project.

4.2.3 Flownex validation model

A heat exchanger was developed using the built-in finned tube heat exchanger component and was assigned a similar layout, flow orientation and operating conditions to that of the heat exchanger represented in Figure 4-6. The Flownex set-up is illustrated in Figure 4-12.

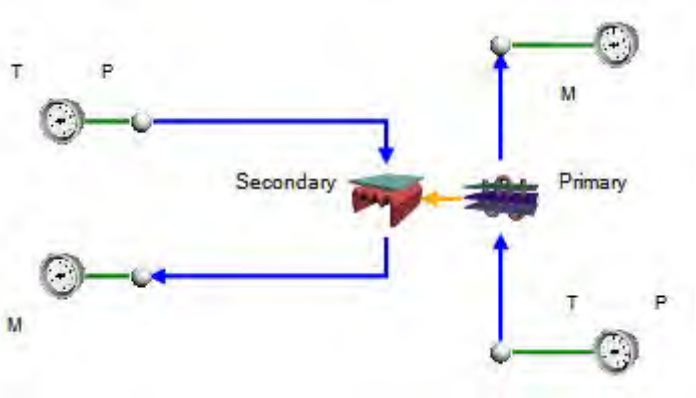

Figure 4-12: Basic layout of Finned Tube Heat Exchanger component in Flownex.

Various geometrical properties were defined by the user and they are explained in full in Appendix A. Custom fluids were developed to match the fluid properties of those in the analytical model in order to have comparable results. All fluid properties were calculated for inlet conditions of both streams as was explained in the modelling methodology of the analytical model.

Primary heat exchanger

The primary side of the finned tube heat exchanger represents the external fluid and geometries associated with it. The general procedure to calculate the heat transfer coefficient differs from that described in Chapter 3 and is described below. The convection heat transfer coefficient is defined by:

$$h = \frac{j_H \cdot \rho \cdot V \cdot c_p}{Pr^{2/3}} \tag{4-13}$$

With the Colburn factor defined as a function of the Stanton and Prandtl numbers:

$$j_H = St \cdot \mathrm{Pr}^{2/3} \tag{4-14}$$

The Colburn factor is not calculated directly, but rather looked up as a function of the Reynolds number from a ***heat exchanger characteristic chart*** that was assigned to the heat exchangers as one of the inputs. There were numerous characteristic charts available in literature, but none could be identified that satisfied this specific layout. A chart was thus developed that accurately represented the typical heat exchanger layout expected in a coal-fired boiler.

The correlation for the Stanton number is:

$$St = \frac{Nu}{\mathrm{Re} \cdot \mathrm{Pr}} \tag{4-15}$$

Replacing the Hilpert correlation for the Nusselt number into equation (4-15), it becomes:

$$St = \frac{C \cdot Re^{n} \cdot Pr^{0.33}}{Re \cdot Pr} = C \cdot Re^{n-1} \cdot Pr^{-0.67} \qquad (4\text{-}16)$$

For simplicity, the Prandtl number was assumed to be a constant value and calculated assuming constant flue gas pressure. The Prandtl numbers for the typical range of flue gas temperatures and the average value used are illustrated in Figure 4-13. Figure 4-13 justifies the assumption of using the average between minimum and maximum Prandtl numbers.

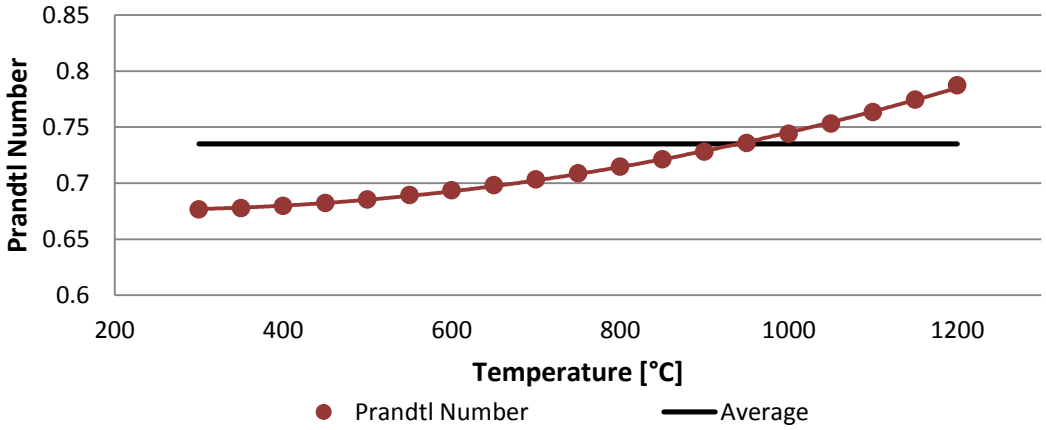

Figure 4-13: Prandtl number range for typical heat exchanger flue gas temperatures.

A range of applicable Reynolds numbers was identified, after which the Stanton number and subsequently the Colburn factor were calculated. This data was transferred into the heat exchanger characteristic chart and can be assigned to a specific group of heat exchangers for which it was developed. The Flownex software then calculates heat transfer coefficient and heat transfer based on values in the chart corresponding to the Reynolds number for the fluid.

In order to ensure simplicity of the validation model, only convective heat transfer was considered and the characteristic chart was developed accordingly. The resultant heat exchanger characteristic chart providing the Colburn factor as a function of the Reynolds number is illustrated in the graph in Figure 4-14.

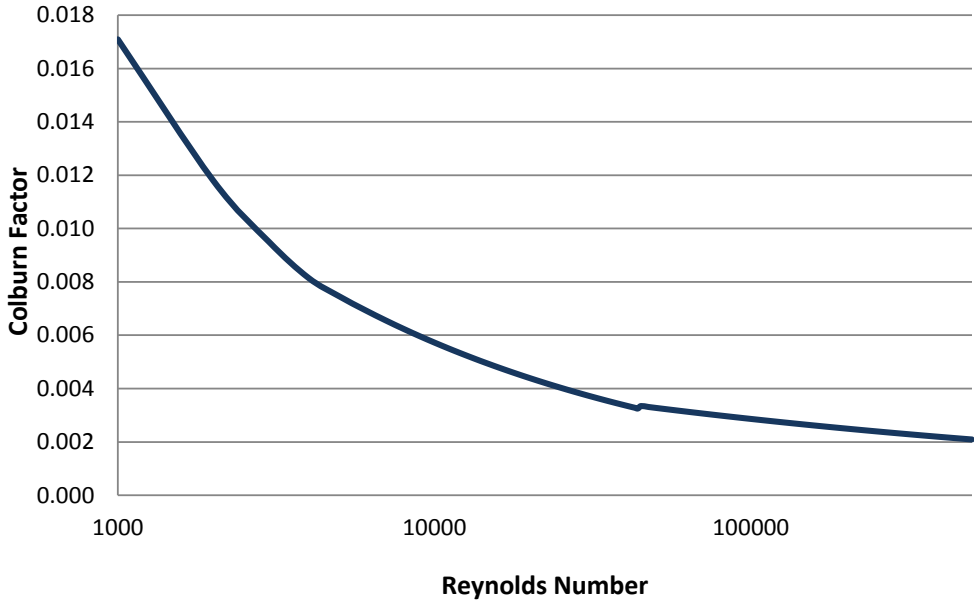

Figure 4-14: Heat exchanger characteristic chart for convection heat transfer only.

Secondary heat exchanger

The secondary side of the finned tube heat exchanger represents the internal fluid and geometries associated with it. Again, the process and fluid properties required to calculate dimensionless numbers were calculated from the inputs defined by the user. The Ditus-Boelter correlation was used to calculate the internal Nusselt number as is commonly done for internal pipe flow situations. The general heat transfer calculation method for the internal fluid was very similar to that of the analytical method and is not explained in detail.

Conclusion

After set-up was completed and sanity checks were done, the validation model was solved and results compared to that of the analytical model. Comparable results indicated that the solving methodology of the Flownex model with the characteristic chart was sufficient and adhered to the required theoretical fundamentals. This modelling methodology was extended and further developed to capture the total physical properties of a typical coal-fired boiler. Validation results are discussed in detail in Chapter 5.

4.2.4 Radiation in convective pass

Until this stage, the only heat transfer mechanism modelled in Flownex was convection. As mentioned, a significant percentage of the total heat transfer to the water-steam cycle in the

convective pass is as a result of radiation heat transfer and an important part of the detail superheater model was to include the contribution of radiation heat transfer.

The approach taken in this project was to include the radiation heat transfer as a constant to the heat exchanger characteristic charts for specific heat exchangers in different locations along the flue gas path. As the flue gas temperature gradually decreases through the convective pass, the characteristic charts were adjusted sequentially. The process of calculating and including radiation to the charts is explained below:

$$h_{total} = h_{conv} + h_{rad} \tag{4-17}$$

Substituting Equation (4-13) into Equation (4-17) yields:

$$h_{total} = \frac{j_{Hconv} \cdot \rho \cdot V \cdot c_p}{Pr^{2/3}} + \frac{j_{Hrad} \cdot \rho \cdot V \cdot c_p}{Pr^{2/3}} \tag{4-18}$$

Because the fluid properties were evaluated at similar conditions, this equation simplifies to:

$$h_{total} = \frac{(j_{Hconv} + j_{Hrad}) \cdot \rho \cdot V \cdot c_p}{Pr^{2/3}} \tag{4-19}$$

Substituting the Colburn factor as in Equation (4-14) yielded:

$$h_{total} = (St_{conv} + St_{rad}) \cdot \rho \cdot V \cdot c_p \tag{4-20}$$

The radiation Stanton number thus became the critical variable that needed to be evaluated. The radiation Stanton number was calculated as a function of the radiation heat transfer coefficient and is represented by the following correlation:

$$St_{rad} = \frac{h_{rad}}{\rho \cdot V \cdot c_p} \tag{4-21}$$

The methodology started by calculating the radiation heat transfer coefficient based on the method developed by Brummel [22] and Vortmeyer [18] which was explained in detail in Chapter 3.3.2. The main correlations used are emphasised below:

$$h_{rad} = \frac{\varepsilon_w \sigma}{\left(\alpha_{gp} + \varepsilon_w - \alpha_{gp}\varepsilon_w\right)} \cdot \frac{\varepsilon_{gp} T_g^{\,4} - \alpha_{gp} T_w^{\,4}}{T_g - T_w} \tag{4-22}$$

With the mean beam length calculation based on a control volume with a round tube inside as given by Taler [19]:

$$s = C\frac{d}{4}\left(\frac{4}{\pi}\frac{s_1 s_2}{d^2} - 1\right) \tag{4-23}$$

In order to calculate the radiation contribution as a constant for multiple boilers, good average values that accurately represent the majority of the boilers in a specific group needed to be used. The groups of boilers investigated in Chapter 2.6 showed that when heat exchangers were compared according to gas flow, various average properties were good representations of the group. Based on that, characteristic charts were developed for both groups of boilers.

The properties required to calculate the radiative heat transfer contribution from flue gas at various stages throughout the process is explained briefly below.

Flue gas composition

Although all the properties for flue gas are represented by those of air elsewhere in the project, the contribution of the actual gasses to radiation needed to be used. An estimate of the flue gas composition commonly found in South African boilers is presented in Table 4-1, these values were obtained from another student based on simplified mass and energy balance equations of typical South African coal. The gasses that contribute to radiation contained in the flue gas were for the purpose of this project accepted as only H_2O vapour and CO_2. It was assumed that the other contributing gasses such as SO_x's and NO_x's were present, but in such small percentages that they can be neglected. Other gasses, such as oxygen and nitrogen which contribute the remainder of the composition but don't contribute to the radiation are omitted from the table.

Table 4-1: Gas composition values for radiation calculation.

Variable	**Ratio**	**Partial pressure**
Ratio of water vapour [$\boldsymbol{H_2O}$]	6%	6 kPa
Ratio of carbon dioxide [$\boldsymbol{CO_2}$]	20%	20 kPa
Flue gas mixture	100%	100 kPa
Partial pressure of contributing gasses [$\boldsymbol{p_{sum}}$]	26%	26 kPa

Mean beam length

As explained in Chapter 2.4.3 the heat exchanger tube elements are typically wider spaced closer to the furnace and tube bundles increase in density as flue gas cools to optimise heat transfer. With the heat exchanger numbering done sequentially along the flue gas path, one would expect to see the average mean beam length decrease systematically as the flue gas cools. Mean beam lengths were calculated from average tube pitch values using Equation (4-23) and the average mean beam length for a specific heat exchanger in sequence is illustrated for the two groups of boilers in Figure 4-15. The group for boilers larger than 300MW shows two trends which represent the superheater and reheater diameters separately as they differ.

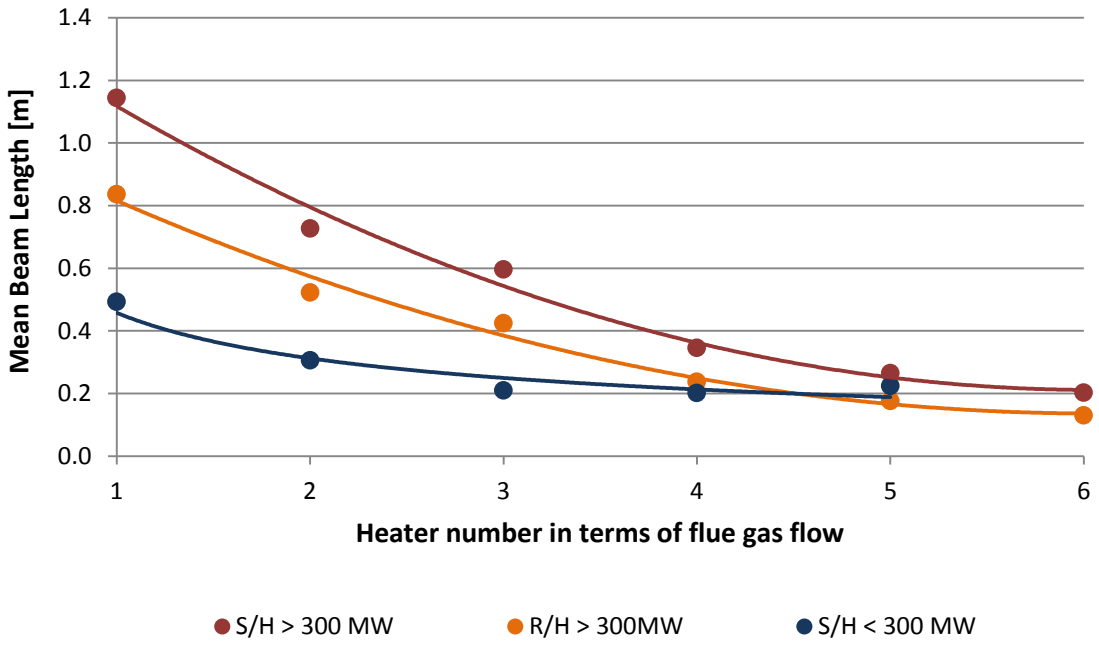

Figure 4-15: Mean beam length average values per heater for both boiler and heater groups.

Flue gas temperature

The heat exchanger characteristic charts were developed using the design data for flue gas temperatures at full load. This was done for two reasons: firstly, the flue gas temperatures don't vary greatly with load as shown in Figure 4-17 and secondly, high to full load operation is the most common range of operation, hence in this region is where the most accurate results were required. The inlet and outlet temperatures of heat exchangers were averaged across the groups and results are illustrated in Figure 4-16.

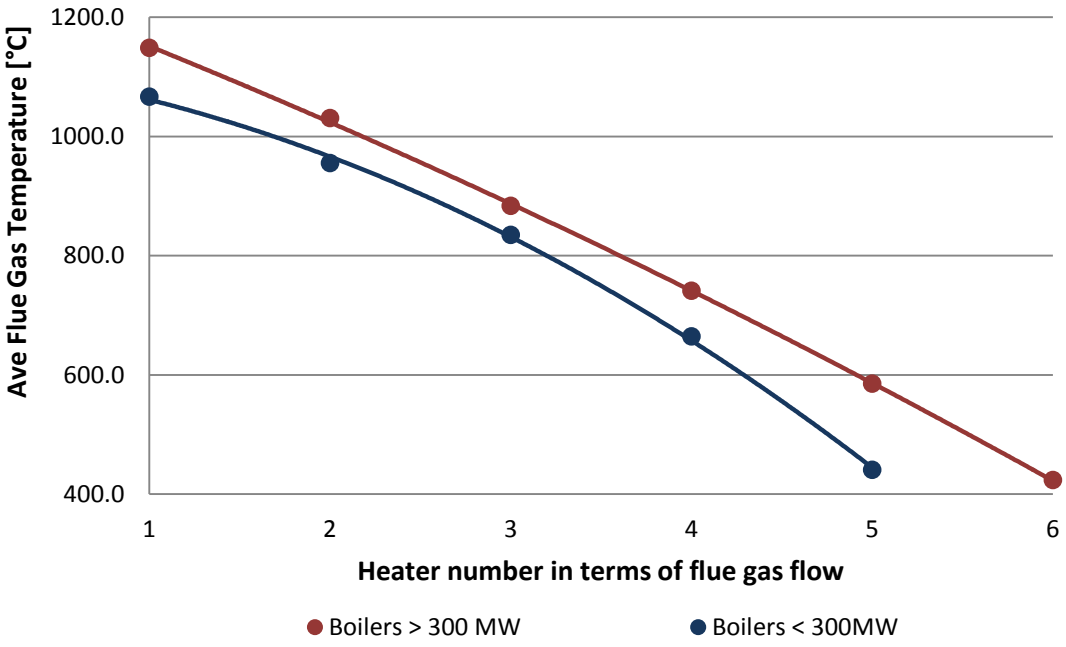

Figure 4-16: Average flue gas temperatures per heat exchanger for both boiler groups.

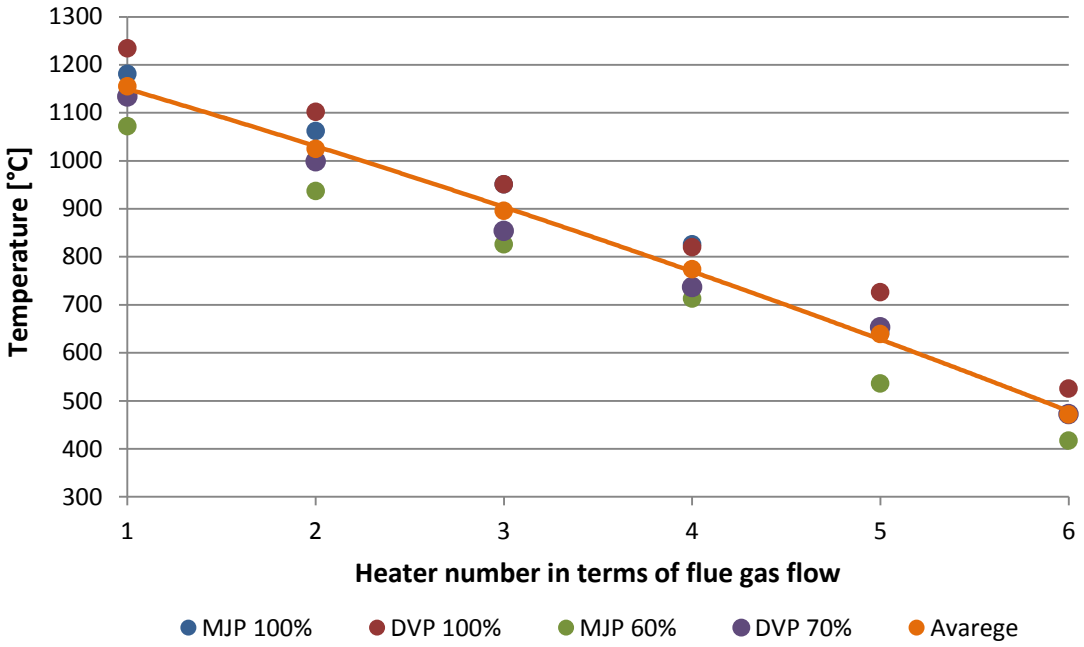

Figure 4-17: Flue gas temperature comparison between 100%, 70% and 60% MCR on two power stations.

Steam temperatures

As the individual boiler layouts typically vary, the average steam temperatures plotted according to the sequential heat exchanger numbering according to the flue gas flow path did not present similarly accurate and representable trends. The impact of the steam temperature on radiation was not as significant as flue gas temperatures and thus any small errors resulting from using the average were accepted. The average steam temperature values are plotted in Figure 4-18.

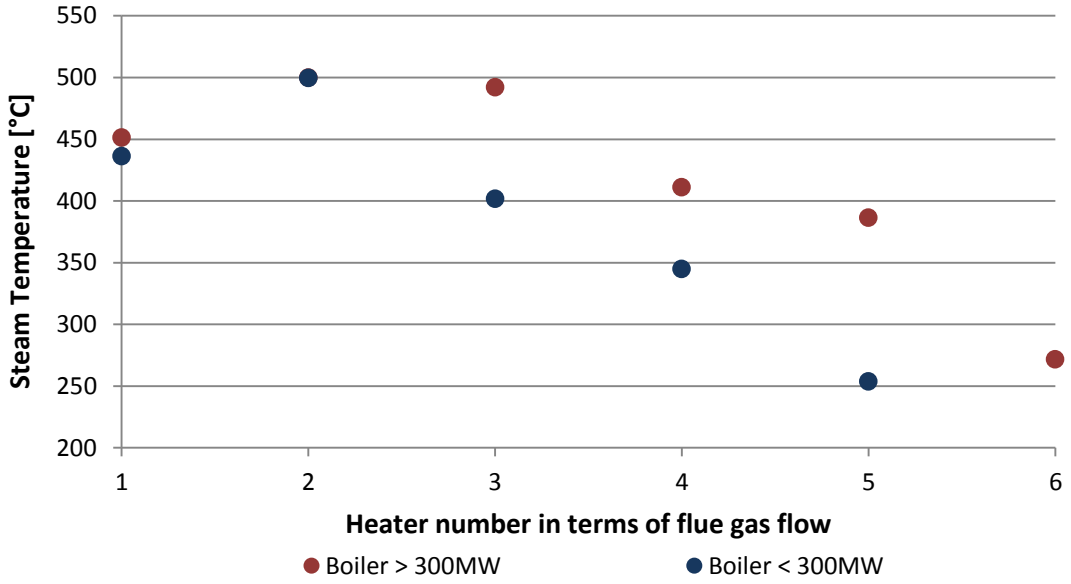

Figure 4-18: Average steam temperatures per heat exchanger for all boilers.

Ash particle emissivity

It was assumed that a thin layer of ash is present on all tubes and that the emissivity of both the tubes and the particles are equal. Obtaining all the information required to utilise the method described in Chapter 3.3.2 fell outside the scope of this project. It was thus assumed that the ash particle emissivity is $\varepsilon_p = 0.35$ for all heat exchangers. This assumption was based on discussions with specialist engineers in the field and is not validated in any specific documentation. Table 4-2 below, however, indicates that the assumed emissivity falls within the range for most sizes of powder ash in the temperature range applicable.

Table 4-2: Ranges for emissivity of different forms of powder ash. [25]

Material	T range (K)	ε range
Powder - 120 µm	500 – 1500	0.8 – 0.4
Powder - 33 µm	500 – 1500	0.7 – 0.3
Powder - 6.5 µm	500 – 1500	0.6 – 0.2

Flue gas velocity

Investigation into the design documentation for flue gas velocities at various loads yielded a strong correlation across different boiler designs for the group of boilers larger than 300MW. This is as a result of fly-ash erosion damage control in which velocities needs to be controlled in order to ensure reliability. Flue gas velocity was found to typically be a function of unit load.

The flue gas velocity for all radiation calculations in this project was assumed to be constant for all loads. This should result in some inaccuracies, specifically at lower loads, as the Stanton number is a function of flue gas velocity as can be seen in Equation (4-21). The average flue gas velocity design values at various loads for both groups of boilers are illustrated in Figure 4-19. Design data for flue gas velocities in smaller boilers was obtained for two boilers only, which resulted in larger errors for the specific group. The correlation between velocities was not as good and the average value indicated is thus not very representative.

The majority of coal-fired power stations were designed as base load stations and thus mainly operate at or close to full load. It thus made sense to use the flue gas velocity in this range for all calculations. The velocity used for boilers larger than 300MW was thus 10m/s. In-depth investigation into the appropriate velocity to use for smaller boilers were done on an individual boiler basis.

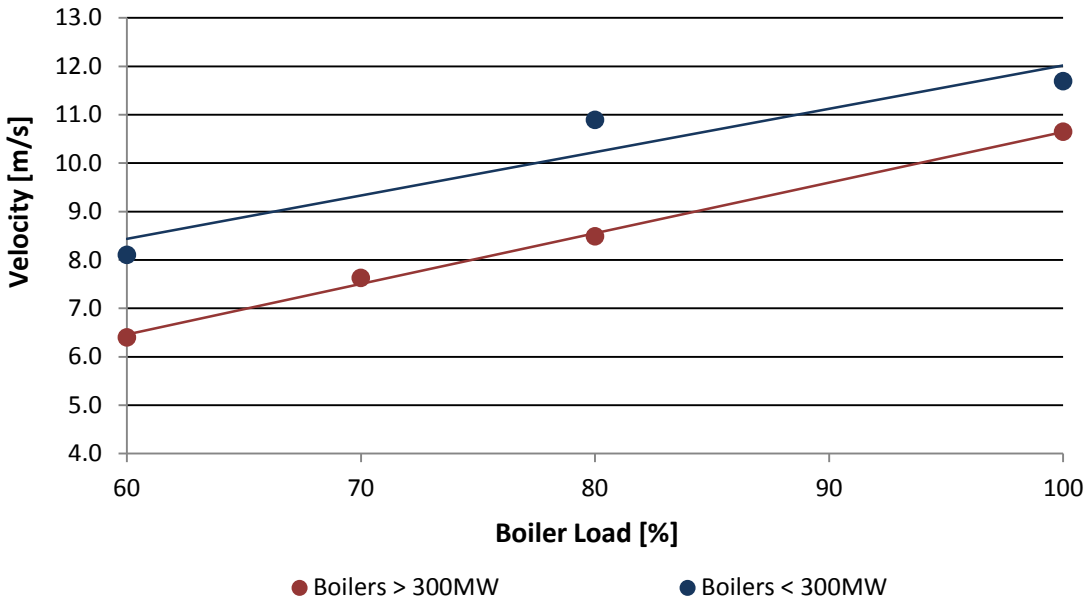

Figure 4-19: Average flue gas velocities for both groups of boilers.

Results

The Stanton numbers representing radiative heat transfer per heat exchanger in the convective pass for all three groups of heat exchangers is plotted in Figure 4-20.

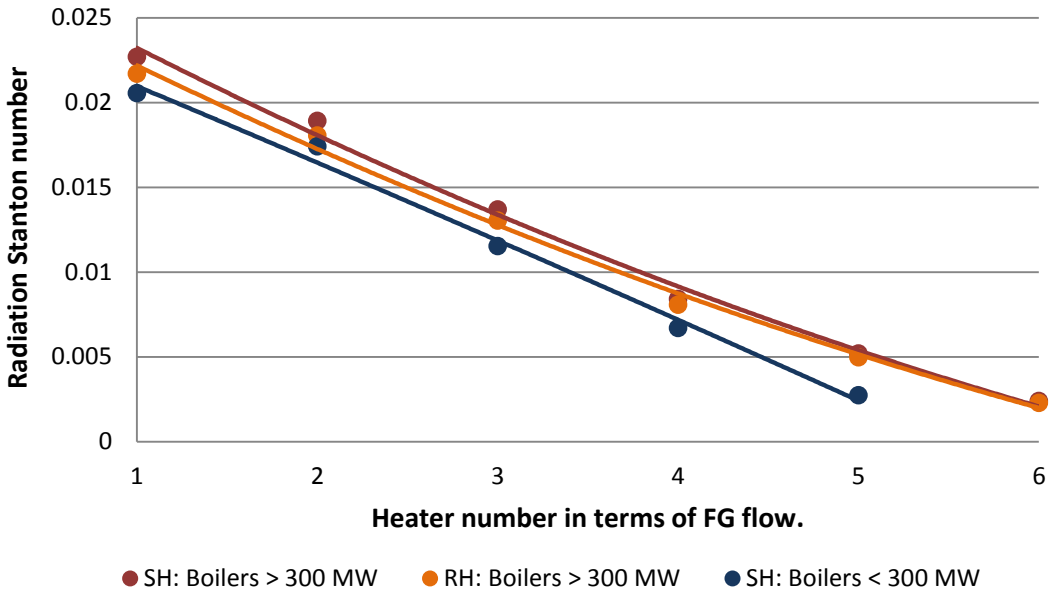

Figure 4-20: Stanton numbers from heat transfer coefficients per heat exchanger.

The Stanton numbers from the graph above were systematically added to the convection heat exchanger characteristic chart to represent radiative heat transfer to specific heat exchangers at various locations along the flue gas path. An example of this is shown in Figure 4-21.

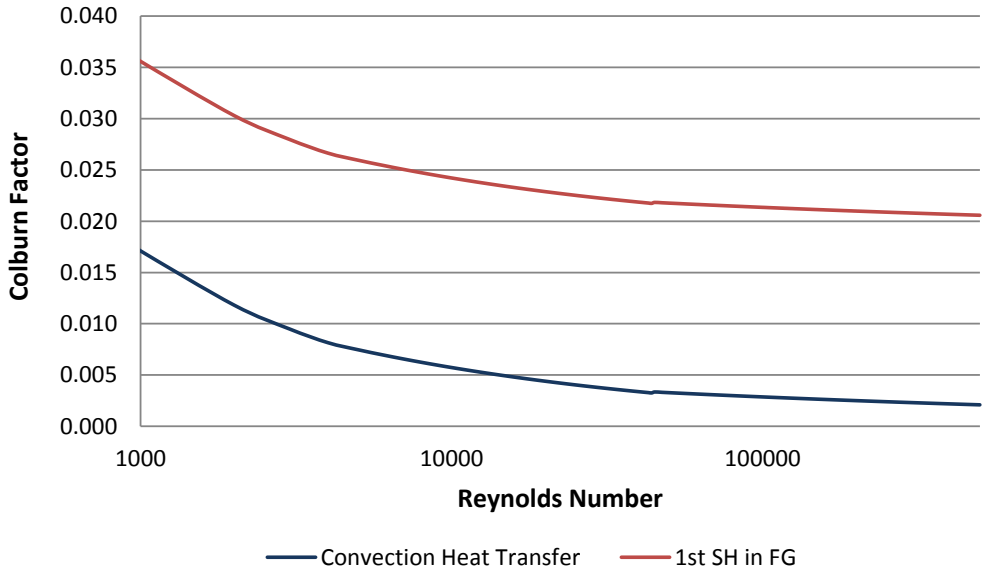

Figure 4-21: Colburn factor as for convection and total heat transfer for 1st heat exchanger.

4.2.5 Fouling

Although the model has the capacity to simulate different fouling scenarios independently, the actual change in conduction due to either internal or external fouling was not modelled in detail. As discussed in Chapter 3.1.1, fouling will lower the effective conductivity of the tube wall material because of the poor conductivity of typical fouling materials. As fouling increases, the delay in response time of steam temperature to transient conditions will increase along with a decrease in total heat transfer for constant temperatures. Thus, in order to accomplish required heat transfer, the temperature difference needs to be greater which leads to increased metal operating temperatures.

The model developed could be used to determine the effect of specific fouling characteristics on boiler performance or to track changes due to fouling over a long period of time. Significant information however is required on the fouling material such as material composition, thermal conductivity and geometrical properties such as basic dimensions or thicknesses.

An effective conductive heat transfer coefficient including the effect of fouling can be calculated as follows:

$$h_{conduction} = \frac{1}{R_{fouling.inner} + R_{tube} + R_{fouling.outer}} \tag{4-24}$$

With:

$$R_{cylinder} = \frac{r_{ave} \cdot ln\left(\frac{r_{outer}}{r_{inner}}\right)}{k_{material}} \tag{4-25}$$

The above method is a simplification as approximate radiuses are used and could be done more accurately should the user require very accurate conduction results. For the high-level boiler model as was developed here, the formulas above will suffice as fouling layers normally are extremely thin and errors will thus be small.

4.2.6 Air versus flue gas

Due to the fact that all modelling was done with air as supposed to the actual flue gas composition, a simple test was set up to evaluate the error that occurred because of it. A basic flue gas was developed and similar models were run with both air and flue gas to compare results. The test was done on a low temperature superheater as well high temperature final stage superheater. The results and conclusion is presented in the next chapter.

4.3 Detail superheater

Once the validation model proved that the solving methodology of Flownex compared well with the analytical model and thus adhered to the various theoretical fundamentals discussed in Chapter 3, a detail model was developed. The final process in the superheater modelling methodology was to elaborate on the validation model to include all the detail and properties of an actual heat exchanger.

This entailed the following changes:

- Replaced custom constant property fluids with real fluids

  This included the fluid properties into the model and thus temperature and pressure variations and subsequent property changes were accounted for.

- Detail geometry included

  The simplified heat exchanger was elaborated to include all geometrical detail of an actual heat exchanger as is commonly found in Eskom boilers.

- Heat exchanger characteristic charts with radiation included

  The appropriate heat exchanger characteristic chart was selected which included the radiation heat transfer according to the location of the heat exchanger.

For full detail of inputs required and options to select, see Appendix A for the calculation procedure.

4.4 Complete boiler

The assembled boiler model consisted of multiple heat exchangers connected in series as is found in an actual boiler. A simplified drawing of the expected model layout is illustrated in Figure 4-22 and a brief summary of components that needed to be included.

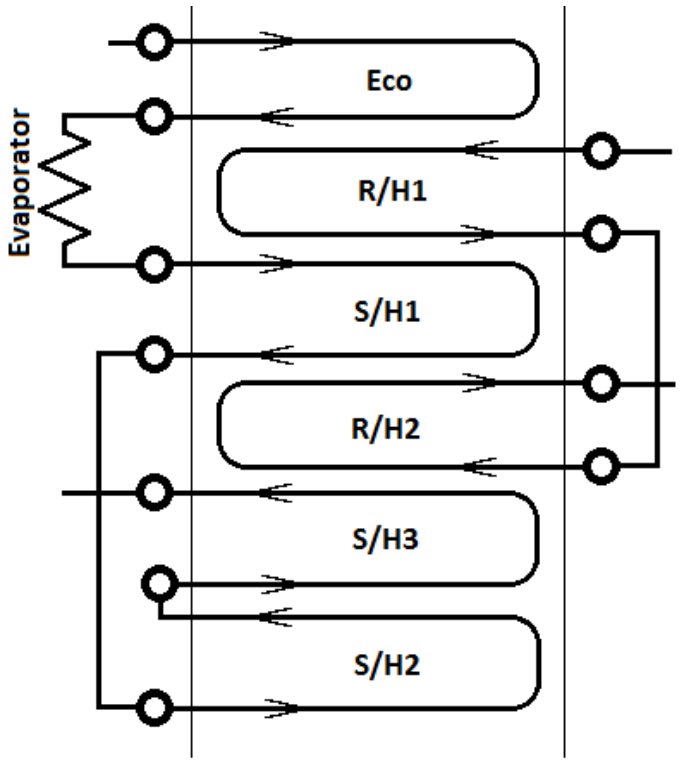

Figure 4-22: Example of an expected software model layout.

- Economiser
  - Finned tube heat exchanger was set up similarly to a superheater as described in Chapter 4.3.
  - The economiser was described by the last heat exchanger characteristic chart under the list of superheater charts.
- Evaporator (Once-through boilers only)
  - Total heat transfer, which was calculated in a separate model, was added to a pipe component that represented the evaporator.
- Vessels
  - Vessels themselves were not included in the model, but the volume of any vessels in the steam path was accounted for to ensure volume inertia was represented.
  - The drum, and thus the drum level, for a drum-type boiler was excluded from the project and might need some additional investigation once a water-wall tube radiation model is developed for this type of boiler.

- Convective pass
    - All components that make up the superheater and reheater heat exchangers in a boiler.
    - Appropriate heat exchanger characteristic charts were selected according to location and type.
- Attemperators
    - Introduced additional flow along the steam path at strategic locations between heat exchanger banks and was represented by mass source components.

4.4.1 Pressure drop

Pressure drop was not investigated in this project and thus not explained or modelled accurately. The impact of pressure on heat transfer however, was significant. It was therefore decided to include a relatively accurate pressure drop to each of the heat exchangers by manually changing the surface roughness and K values for each.

Due to the geometrical simplicity of how the evaporator model was represented in the Flownex model, the total pressure drop calculation was not sufficient. The boiler inlet pressure therefore was set slightly lower than design to ensure the required superheater pressure was obtained in order to achieve optimal results in the convective pass. This could be as a result of the elevation difference between the inlet and outlet of the evaporator which was ignored.

4.5 Transient scenarios

Illustrating the transient capabilities of the boiler model was done by running transient scenarios on both a single heat exchanger and a complete superheater consisting of three heat exchangers in series with a single reheater installed within. The aim of the transient testing was to prove that the model is capable of simulating various transient characteristics on a high level and these characteristics are described below. The results were evaluated against expected trends rather than actual plant conditions because of the lack of an integrated control system. An integrated control system would manipulate multiple process properties simultaneously during a transient scenario and thus lead to unnecessary complexities.

4.5.1 Thermal mass inertia

Thermal mass inertia [TMI] is a term describing the delay in response time of the boiler model outputs after an operating condition changed and is caused by the huge mass of steel and water volume in modern boilers that contribute a significant overall thermal inertia. To accurately represent the thermal inertia caused by the mass of the steel in transient calculations and incorporate the thermal delay, the heat capacities of the various heat exchangers were calculated. Heat capacity is defined as the product of the material mass and the specific heat of the material at a specific temperature. The approximate specific heat values of typical boiler tube materials are shown in Table 4-3 below.

Table 4-3: Approximate specific heat values for typical boiler tubes. [8]

Temperature	**200°C**	**300°C**	**400°C**	**500°C**
Heat Capacity [J/gK]	0.50	0.54	0.63	0.71

Two sets of transient simulations were run on a single heat exchanger. In the first scenario, the heat capacity of the heat exchanger was ignored completely, which effectively meant any change in flue gas temperature for instance was immediately transferred directly to the steam temperature. The second scenario included an approximate heat capacity of an actual boiler tube and thus attempted to represent how an actual heat exchanger responds. The values of the heat capacities are shown in Table 4-4.

Table 4-4: Heat capacities for two different scenarios.

Scenario	Material heat capacity [kJ/K]
TMD – Not included	0
TMD – Included	165 000

Volume flow inertia

Plant layout and geometry also plays a role in transient reaction. The flow of water and steam through the volume of the headers, tubes and connecting pipes creates a delay in model output response. Although small when compared to TMI, the volume of all applicable plant for both fluid streams needs to be accounted for to ensure optimal results. This aspect of boiler geometry was included in all transient simulations, but was not tested separately. It is automatically considered by the Flownex solver.

4.5.2 Steam temperature control

The complete power station simulation model will be integrated with a distributed control system [DCS] that will be developed in Flownex. This control system will be developed to control system and sub-system inputs and set-points based on measured outputs and set-points of other systems in the same way an actual power plant is controlled. A good example of this is the spraywater control valves which regulate the mass flow rate of spraywater. The valve position and thus flow rate is controlled by temperature measurements downstream of the valves. Using the rate of change in temperature and actual temperature difference between the measured and the set-point value, a proportional-integral-derivative [PID] controller calculates an output value which manipulates the valve position to best control flow rate and thus steam temperature.

It is crucial from the global objective point of view that all systems are controllable by the developed DCS. It was thus proved that the boiler model can in principle comply with the control philosophy of a DCS. The boiler needs to deliver steam at a specified temperature and pressure regardless of other plant conditions and within certain upper and lower boundaries. As a result of complexities in plant layout, physical properties and lack of an operational control system, the compliance to control requirements was tested on a very simplified scenario on a proof of concept principle. A Simple PID component was set up to control the superheater outlet temperature by manipulating the spraywater flow rate in the final attemperator. Successful control of steam temperature in this simplified set-up implied that boiler control is possible with more complex control system set-ups.

5. Model evaluation and results

5.1 Evaporator model

The evaporator model was developed to calculate heat transfer and subsequently the inlet conditions to the superheater section of the boiler on once-through type boilers. This model was not used for drum-type boilers as the inlet conditions are known to be that of saturated steam. Data used for all calculations were obtained from the C-schedule and other design documents and not actual plant data. Various mill combinations can be simulated, but for the purpose of this project, the mill combinations were set to be the bottom rows of burners only. The model does, however, have the capability to adjust the firing combination should the need arise.

Figure 5-1 illustrates the comparison between the calculated heat transfer distribution profile to a single tube and the heat transfer profile to the height of the boiler as per design documentation [27].

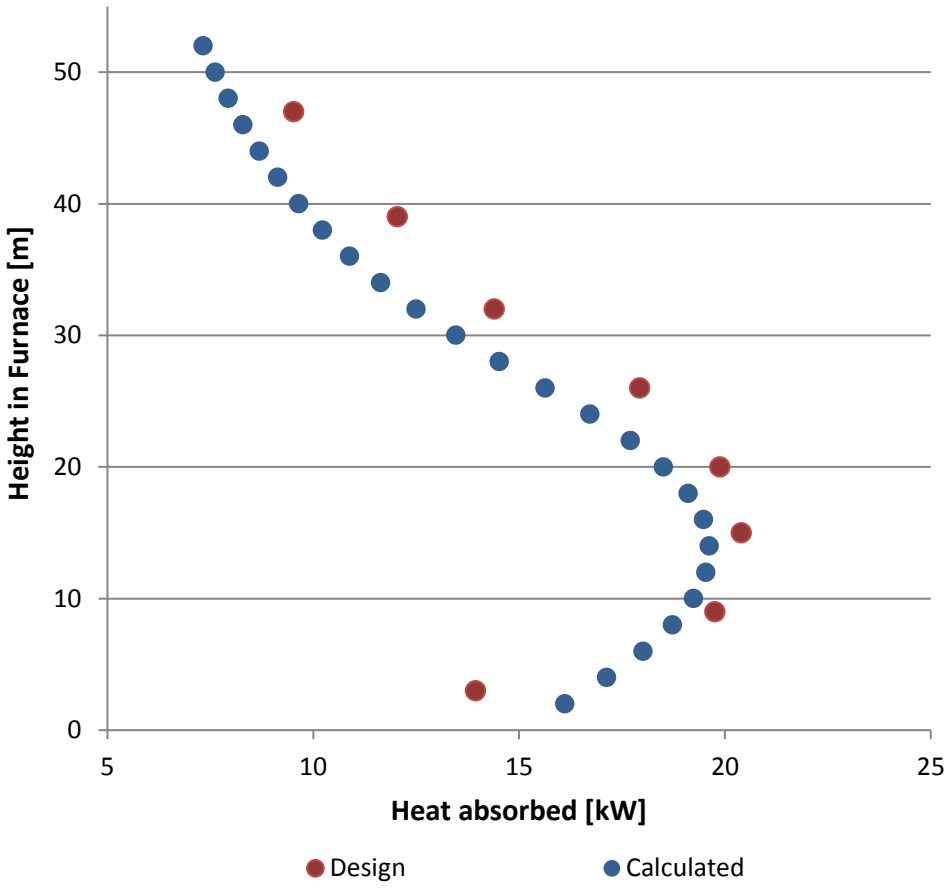

Figure 5-1: Heat transfer profiles of design data versus calculated data for PS-13.

There is a slight discrepancy between calculated and design data as the exact geometry was not modelled and the design data was manipulated slightly. This, however, proved that the results yielded by the model were representative of what is expected in an actual furnace. The heat transfer to additional tubes which was not included in the evaporator model was equally divided across the total length of tube. The additional tubes were excluded due to geometrical complications.

Integration across the profile yielded the total heat transfer to the tube, which was extrapolated to the total number of tubes. This process was repeated for all load cases for which operating data was available and total heat transfer profile created.

5.1.1 Evaporator results for PS-12 and PS-13

The flame temperatures calculated for various load set-points were used in the evaporator model to determine the inlet temperature to the superheaters. The flame temperatures for both power stations are illustrated in Figure 5-2.

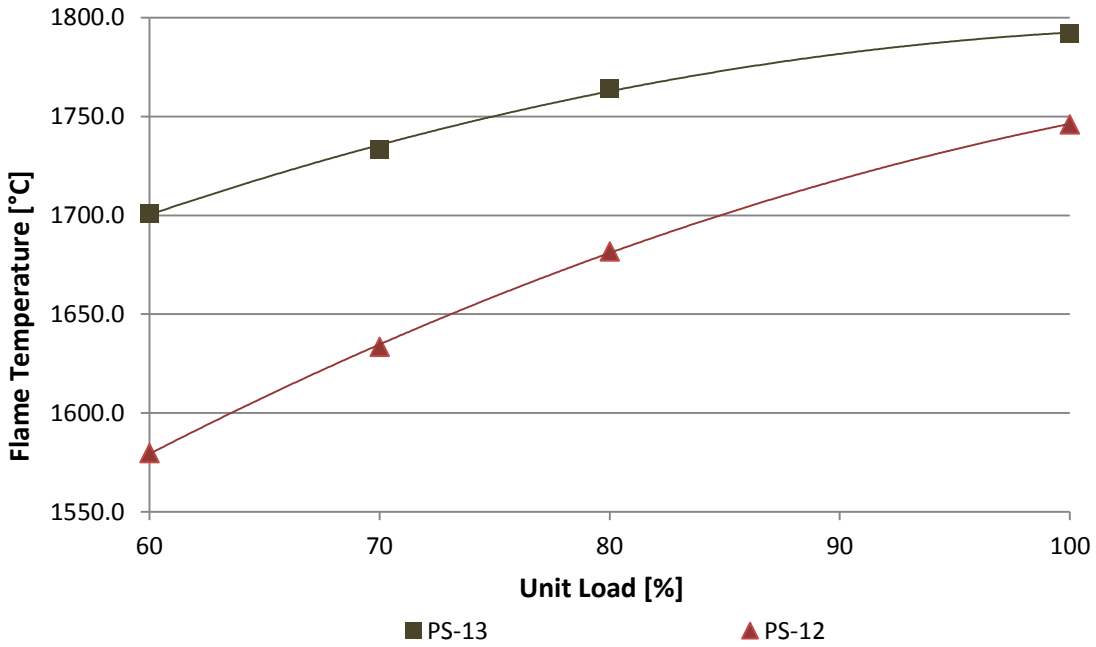

Figure 5-2: Flame temperature results for various loads at PS-12 and PS-13.

Using the above flame temperatures, the heat transfer was calculated by adjusting the opacity factor to yield the desired steam inlet temperature to the first stage superheater. The design and actual values for heat absorbed and opacity factor was evaluated and results are plotted in Figure 5-3.

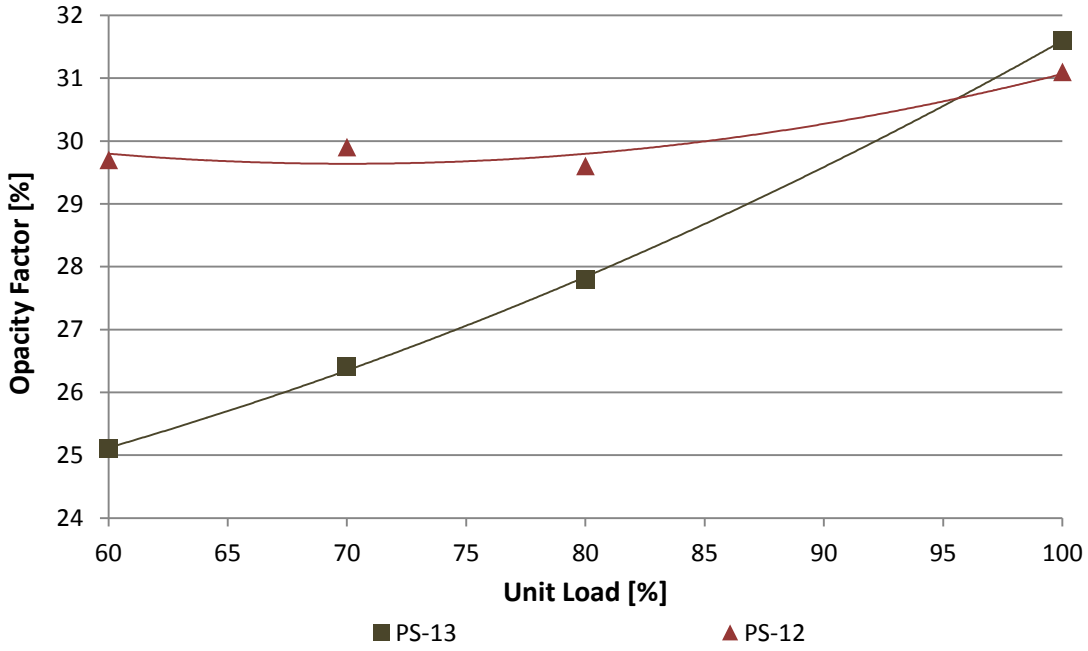

Figure 5-3: Opacity factor results for evaporator models on PS-13 and PS-12.

To verify the accuracy of results, the furnace exit temperature (FET) was calculated using the flame temperature and the associated heat transfer value calculated by the model. This was evaluated against the FET values given in the design documentation and results are plotted in Figure 5-4.

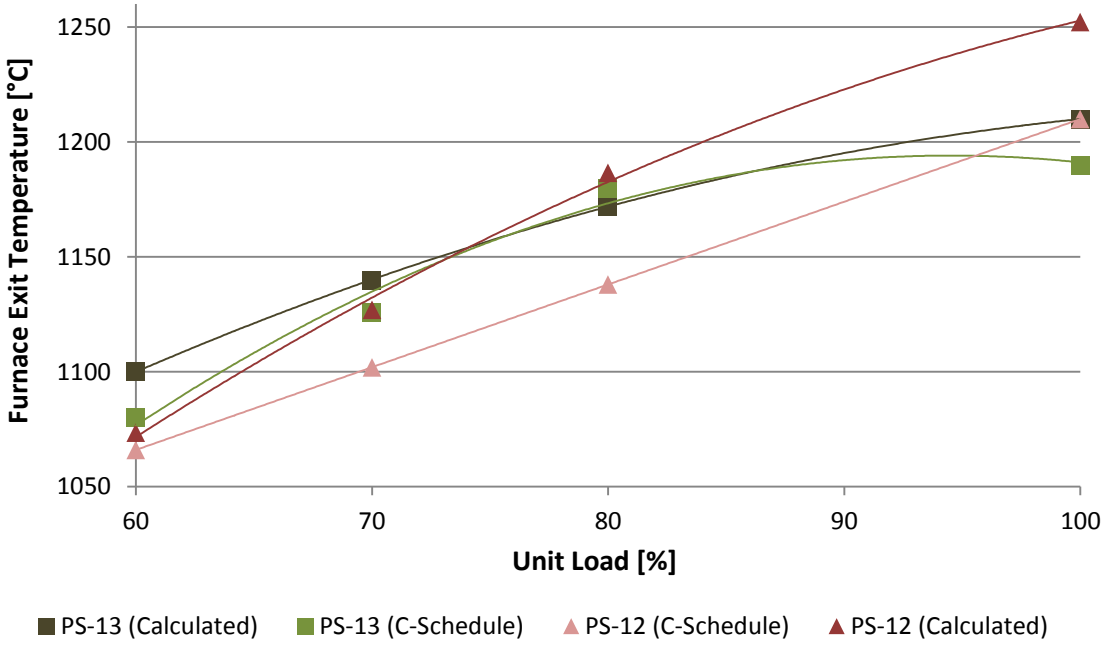

Figure 5-4: Design versus calculated FET for PS-13 and PS-12.

5.1.2 Conclusions

One of the major drawbacks of this model was the need to have access to geometrical and process information regarding the evaporator. The total length of tube and number of tubes was essential and often information that was not easily accessible. The opacity factor of the model also had to be re-calibrated at various loads which mean that a single model would not be sufficient for various load point simulations.

The validity of the model was illustrated in a couple of different ways: firstly it was successful in calculating a heat transfer profile across the length of a single helical evaporator tube which generally matches that of the profile represented in the design documentation. Secondly it can be used to calculate total heat transfer by manipulating the opacity factor at various loads in order to yield appropriate evaporator outlet temperatures. Both the opacity factors at various loads, for various coal supplies, and the heat transfer profiles generated could be useful information for future work into the radiative heat transfer in coal-fired boiler furnaces.

An attempt was made to establish whether the opacity factor calculated for one boiler could be applied to another, but this didn't yield much success. It was however not done on boilers with similar coal supply which could be the main reason for the difference. Similar coal and ash loadings could result in similar opacity factors and might be worth testing, but it was not done in this project.

5.2 Superheater model validation

An analytical and a Flownex model were developed for a fictitious heat exchanger scenario. Convection was assumed to be the only heat transfer mechanism at work. Identical geometrical, process and fluid properties were specified for both models to ensure comparability of solving methods and these are indicated in Figure 5-5 below.

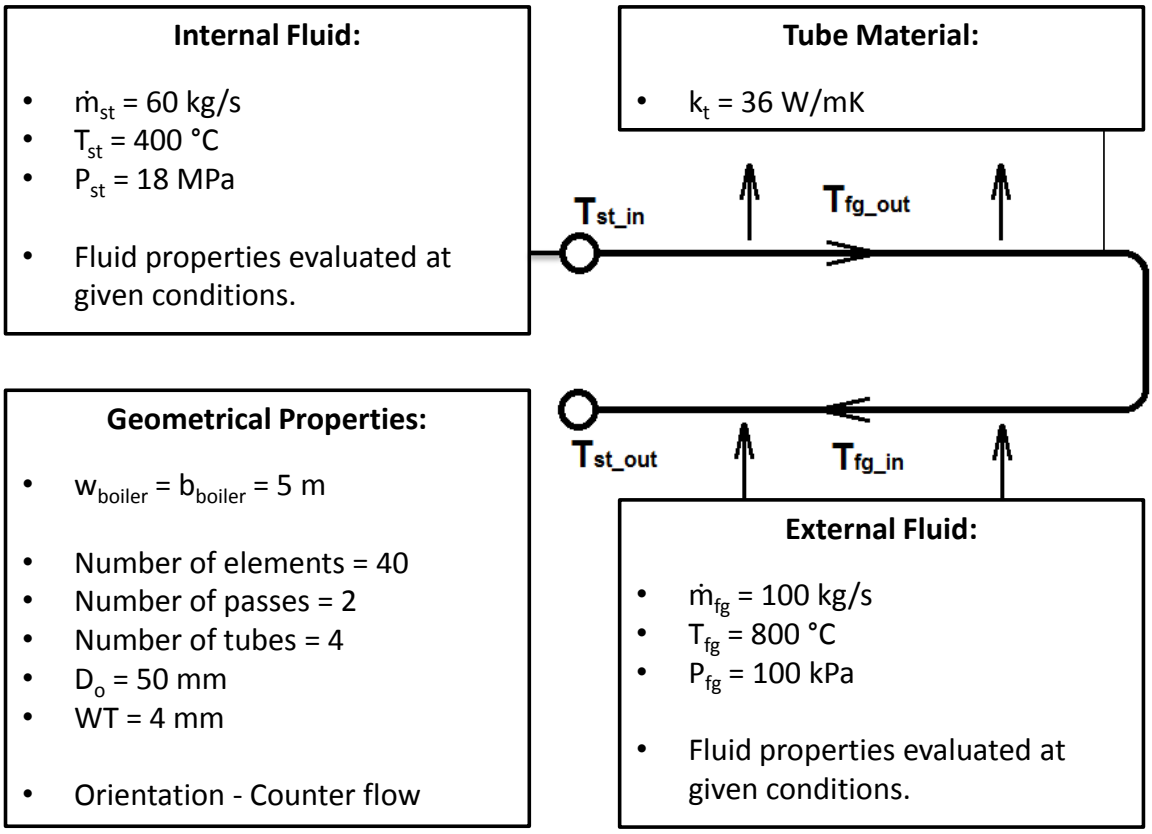

Figure 5-5: Input properties and layout for validation heat exchanger.

The analytical model was set up in two different ways: firstly solving the two pass heat exchanger with the effectiveness correlation for a single pass cross flow heat exchanger, and secondly split the two passes into two single pass heat exchangers and solved simultaneously. Fluid properties were assumed to be constant and calculated at inlet conditions for both streams. Custom fluids were developed in Flownex to ensure consistency across the models. The results obtained are indicated in Table 5-1.

Table 5-1: Results from superheater model validation.

Property	**Analytical model**	**Analytical model**	**Flownex model**
ε-correlation	**two single passes**	**single pass cross flow**	**-**
Q [MW]	3.86	3.859	3.861
$T_{st.out}$ [°C]	412.22	412.22	412.23
$T_{fg.out}$ [°C]	766.91	766.93	766.724
Effectiveness [-]	0.0426 per pass	0.083	0.083

The two analytical model results are similar because of the constant property fluids used. If real fluids were used, the successive single pass heat exchangers would yield different results. The results however, validated the solving methodology of Flownex and all further modelling was done on this platform.

It should be noted that the Flownex model does not use the ε-NTU method, but rather solves an internally discretized pipe network. The effectiveness is then calculated as a result. The fact that the results are so similar makes the Flownex model even more trustworthy.

5.3 Full heat exchanger in Flownex

The full detail single heat exchanger was the first attempt to model an actual heat exchanger as is used in coal-fired boilers. All heat exchangers of PS-13 were tested independently and input data for geometry, inlet fluid conditions and layout were acquired from the design documentation. An example of the model set-up for layout and fluid inputs is given in Figure 5-6. Geometrical inputs also form part of the set-up, although not shown in the figure.

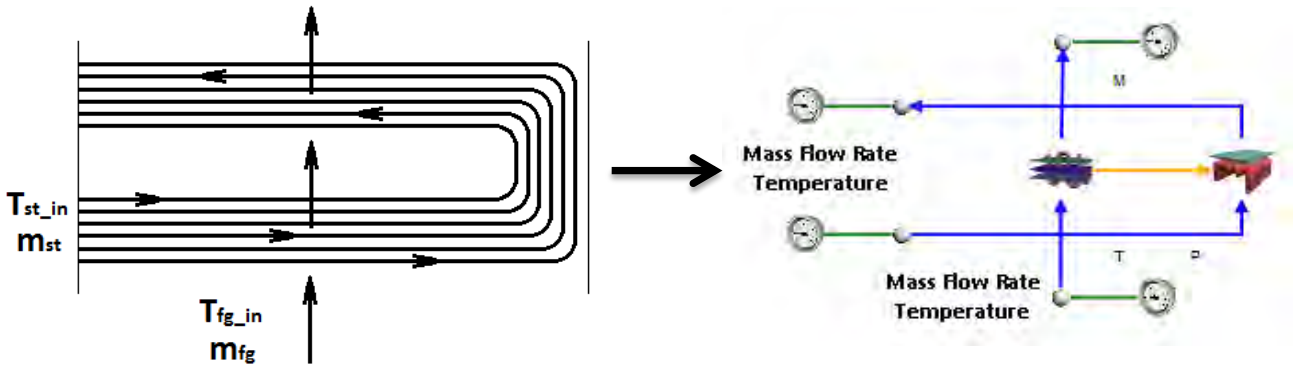

Figure 5-6: Heat exchanger set-up example showing inputs.

Accuracy of results yielded was evaluated against design data for fluid outlet temperatures and total heat transfer. The acquired results are given in Table 5-2, Table 5-3 and Table 5-4. Errors are calculated as follows:

$$\%_{Error\_Temp} = \left| \frac{T_{out.actual} - T_{out.design}}{T_{out.design} - T_{in.design}} \right| \quad (5\text{-}1)$$

$$\%_{Error\_Q} = \left| \frac{Q_{design} - Q_{actual}}{Q_{design}} \right| \quad (5\text{-}2)$$

Table 5-2: Steam conditions and error for all heat exchangers of PS-13 solved individually.

Heat Exchanger	Inlet Temp [°C] (Design)	Outlet Temp [°C] (Design)	Outlet Temp [°C] (Calculated)	Error [%]
Eco	249	287	292.9	
RH1	333	458	461.7	**2.96**
SH1	397	469	471.2	**3.06**
RH2	443	540	548.4	**8.66**
SH3	482	540	540.6	**1.03**
SH2	442	499	497.4	**2.81**

Table 5-3: Flue gas conditions and error for all heat exchangers of PS-13 solved individually.

Heat Exchanger	Inlet Temp [°C] (Design)	Outlet Temp [°C] (Design)	Outlet Temp [°C] (Calculated)	Error [%]
Eco	471	361	334.76	**23.85**
RH1	641	471	462.1	**5.24**
SH1	826	641	638.1	**1.57**
RH2	951	826	821.4	**3.68**
SH3	1062	951	958.3	**6.58**
SH2	1181	1062	1076.2	**11.93**

Table 5-4: Heat transfer and error for all heat exchangers of PS-13 solved individually.

Heat Exchanger	Heat Transfer [MW] (Design)	Heat Transfer [MW] (Calculated)	Error [%]
Eco	98.1	115.1	**17.33**
RH1	152	156.7	**3.09**
SH1	170	172.3	**1.35**
RH2	115	123.9	**7.74**
SH3	105	102.9	**2.00**
SH2	112	108.4	**3.21**

It is clear from the results that the boiler software model yields accurate results, especially when considering the amount of input data used to calculate the radiative heat transfer contribution to each heat exchanger. This proves that the model is sufficient in modelling individual heat exchangers.

The obvious concern is the accuracy of the results that economiser model yielded. The higher error could perhaps be contributed to the external fluid description as it was not modelled as an unmixed fluid, but rather a fully mixed fluid. The actual fluid could be considered a mix between unmixed and mixed due to the addition of fins to the tube, but was not modelled as such. No further investigation was done into the matter.

5.3.1 Effect of flue gas properties

All models used thus far use air as the external fluid for simplicity as it has similar gas properties to that of common flue gas. As explained in section 4.2.6, a test comparing results using air and representative flue gas was done to determine whether using air as a working fluid would suffice. The composition of the test flue gas is indicated in Table 5-5, which was directly used to define the custom fluid in Flownex.

Table 5-5: Gas composition values for external fluid evaluation.

Variable	**Ratio**
Ratio of water vapour [H_2O]	6%
Ratio of carbon dioxide [CO_2]	20%
Nitrogen [N_2]	69%
Oxygen [O_2]	5%

The results illustrated in Figure 5-7 compare the steam outlet temperature, flue gas outlet temperature and external heat transfer coefficient of two heat exchangers at various ends of the flue gas temperature range with each other.

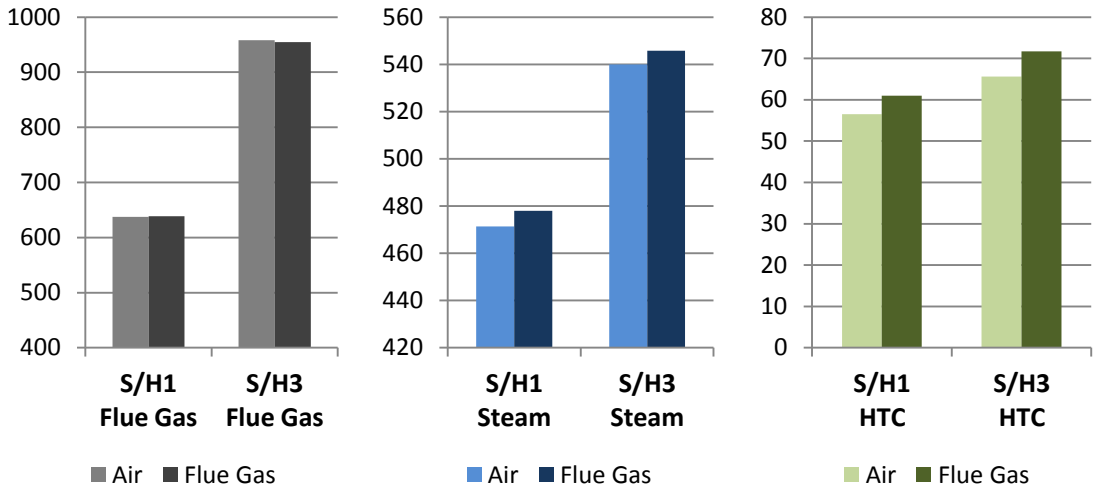

Figure 5-7: Comparative results of using air versus using flue gas as the external fluid.

The results indicate a larger heat transfer coefficient from the flue gas, resulting in higher steam temperatures. The difference is however fairly small in terms of steam outlet temperature, thus justifying the use of air as the external fluid for a generic model. The remainder of modelling was done using air.

5.4 Full boiler model steady state

Having already evaluated individual heat exchangers with acceptable results, the next step was to assemble a complete boiler model with all heat exchangers and subsystems included. This was done to evaluate the calculation methodology across the complete scope of a boiler system.

The main concern which needed to be addressed was how the propagation of errors will impact the final results when only high level properties such as inlet and outlet temperatures of the two fluids were evaluated. The net-effect of small errors in sequential heat exchangers could be magnified as all heat exchangers are inter-connected and individual heat exchanger outputs could have a significant effect on the surrounding heat exchangers. A small error on outlet temperature, for example, is transferred to the downstream heat exchanger inlet conditions and this process continues throughout the boiler.

5.4.1 PS-13 boiler model

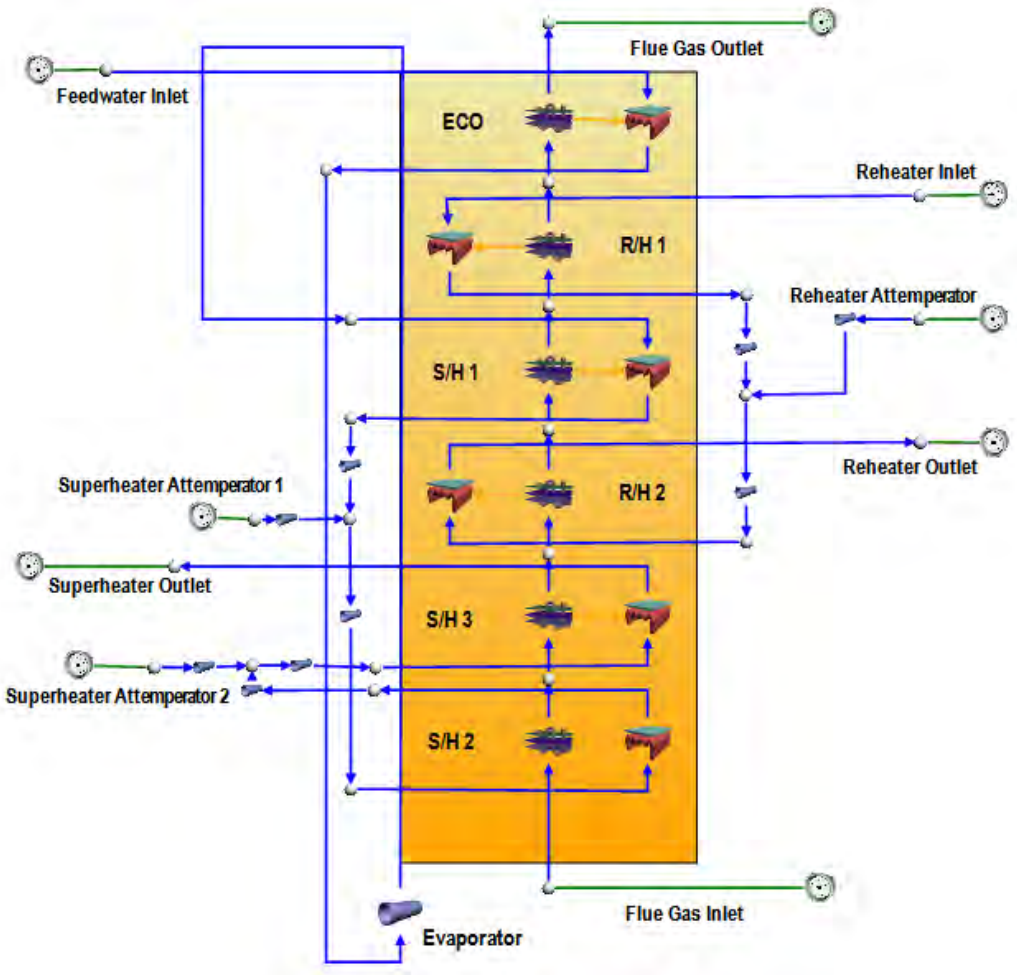

Figure 5-8: Model set-up for steady state modelling on PS-13.

Full load – 100% MCR

PS-13 consists of a HP cycle that includes an economiser, an evaporator and a three stage superheater with two attemperators. It also utilises a two stage reheater with a single attemperator for the LP cycle as is illustrated in Figure 5-8. There were thus 12 sets of water-steam and seven sets of flue gas temperature results to compare with design data. The comparison of the results against design data is illustrated in Figure 5-9 and Figure 5-10.

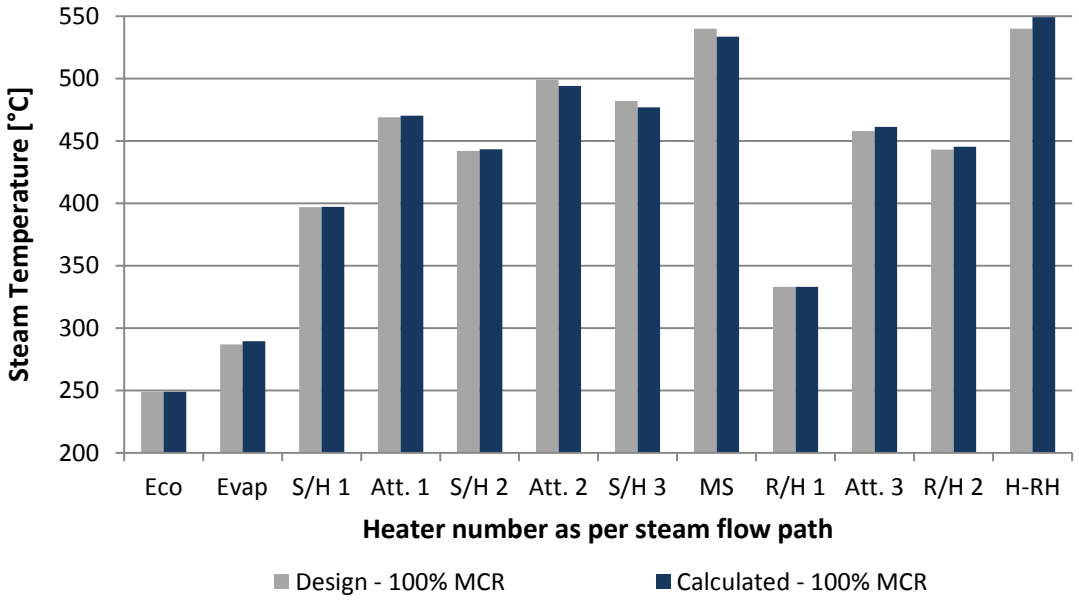

Figure 5-9: Steam temperature comparison for PS-13 superheater and reheater at 100% MCR.

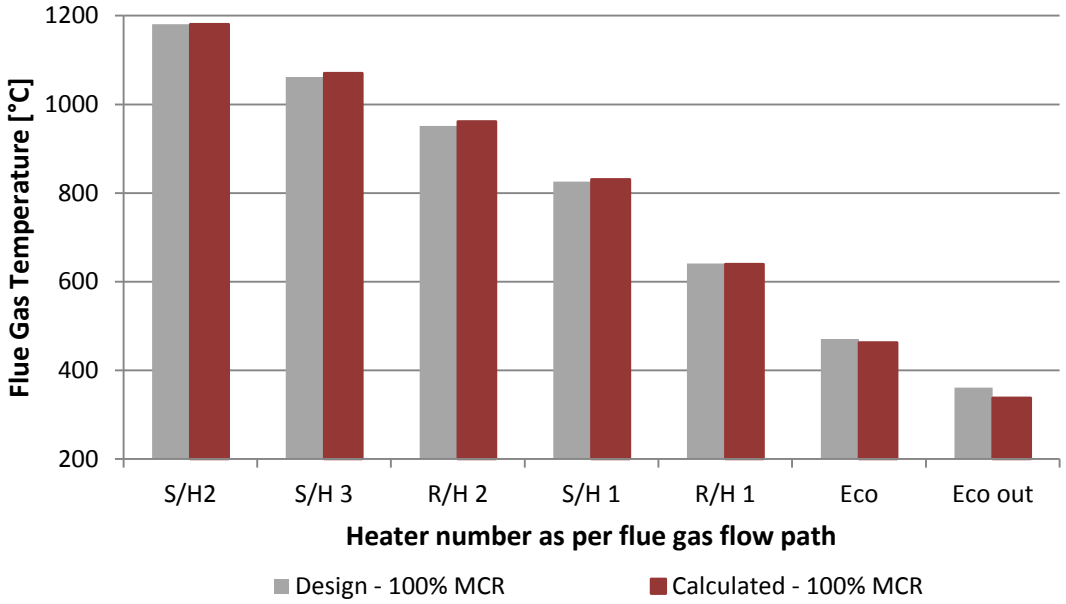

Figure 5-10: Flue gas temperature comparison for PS-13 at 100% MCR.

Low load - 60% MCR

A similar process was followed for evaluating the model at operating conditions for lower loads. The lowest load for which design data was available is 60% MCR. Similar to the full load evaluation results, the low load comparison results are illustrated in Figure 5-11 and Figure 5-12:

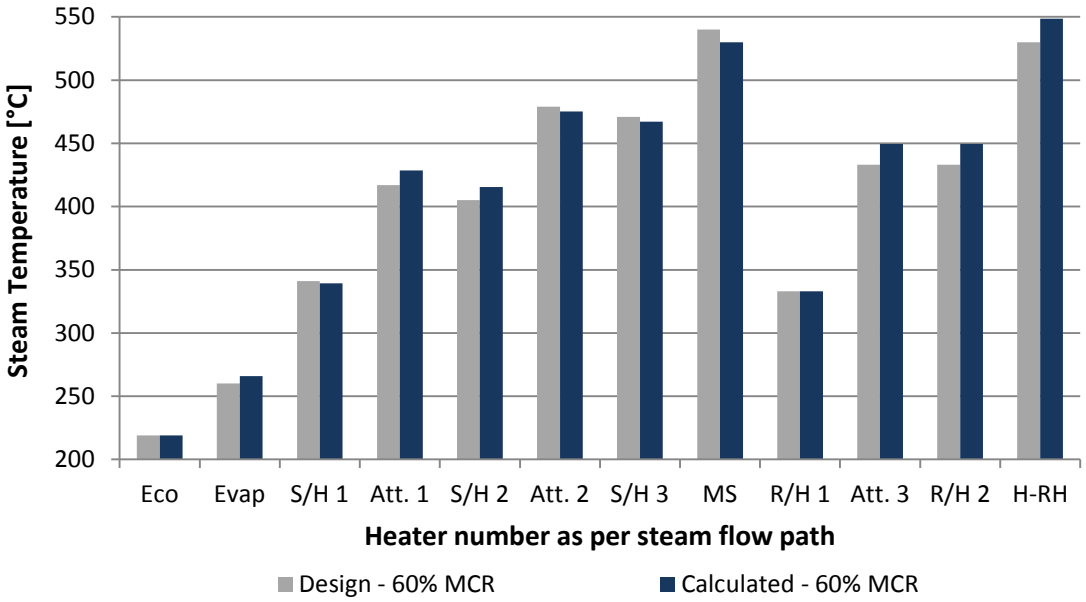

Figure 5-11: Steam temperature comparison for PS-13 superheater and reheater at 60% MCR.

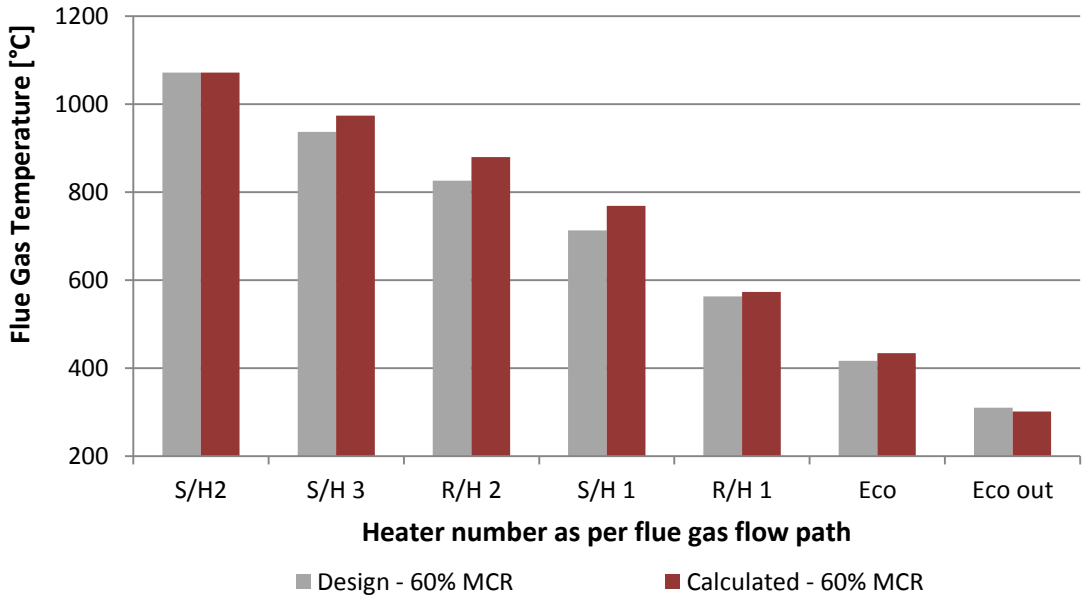

Figure 5-12: Flue gas temperature comparison for PS-13 at 60% MCR.

5.4.2 PS-04 Unit 1 boiler model

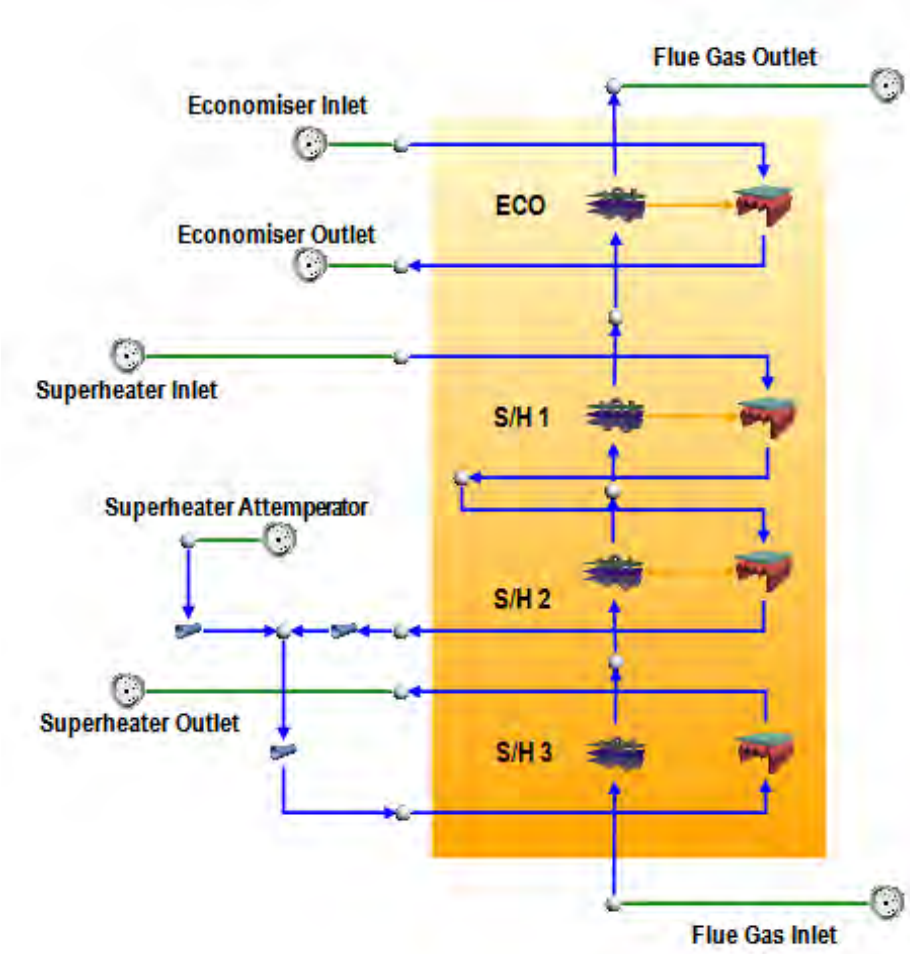

Figure 5-13: Model set-up for steady-state modelling on PS-04.

The methodology for the small group of boilers was evaluated against design data from PS-04 Power Station, Unit 1. Design data for the older, smaller power stations were not as detailed as the newer stations and there were thus fewer results to compare. This is a drum-type boiler, hence no evaporator was modelled.

Full load – 100%MCR

PS-04 Unit 1 utilises four heat exchangers as is illustrated in Figure 5-13. The design data was analysed and the appropriate heat exchanger characteristic charts were selected based on flue gas temperatures. This boiler was selected as it was one of few where flue gas velocity design values could be obtained. Heat exchanger charts were developed for an average velocity of 9m/s as the design velocity of PS-04 was substantially lower.

The economiser and superheater are modelled as two separate systems with the inlet conditions to the superheater accepted as saturation and the appropriate temperature calculated for the given pressure. The results are illustrated in Figure 5-14 and Figure 5-15 below.

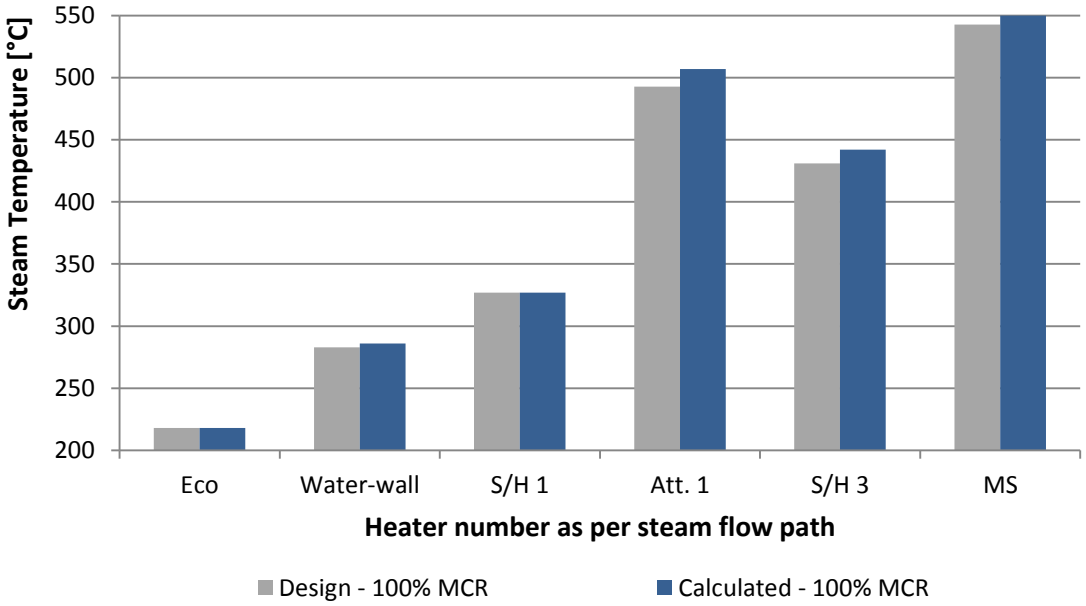

Figure 5-14: Steam temperature comparison for PS-04 superheater at 100% MCR.

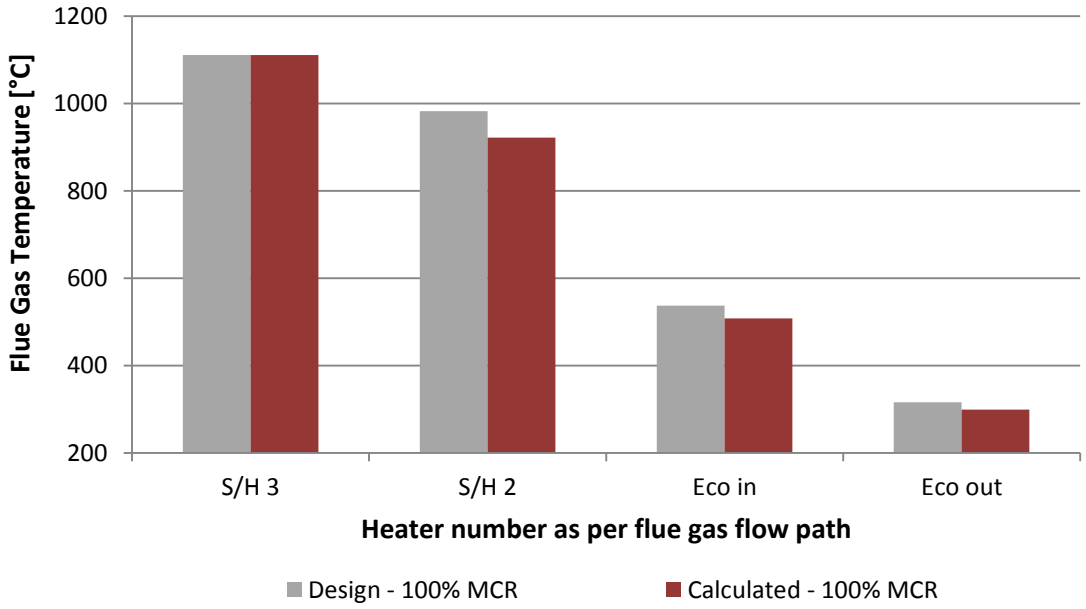

Figure 5-15: Flue gas temperature comparison for PS-04 at 100% MCR.

Low load – 60% MCR

A similar process was followed for evaluating the model at operating conditions for lower loads. The low load comparison results are illustrated in Figure 5-16 and Figure 5-17.

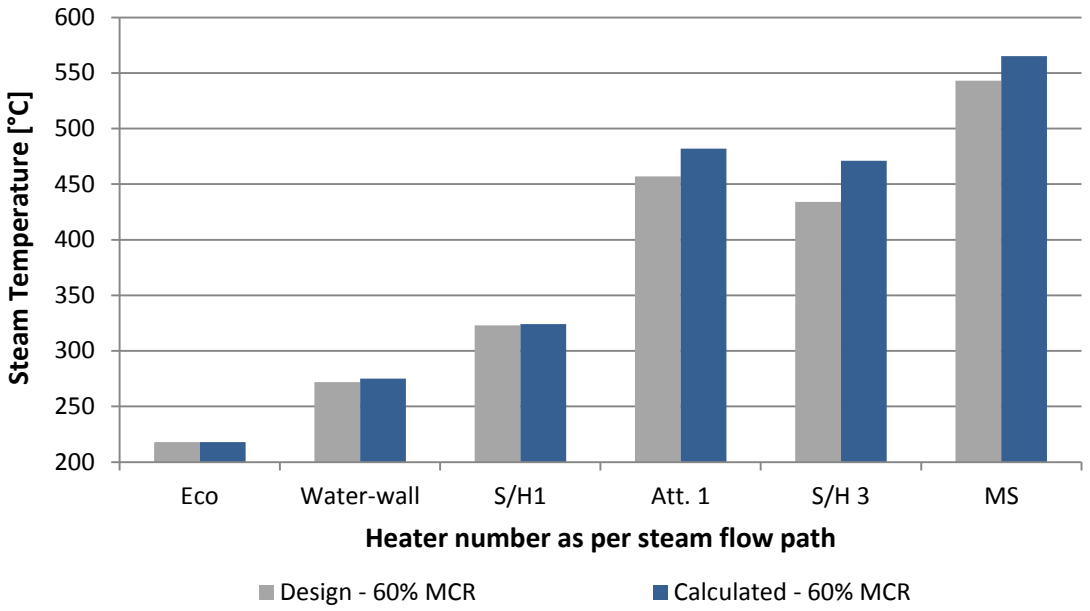

Figure 5-16: Steam temperature comparison for PS-04 superheater at 60% MCR.

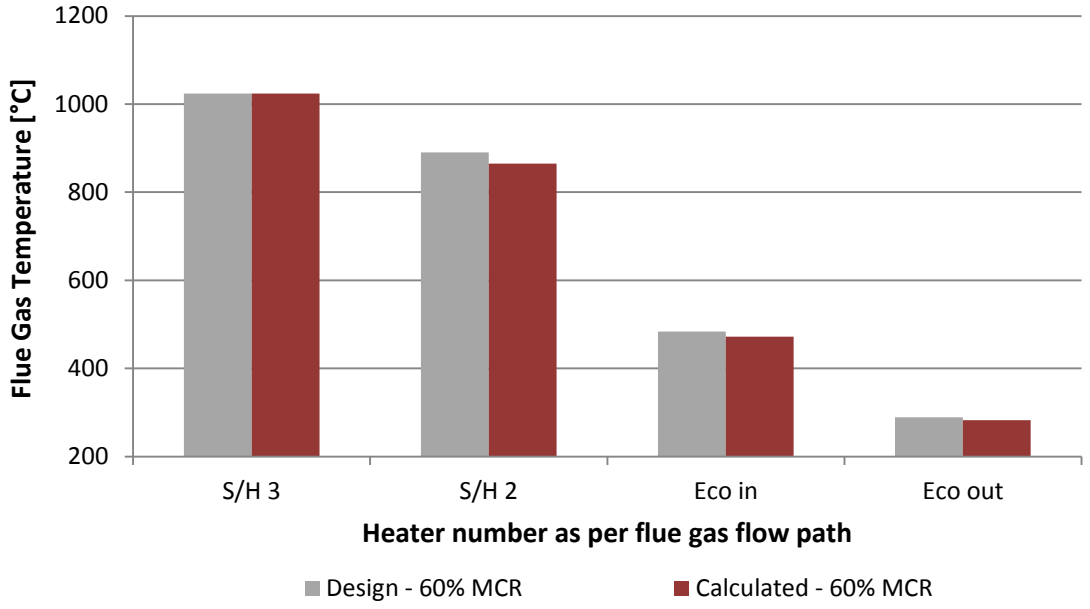

Figure 5-17: Flue gas temperature comparison for PS-04 at 60% MCR.

5.5 Summary of steady-state results

It is clear from the results that the smaller power stations yielded less accurate results. This is partly due to the amount of design data available, thus averaging errors across multiple heat exchangers became more significant. Design data for flue gas velocities also indicated that a representable value was not as easy to obtain as velocities tend to vary more through the heat exchangers of the convective pass.

Due to the fact that the test of a complete set of heat exchangers forming a boiler is not as controlled as the test of a single heat exchanger, the error was a function of two variables. The two variables were the inlet and outlet temperatures of both fluids and either could inherently have some error. The range of errors was thus expected to be wider.

The following is a summary of all the results obtained for steady state modelling on different boiler designs and at different loads. The accuracy of the results are illustrated in Figure 5-18 and Figure 5-19 and evaluated against the error which is calculated as follows.

$$\%_{Error} = \left| \frac{T_{in.actual} - T_{in.design}}{T_{in.design} - T_{out.design}} \right| \quad (5\text{-}3)$$

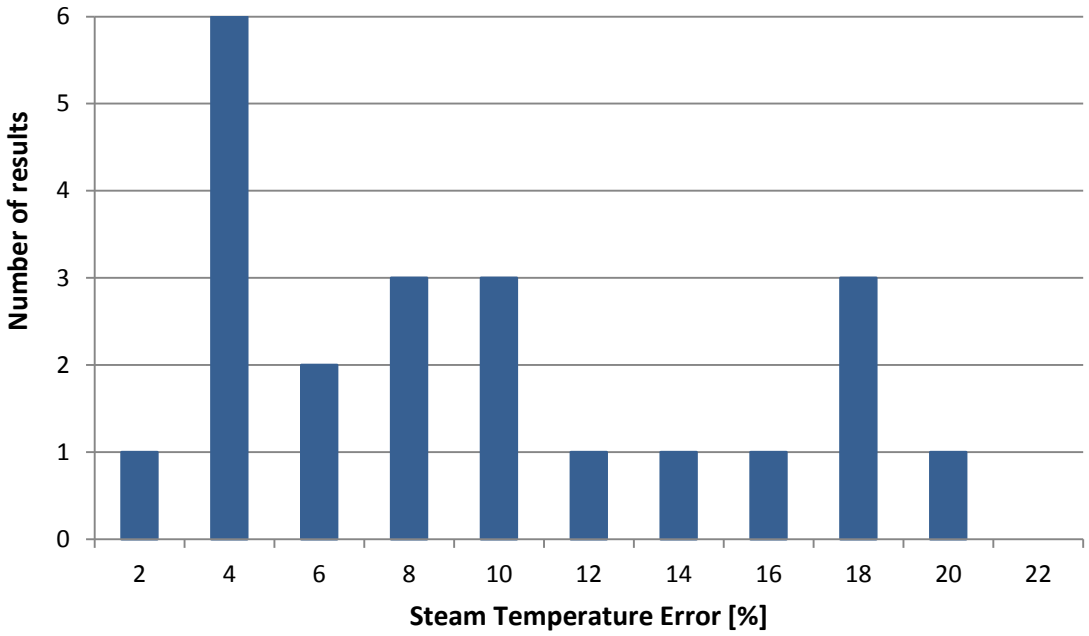

Figure 5-18: Histogram of errors in steam temperature results.

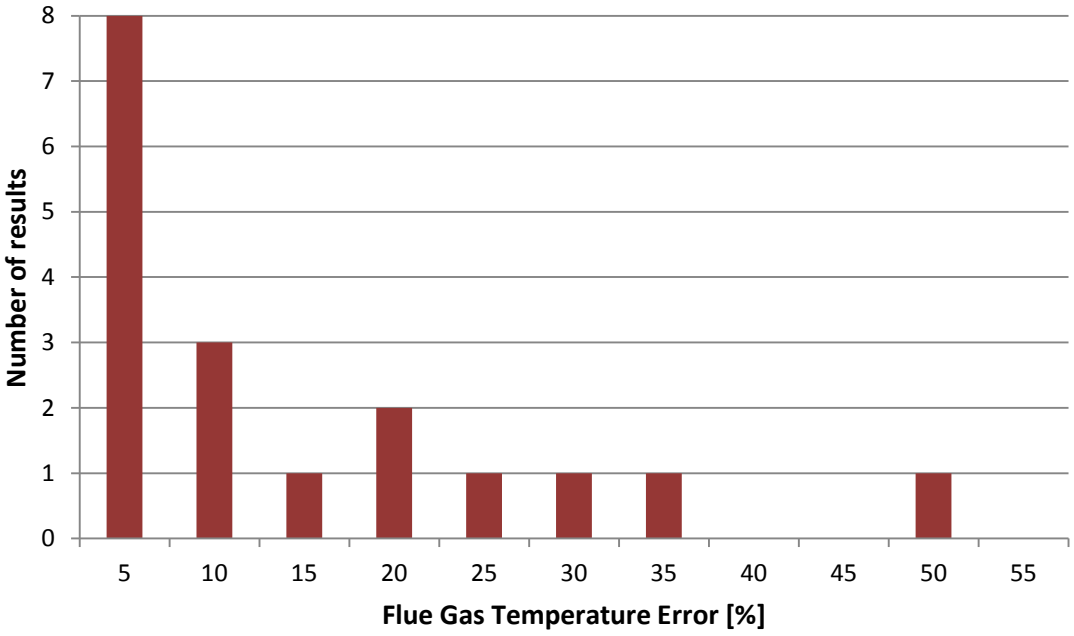

Figure 5-19: Histogram of errors in flue gas temperature results.

The average errors of individually evaluated heat exchangers are compared to that of heat exchangers evaluated as an integrated set and the comparison is illustrated in Figure 5-20.

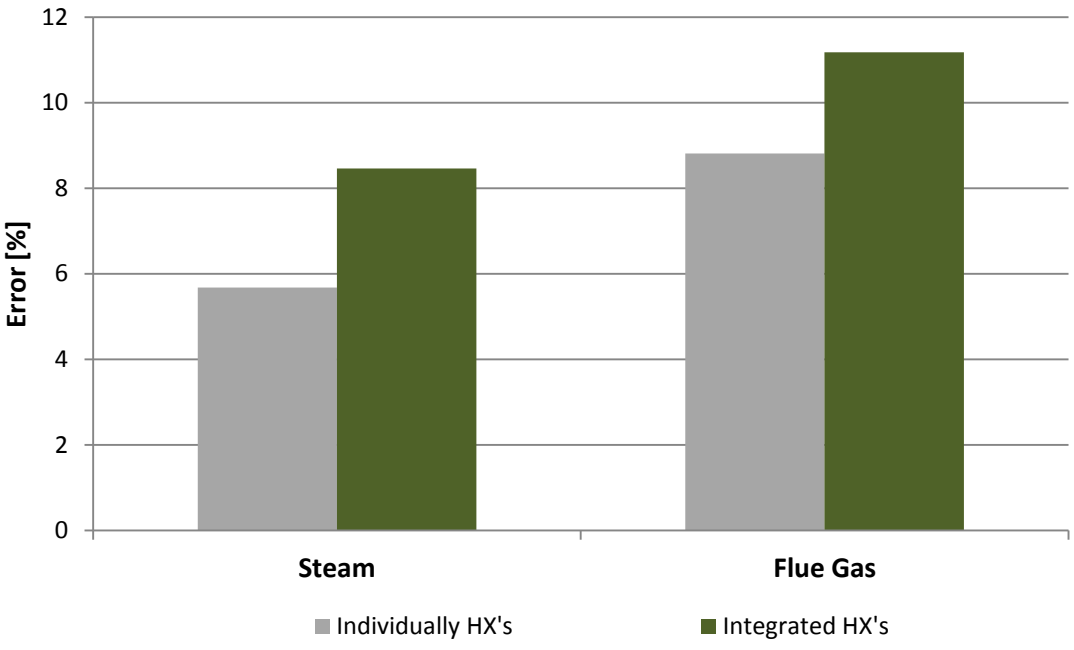

Figure 5-20: Error comparison between individual and integrated heat exchangers.

The results above illustrate the role that error propagation plays in the integrated set of heat exchangers. One of the main contributing factors to the wider error range is the calculated inlet conditions that are a function of the upstream heat exchangers.

5.6 Transient simulation results

5.6.1 Thermal mass inertia

The effect of thermal mass inertia on the outlet temperature response during transient conditions was tested on an actual heat exchanger from PS-13. The temperatures indicated represent the temperature inside the outlet header and volume flow delays were thus limited to only that of the tubes.

The transient scenario triggered a flue gas inlet temperature step-change from 825°C down to 600°C at a time of 0 seconds while all other operating conditions remained constant. A temperature step change which occurs instantaneously, like modelled here, is not realistic but it enables evaluation of the output and visualisation of the effect of TMI more effectively. This is important as, firstly, the temperature change during actual plant incidents occurs too slowly to yield any significant evaluation data for TMI. Secondly, the process control system adjusts multiple parameters to control steam temperature and thus the effects of TMI is further disguised. The model was run for both sets of heat capacity values as mentioned earlier and the results are superimposed and illustrated in Figure 5-21.

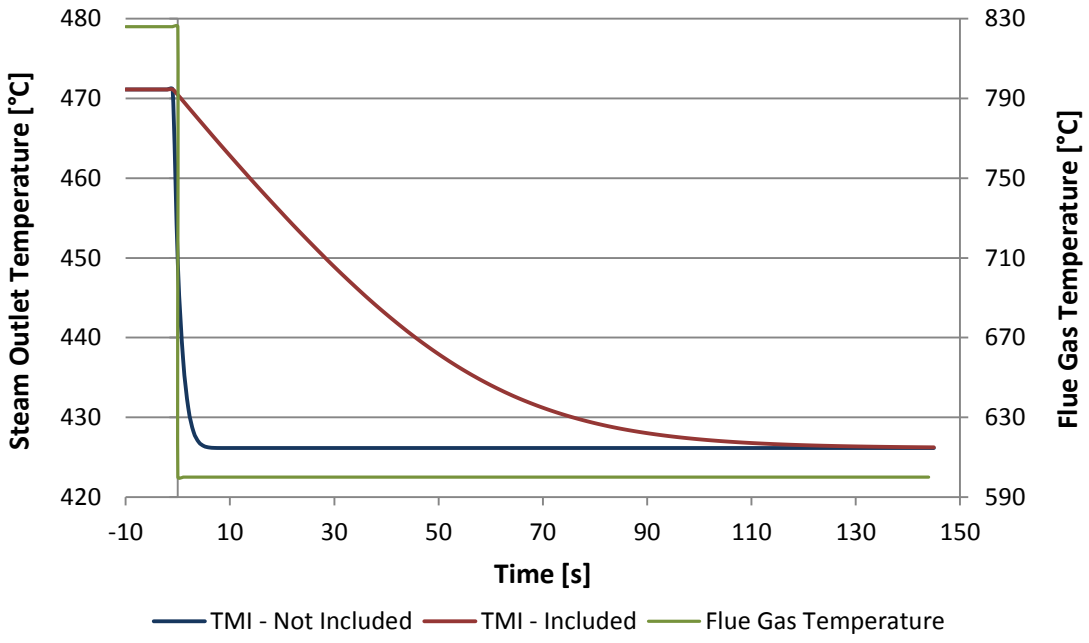

Figure 5-21: Results for transient simulation illustrating the effect of TMI.

The data representing the scenario where the TMI was not included displays a delay in temperature change of less than 10 seconds and which is exclusively due to the flow conditions of steam

throughout the tubes and into the outlet header. The data representing the scenario where the TMI was included shows a significant delay in response illustrating the effect of material mass on response time.

5.6.2 Steam temperature control

In proving controllability of the boiler model, a transient scenario was set up. The model was based on a PS-13 superheater and consisted of three superheater heat exchangers in series with a reheater heat exchanger in between. Figure 5-22 below illustrates the physical set-up of the model along with the location of the PID controller and associated inputs and outputs connected to it.

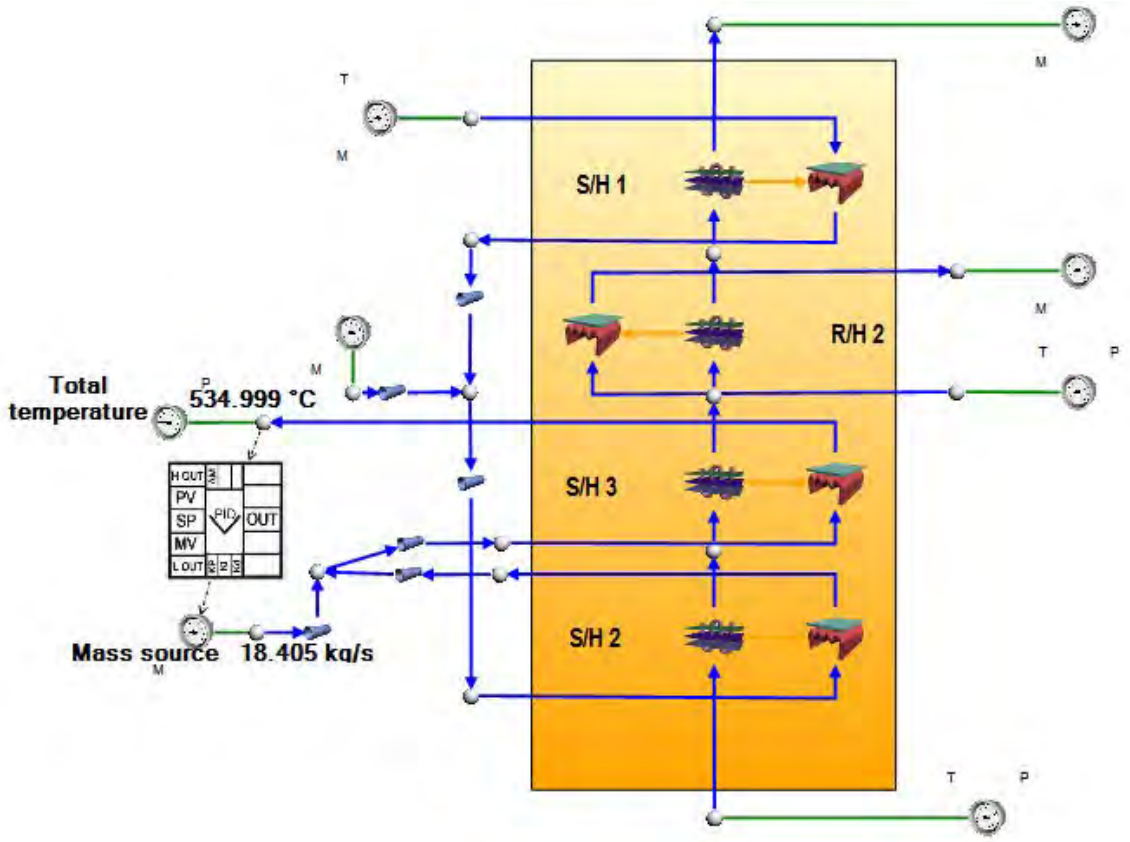

Figure 5-22: Set-up of model for controller transient test.

The steam inlet flow rate was given a step change from 536kg/s down to 520kg/s over a period of 16 seconds while the flue gas conditions remained unchanged. The lower flow rate led to an increase in steam temperature to above the set-point of 535°C. The ability of the PID controller to adjust the spraywater flow rate to manipulate the steam temperature back to the set-point was tested in the transient scenario and the results are given below.

The results are plotted from 100 seconds before initiation of the transient and until the control has restored to a steady-state operation.

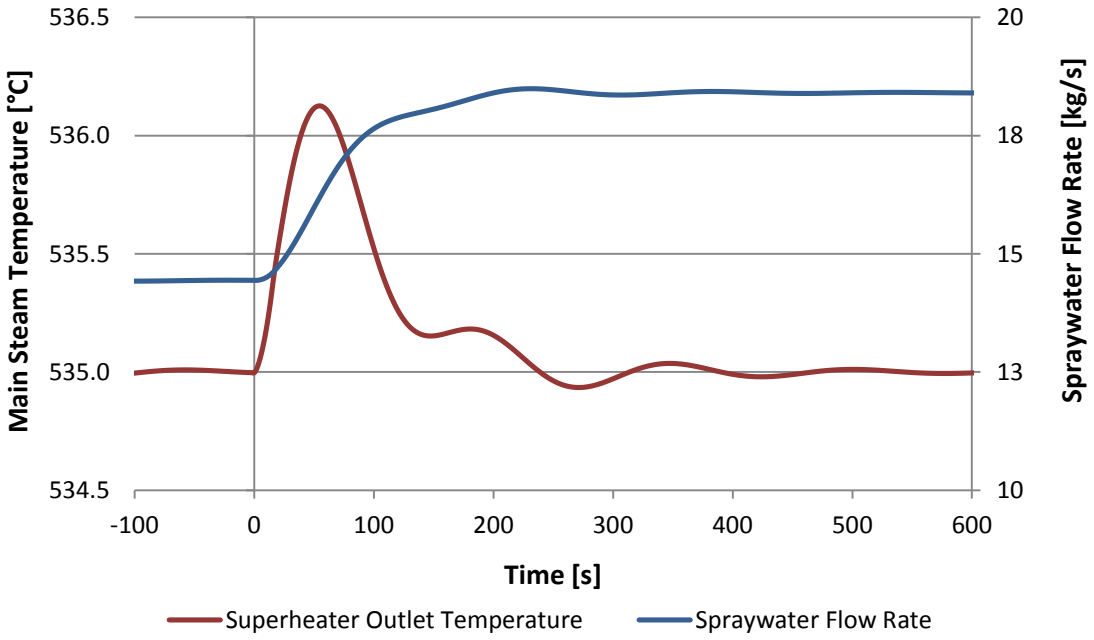

Figure 5-23: Results from transient simulation testing control.

It is clear from Figure 5-23 above that the simple control component was capable of controlling the steam temperature similarly to how an actual boiler is controlled. Although it was not evaluated against actual plant data, this in principle proves that the boiler model complies to control requirements of the final coal-fired power station model.

The oscillations are also to be expected, since the measurement point is a distance downstream of the attemperation. There is thus a feedback delay which will naturally cause the controller to slightly overcompensate. With proper control tuning, this can be minimized.

6. Conclusion and recommendations

6.1 General

The requirement of the Energy Efficiency Centre for a modelling methodology describing the process of developing an operational boiler software model that can be included in the full power station model was investigated. The model represented the complete convective pass as an integration of similar components with the evaporator or water-wall tubes included as a sub-component. The model is required to adhere to several requirements set by the research centre in order to be successfully integrated into the full power station model.

The boiler simulation model needed to be developed in Flownex, which is a thermo-hydraulic network solver, in which the full power station model will be developed. It needed to be a generic model capable of simulating results for the majority of boiler designs utilised in the Eskom fleet. The model had to be set up with relatively easily accessible process and geometrical input properties. Because the model will be used in a transient software model, important transient characteristics had to be accounted for to ensure that results are comparable to that of an actual boiler plant. The final power station model will be controlled by a DCS and thus sub-systems of the power station model needed to be individually controllable as well.

In order to meet all the requirements for the boiler model, several objectives were identified and organised systematically in order to guide the development process. Due to the generic nature of the model, knowledge of current operational boilers was essential to ensure all designs were accounted for in the modelling process. Plant documentation of as many boilers as possible was obtained and common process and geometrical properties applicable in heat transfer calculations were studied. It was identified that the total fleet could be split into two groups of boilers based on size which would distinguish between specific properties that impacted the modelling methodology or accuracy thereof. The two main properties were identified as whether the boiler utilises a reheat section or not and the number of heat exchangers utilised. It was shown in the study that similar types and sizes of boilers, as was grouped together, had many common characteristics which would be well represented by an average value trend calculated from design data from the two groups respectively.

A literature study was done on the different heat transfer mechanisms, where they are applicable in coal-fired boiler heat exchangers and how to model them. Analytical models of simplified heat exchangers were developed from the fundamental theoretical basics that were identified for all required locations and mechanisms. Accepted modelling methodologies were studied which also

attempted to model boilers from a high level point of view. The DimBo model was identified as another as it is simulates boilers, and heat exchangers, on a high level basis. One drawback is that it does not include all of the transient characteristics required by this project. Acquiring appropriate licencing to enable modelling using DimBo also becomes a problem and it was decided that actual plant design data is a better validation platform to evaluate results of analytical models, rather than unknown correlations utilised in DimBo.

The finned tube heat exchanger, which is a built-in Flownex component, was identified as the best way to model the layout and geometry of a typical coal-fired boiler heat exchanger as, amongst other things, it was developed for heat exchangers with similar flow conditions. It consists of two sub-components, one representing the water-steam flow inside the tubes and the other the flue gas flow around the tubes with either an overall counter or overall parallel flow orientation. The internal fluid was relatively straight-forward and solved as convective heat transfer to a fluid flowing inside a tube. The flow orientation of the external fluid was cross-flow across a bundle of tubes and a heat exchanger characteristic chart was used to calculate external heat transfer as a function of the Reynolds number of the fluid.

A heat exchanger characteristic chart representing convective heat transfer only was developed and used in simplified models similar to the analytical models as described above. Flownex results were validated against results from analytical models ensuring adherence to identified theoretical fundamentals. Various simplifications and assumptions were made in the validation process, such as simple geometry, constant property fluids and convection heat transfer only.

Following successful model validation, full detail heat exchangers and combinations of heat exchangers capturing the true geometries, fluid and flow conditions were developed including actual heat transfer on the external side. The external heat transfer was much more complex as a result of the high temperatures and the subsequent effect of radiation. The effect of radiation was calculated as a constant value per heat exchanger at specific locations along the flue gas path. It was calculated by average values of properties as obtained from boiler design data discussed earlier. Heat exchanger characteristic charts were developed for various locations along the flue gas path by adding the radiation constant to the convection component which is a function of the Reynolds number. Final steady-state models were evaluated against plant design data.

Transient capabilities were illustrated on single heat exchangers and combinations of heat exchangers respectively. Due to the lack of an actual operational control system and acceptable plant data, transient scenario results were evaluated against expected result trends as supposed to actual plant data.

Steady-state results for both fluid streams across both groups of boilers proved to be more accurate than was anticipated and thus fulfils the main objective of delivering a generic boiler model. The methodology to do this was explained in detail and it is expected that repeatability of the process when the model will eventually be implemented into the final software model should not become a concern. Various transient characteristics were captured and will be of great value when high-level plant transient analyses are run with all systems integrated together with the DCS.

6.1.1 Outliers, specific plant studies and limitations

Due to the fact that the main objective was not only a generic model, but the methodology to develop it, outliers or specific detail boiler studies would be possible as a result of this project. The term outlier is used for boilers with physical or process properties which do not match that of the trends illustrated for the groups of boilers in this project. Using plant specific trends as supposed to average trends, and following the process explained in this document, a boiler model can be developed for individual systems. This would be done when the boiler at hand has a substantially different layout or when very plant specific studies are done.

As a preceding step before the model is to be used within an integrated model, it is recommended that a sanity check be done on the boiler model, or individual heat exchanger, alone with some known system parameters to verify accuracy of model on specific study.

6.2 Future work

6.2.1 Radiation heat transfer

A full detail furnace heat transfer model needs to be developed. This model should be applicable to both once-through and drum-type boilers. This model should focus on direct radiation between the heat source and all surfaces in view of it. This should include the first few rows of heat exchanger tubes where direct radiative heat transfer is still significant.

The radiation model is sufficient for high level analyses, but full detail model could need to include the ash properties per heat exchanger. In order to do this significant knowledge of the coal and ash loadings and compositions is required. The method of how to implement this is described briefly in this document. Radiation is modelled based on full load data and this can cause some inaccuracies. The inaccuracies were not completely quantified and could become an issue, specifically in lower load studies. Future studies should consider modifying the heat exchanger chart in real time, based on prevailing flue gas temperatures and velocities.

Design data for plant geometry and operating conditions from older power stations were quite scarce. Simulating any of them with significant accuracy would require better representative data.

6.2.2 Model response and prediction

It is clear from the results obtained in the transient models that this methodology enables the user to simulate actual transient plant conditions. A study investigating the possibility of optimising plant control based on expected responses in specified plant conditions could be initiated. This study would predict heat exchanger or boiler response to a predetermined set of operating conditions and thereby adjust or optimise control parameters to prevent certain unwanted conditions from occurring. A good example of this would be to predict main steam temperature response to various furnace incidents and attempt to prevent excessively high temperatures with subsequent control optimisation.

6.2.3 Pressure drop

The pressure drop experienced in typical pipe flow scenarios was not investigated in any detail in this project. The fluid pressure, especially on the steam side, is a significant characteristic in terms of heat transfer and needs to be included in the final power station model. Further work is required to investigate and determine the best way to include the pressure drop in the heat exchangers in order to replace the assumed or manually set values with acceptable calculations.

7. List of References

[1] L. Jestin, M. Fawkes, B. Maccoll and M. Koko, “Eskom Power Platn Institute (EPPEI) 5-years research strategic plan.,” in *POWER-GEN AFRICA CONFERENCE*, Cape Town, 2014.

[2] Unknown, “Enhancements of Rankine Cycles [8.6],” MIT, [Online]. Available: http://web.mit.edu/16.unified/www/FALL/thermodynamics/notes/node66.html. [Accessed 12 05 2016].

[3] K. Rayaprolu, BOILERS for POWER and PROCESS, Taylor & Francis Group, 2009.

[4] C. Cantrell and S. Idem, “U-Tube Assembly Heat Exchanger Performance Analysis Using Cyclic Iteration,” *Heat Transfer Engineering,* pp. 1042-1060, 2010.

[5] “Reliance Tech-Service Co. Ltd,” [Online]. Available: http://reliance-techservice.com/fin_tubes.php. [Accessed 08 December 2015].

[6] “Industrial and Financial Corporation "MUST-IPRA",” 01 February 2009. [Online]. Available: http://www.must-ipra.com/?act=fullnews&id=2&lang=en. [Accessed 08 December 2015].

[7] L & C Steinmuller, “Description of Steam Generation Plant at PS-13,” N/A, Sandton, 1999.

[8] R. B. Dooley and W. P. McNaughton, EPRI: Boiler and Heat Recovery Steam Generator Tube Failures: Theory and Practice, vol. 1: Fundamentals, Charlotte: EPRI, 2007.

[9] Mannesmannröhren-Werke, High-Temperature Steels.

[10] K. C. Mills, L. Yuan and R. Jones, “Estimating the physical properties of slags,” *The Journal of The Southern African Institute of Mining and Metallurgy,* pp. 649-658, 2011.

[11] R. S. Subramanian, “Reynolds Number,” Department of Chemical and Biomolecular Engineering, Clarkson University, Clarkson .

[12] M-Tech industrial, “Flownex Library Manual,” 2014.

[13] F. P. Incropera, D. P. Dewitt, T. L. Bergman and A. S. Lavine, Fundamentals of Heat and Mass Transfer, John Wiley & Sons, 2007.

[14] F. Kreith, R. F. Boehm, G. D. Raithby, K. G. Hollands, N. V. Suryanarayana, M. F. Modest, V. P. Carey, J. C. Chen, N. Lior, R. K. Shah, K. J. Bell, R. J. Moffat, A. F. Mills, A. E. Bergles, L. W. Swanson, V. W. Antonetti, T. F. Irvine, Jr. and M. Capobianchi, Heat and Mass Transfer, CRC Press LLC, 1999.

[15] V. Gnielinski, "Heat Transfer in Cross-flow Around Single Tubes, Wires and Profiled Cylinders," in *VDI Heat Atlas*, 2nd ed., Düsseldorf, Springer, 2010, pp. 723-724.

[16] V. Gnielinski, "Heat Transfer in Cross-flow Around Single Rows of Tubes and Through Tube Bundles," in *VDI Heat Atlas*, 2nd ed., Düsseldorf, Springer, 2010, pp. 725-729.

[17] V. Gnielinski, "Heat Transfer in Pipe Flow," in *VDI Heat Atlas*, 2nd ed., Düsseldorf, Springer, 2007, pp. 693-751.

[18] R. Govindsamy, "Thermal Performance Evaluation of Heat Exchangers in Pulverised Coal Boilers," Johannesburg, 2013.

[19] D. Vortmeyer and S. Kabelac, "Gas Radiation: Radiation from Gas Mixtures," in *VDI Heat Atlas*, Second ed., Düsseldorf, Springer, 2010, pp. 979-988.

[20] D. Taler and J. Taler, "Simplified Analysis of Radiation Exchange in Boiler Superheaters," *Heat Transfer Engineering,* vol. 30, no. 8, pp. 601-609, 2009.

[21] L. I. Díez, C. Cortés and A. Campo, "Modelling of pulverized coal boilers: review and validation of on-line simulation techniques," *Applied Thermal Engineering,* pp. 1516-1533, 2005.

[22] H. Hausen, Heat Transfer in Counterflow, Parallel Flow and Cross Flow, McGraw-Hill, 1983.

[23] H.-G. Brummel, "Thermal Radiation of Gas-Solids-Dispersion," in *VDI Heat Atlas*, 2nd ed., Düsseldorf, Springer, 2010, pp. 989-999.

[24] F. P. Incropera, D. P. Dewitt, T. L. Bergman and A. S. Lavine, Principles of Heat and Mass Transfer Supplemental Material, 7th Edition ed.

[25] F. P. Incropera, D. P. DeWitt, T. L. Bergman and A. S. Lavine, Fundamentals of Heat and Mass Transfer.

[26] A. Zbogar and F. Frandsen, "Surface Emissivity of Coal Ashes," *IFRF Combustion Journal,* p. Article Number 200305, 2003.

[27] L & C Steinmuller, "C-Schedules: PS-13 Units 1-3," N/A, N/A, 1996.

[28] D. V. T. Sathyanathan, "Bright Hub Engineering," 20 10 2010. [Online]. Available: http://www.brighthubengineering.com/power-plants/61781-once-through-and-drum-type-boiler-designs-compared/.

[29] C. C. A. C. Luis I. Díez, "Modelling of pulverized coal boilers: review and validation of on-line simulation techniques.," *Applied Thermal Engineering,* vol. 25, no. 10, pp. 1516 - 1533, 2005.

[30] S. Kabelac and D. Vortmeyer, "Radiation of Surfaces," in *VDI Heat Atlas*, 2nd ed., Düsseldorf, Springer, 2010, pp. 947-959.

[31] D. Vortmeyer and S. Kabelac, "View Factors," in *VDI Heat Atlas*, 2nd ed., Düsseldorf, Springer, 2010, pp. 961-977.

[32] D. Taler, M. Trojan and J. M. Taler, "Mathematical Modeling of Cross-Flow Tube Heat Exchangers With a Complex Flow Arrangement," *Heat Transfer Engineering,* pp. 1334-1343, 2014.

[33] R. B. Dooley and W. P. McNaughton, EPRI: Boiler and Heat Recovery Steam Generator Tube Failures: Theory and Practic, Vols. 2: Water-Touched Tubes, Charlotte: EPRI, 2007.

[34] G. E. Dieter, Mechanical Metallurgy, London: McGraw-Hill, 1988.

[35] K. Mills, "The estimation of slag properties," Imperial College, London, 2011.

[36] K. G. Schmidt, "Heat Transfer to Finned Tubes," in *VDI Heat Atlas*, 2nd ed., Düsseldorf, Springer, 2010, pp. 1273-1418.

[37] G. V. u. C. (. Editor, VDI Heat Atlas, Berlin - Heidelberg: Springer, 2010.

[38] "Basic Electricity," [Online]. Available: http://www.energy.gov.za/files/electricity_frame.html. [Accessed 18 November 2015].

[39] "SouthAfrica.info," 27 November 2012. [Online]. Available: http://www.southafrica.info/business/economy/infrastructure/energy.htm#.VkyMfXYrLIU. [Accessed 18 November 2015].

[40] Energy 2D, The Concord Consortium, [Online]. Available: http://energy.concord.org/energy2d/prandtl.html. [Accessed 08 December 2015].

Appendix A. Finned tube heat exchanger set-up

The following paragraphs will look at the important variables to take note of when developing a heat exchanger in Flownex using a finned tube heat exchanger:

Finned tube heat exchanger – Primary side

The table below illustrates all the various inputs that are required when setting up the flue gas side of the finned tube heat exchanger.

Table A 1: Set-up for primary finned tube heat exchanger.

Property:	**Comment**	**Options**
Fluids:		
Fluid data reference	Select appropriate fluid from list of fluids or develop custom fluid.	Air / Gasses (Pure fluids) or custom flue gas fluid.
Heat Transfer and Friction Factor Data:		
Characteristic Chart	Select appropriate number of heat exchanger for specific boiler from drop down menu. Select heat exchanger with closest flue gas temperature from Chapter 4.2.4. If not available, populate it from Appendix B.	Boiler 300+ SH Boiler 300+ RH Boiler 300-
Geometry:		
Flow Direction	Overall flow direction of heat exchanger.	Counter / Parallel
Heat transfer area	Total external tube surface area from design data or as calculated.	
Area ratio	Ratio of external to internal tube surface.	Can use 1.1 for normal, un-finned tubes. Calculate for finned tubes.

Material Data:	
Material Option	Specify locally
Wall heat transfer coefficient	Heat transfer coefficient representing conduction heat transfer: $h_{conduction} = \left[\frac{r_o}{k_t} \cdot ln\left(\frac{r_o}{r_i} \right) \right]^{-1}$ If fouling needs to be included, see Chapter 4.2.5.
Heat Capacity	Product of mass of tube material and specific heat at given temperature. The values in Table 4-3 should suffice for generic modelling. Use accurate values from literature for high detail modelling.
Fin Side Flow Data:	
Using advanced model	No
Fluid Volume	Total volume of fluid $V_{fluid} = A_{furnace} \cdot L_F$
Fluid path length	Distance gas needs to travel through heat exchanger: $L_F = D_o + tubes_{vertical} \cdot S_F$ $tubes_{vertical}$ – Total number of tubes installed in direction of flow.
# of increments	A minimum of three have proven successful.
Area	Cross-section area of furnace in flue gas flow direction. Inlet and outlet is equal in once-through boilers and back pass. Values will differ for pendant heat exchangers in drum-type boilers. $A_{frontal} = width \cdot breadth$
Area Ratio	Ratio of free flow area to total frontal area. Calculated as follows:

	$A_{frontal} = width \cdot breadth$ $A_{free\_flow} = A_{frontal} - (L_{tube} \cdot D_o \cdot Elm)$ $R_{Area} = \frac{A_{free\_flow}}{A_{frontal}}$ width / breadth – Furnace dimensions L_{tube} – Lengh of tube D_o – Outer tube diameter Elm – Number of horizontal elements in heat exchanger Note: Be sure to check whether the inlet and outlet ratios are equal.

Finned tube heat exchanger – Secondary side

The table below illustrates all the various inputs that are required when setting up the steam side of the finned tube heat exchanger.

Table A 2: Set-up for secondary finned tube heat exchanger.

Drop-Down Option:	Comment	Options
Fluids:		
Fluid data reference	Select appropriate fluid from list.	Water General (Two-phase)
Tube Side Flow Data:		
Number of parallel circuits	Tubes per bundle	See Figure A-1 and Figure A-2 below.
Number of passes	Single direction flow equals one pass.	See Figure A-1 and Figure A-2 below..
Tube rows	Number of elements along the width of boiler.	See Figure A-1 and Figure A-2 below.

Tube inside diameter	Average internal diameter of tube.
Tube pass length	Average length of tube per pass.
Inside roughness	Manually set to achieve approximate pressure drop.
K actual inlet	Manually set to achieve approximate pressure drop.
K actual outlet	Manually set to achieve approximate pressure drop.

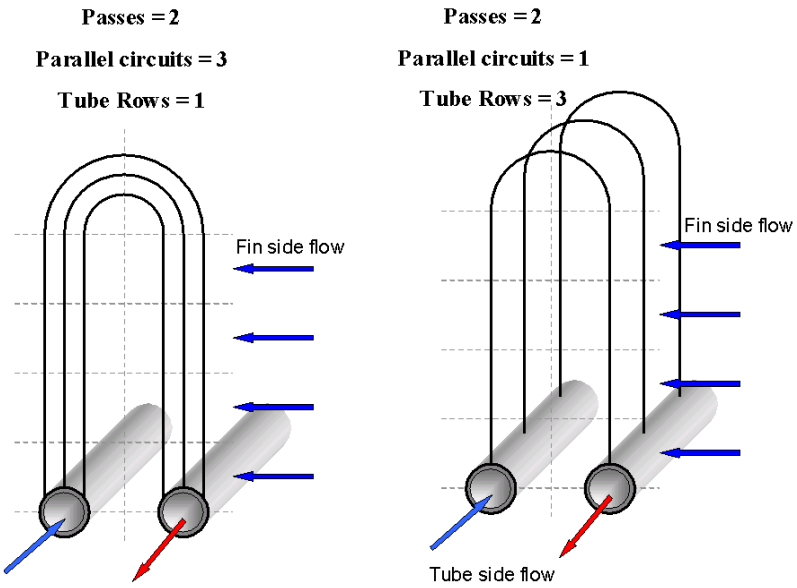

Figure A-1: Layout and tube component description. [11]

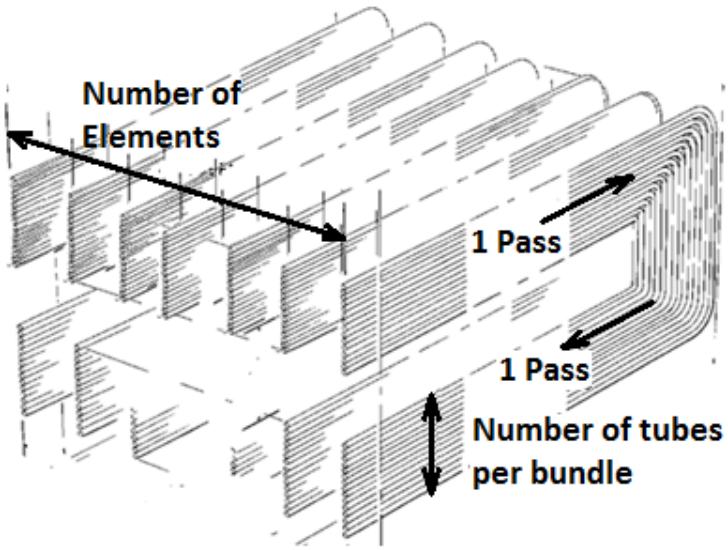

Figure A-2: Layout of heat exchanger with physical descriptions.

Appendix B. Heat exchanger characteristic charts

Convection heat transfer only

Table B-1: Colburn factor data for a convection only heat exchanger characteristic chart.

Reynolds Number	Colburn: Convection	Reynolds Number	Colburn: Convection
1000	0.01709	35000	0.00355
2000	0.01181	36000	0.00351
3000	0.00951	37000	0.00347
4000	0.00815	38000	0.00344
5000	0.00746	39000	0.00341
6000	0.00696	40000	0.00337
7000	0.00656	41000	0.00334
8000	0.00624	42000	0.00331
9000	0.00596	43000	0.00328
10000	0.00573	44000	0.00325
11000	0.00552	45000	0.00335
12000	0.00534	47500	0.00331
13000	0.00518	50000	0.00328
14000	0.00504	52500	0.00325
15000	0.00491	55000	0.00322
16000	0.00479	57500	0.00319
17000	0.00468	60000	0.00316
18000	0.00458	62500	0.00314
19000	0.00448	65000	0.00311
20000	0.00440	67500	0.00309
21000	0.00431	70000	0.00307
22000	0.00424	72500	0.00305
23000	0.00417	75000	0.00303
24000	0.00410	77500	0.00301
25000	0.00404	80000	0.00299
26000	0.00398	82500	0.00297
27000	0.00392	85000	0.00296
28000	0.00387	87500	0.00294
29000	0.00381	90000	0.00292
30000	0.00376	92500	0.00291
31000	0.00372	95000	0.00289
32000	0.00367	97500	0.00288
33000	0.00363	100000	0.00286
34000	0.00359		

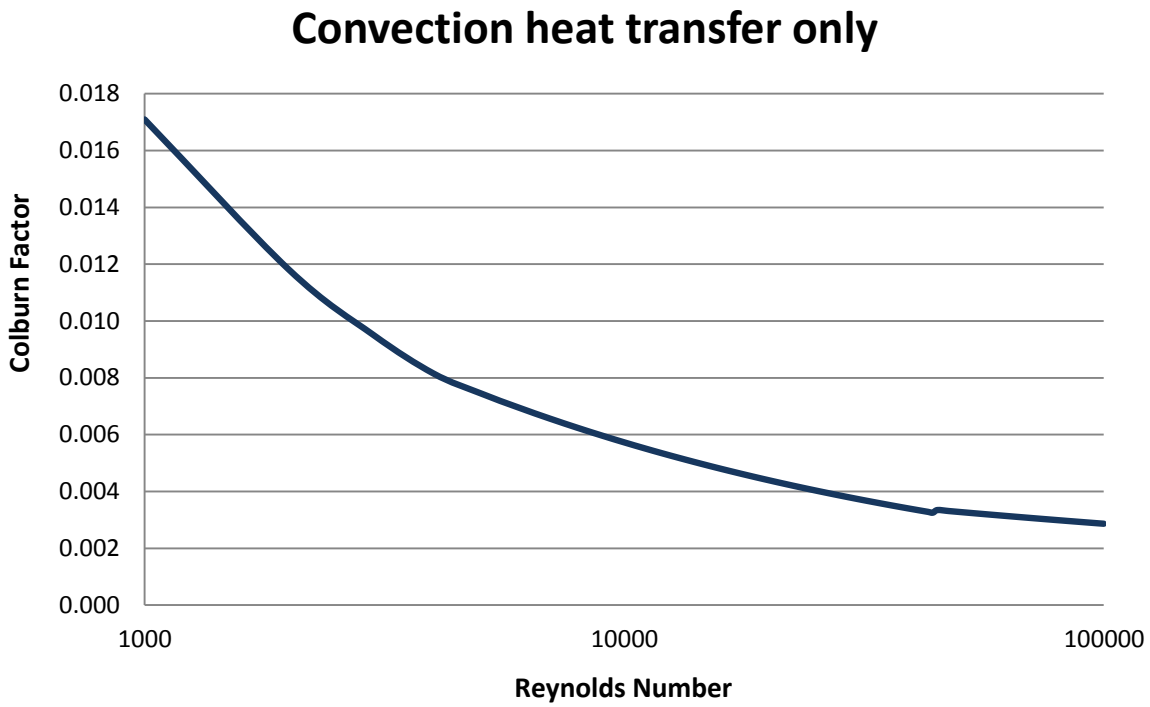

Figure B-1: Heat exchanger characteristic chart for the convection only HX.

1st Heat exchanger in terms of flue gas flow:

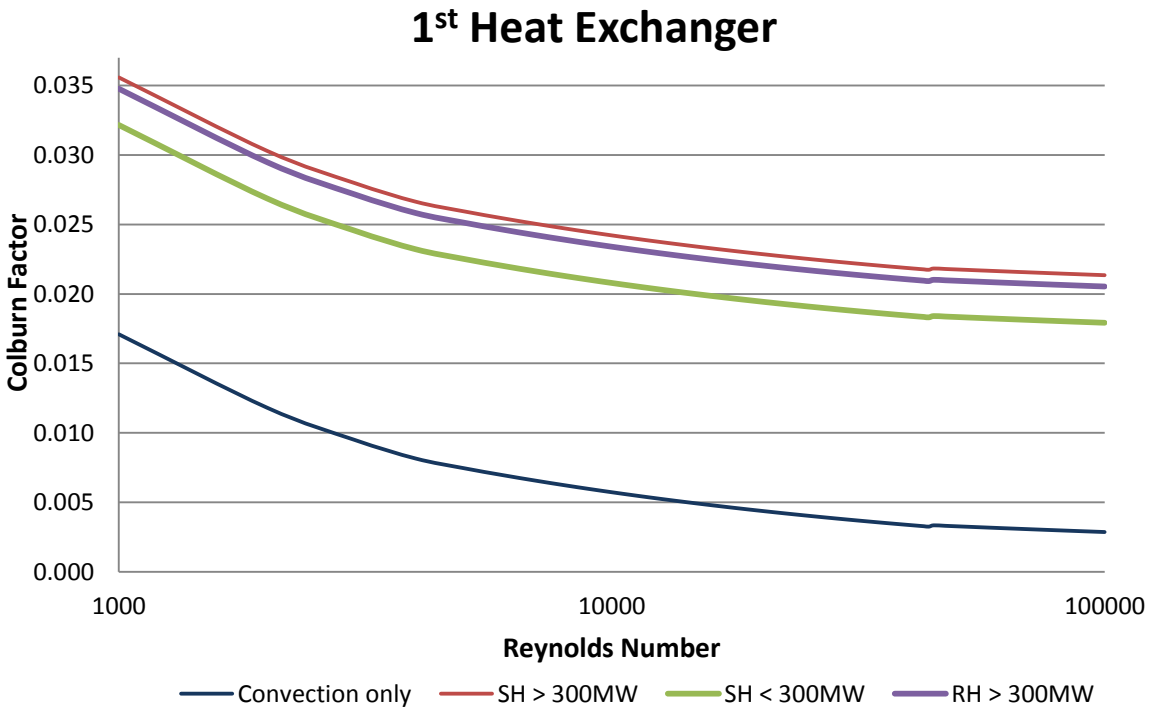

Figure B-2: Heat exchanger characteristic chart for the 1st HX in all boiler groups.

Table B-2: Colburn factor data for 1st heat exchanger characteristic chart.

Reynolds Number	SH Colburn: 300+ HX 1	RH Colburn: 300+ HX 1	SH Colburn: 300 HX 1	Reynolds Number	SH Colburn: 300+ HX 1	RH Colburn: 300+ HX 1	SH Colburn: 300 HX 1
1000	0.03558	0.03477	0.03216	35000	0.02204	0.02122	0.01861
2000	0.03029	0.02948	0.02687	36000	0.02200	0.02118	0.01857
3000	0.02800	0.02718	0.02457	37000	0.02196	0.02115	0.01854
4000	0.02664	0.02583	0.02322	38000	0.02193	0.02111	0.01850
5000	0.02595	0.02514	0.02253	39000	0.02189	0.02108	0.01847
6000	0.02545	0.02464	0.02203	40000	0.02186	0.02105	0.01844
7000	0.02505	0.02424	0.02163	41000	0.02183	0.02101	0.01840
8000	0.02473	0.02391	0.02130	42000	0.02180	0.02098	0.01837
9000	0.02445	0.02364	0.02103	43000	0.02177	0.02095	0.01834
10000	0.02422	0.02340	0.02079	44000	0.02174	0.02093	0.01832
11000	0.02401	0.02320	0.02059	45000	0.02183	0.02102	0.01841
12000	0.02383	0.02302	0.02041	47500	0.02180	0.02098	0.01837
13000	0.02367	0.02286	0.02024	50000	0.02177	0.02095	0.01834
14000	0.02352	0.02271	0.02010	52500	0.02173	0.02092	0.01831
15000	0.02339	0.02258	0.01997	55000	0.02170	0.02089	0.01828
16000	0.02327	0.02246	0.01985	57500	0.02168	0.02086	0.01825
17000	0.02316	0.02235	0.01974	60000	0.02165	0.02084	0.01823
18000	0.02306	0.02225	0.01964	62500	0.02163	0.02081	0.01820
19000	0.02297	0.02216	0.01955	65000	0.02160	0.02079	0.01818
20000	0.02288	0.02207	0.01946	67500	0.02158	0.02076	0.01815
21000	0.02280	0.02199	0.01938	70000	0.02156	0.02074	0.01813
22000	0.02273	0.02191	0.01930	72500	0.02154	0.02072	0.01811
23000	0.02265	0.02184	0.01923	75000	0.02152	0.02070	0.01809
24000	0.02259	0.02177	0.01916	77500	0.02150	0.02068	0.01807
25000	0.02252	0.02171	0.01910	80000	0.02148	0.02066	0.01805
26000	0.02246	0.02165	0.01904	82500	0.02146	0.02065	0.01804
27000	0.02241	0.02159	0.01898	85000	0.02144	0.02063	0.01802
28000	0.02235	0.02154	0.01893	87500	0.02143	0.02061	0.01800
29000	0.02230	0.02149	0.01888	90000	0.02141	0.02060	0.01799
30000	0.02225	0.02144	0.01883	92500	0.02139	0.02058	0.01797
31000	0.02221	0.02139	0.01878	95000	0.02138	0.02057	0.01795
32000	0.02216	0.02135	0.01874	97500	0.02136	0.02055	0.01794
33000	0.02212	0.02130	0.01869	100000	0.02135	0.02054	0.01793
34000	0.02208	0.02126	0.01865				

2nd Heat exchanger in terms of flue gas flow

Table B-3: Colburn factor data for 2nd heat exchanger characteristic chart.

Reynolds Number	SH Colburn: 300+ HX 2	RH Colburn: 300+ HX 2	SH Colburn: 300 HX 2	Reynolds Number	SH Colburn: 300+ HX 2	RH Colburn: 300+ HX 2	SH Colburn: 300 HX 2
1000	0.03250	0.03180	0.02985	35000	0.01896	0.01826	0.01631
2000	0.02722	0.02652	0.02456	36000	0.01892	0.01822	0.01627
3000	0.02492	0.02422	0.02227	37000	0.01888	0.01818	0.01623
4000	0.02356	0.02286	0.02091	38000	0.01885	0.01815	0.01620
5000	0.02287	0.02217	0.02022	39000	0.01881	0.01811	0.01616
6000	0.02237	0.02167	0.01972	40000	0.01878	0.01808	0.01613
7000	0.02197	0.02127	0.01932	41000	0.01875	0.01805	0.01610
8000	0.02165	0.02095	0.01900	42000	0.01872	0.01802	0.01607
9000	0.02137	0.02067	0.01872	43000	0.01869	0.01799	0.01604
10000	0.02114	0.02044	0.01849	44000	0.01866	0.01796	0.01601
11000	0.02093	0.02023	0.01828	45000	0.01875	0.01805	0.01610
12000	0.02075	0.02005	0.01810	47500	0.01872	0.01802	0.01607
13000	0.02059	0.01989	0.01794	50000	0.01869	0.01799	0.01603
14000	0.02045	0.01975	0.01779	52500	0.01866	0.01795	0.01600
15000	0.02032	0.01961	0.01766	55000	0.01863	0.01793	0.01597
16000	0.02020	0.01950	0.01754	57500	0.01860	0.01790	0.01595
17000	0.02009	0.01939	0.01743	60000	0.01857	0.01787	0.01592
18000	0.01999	0.01928	0.01733	62500	0.01855	0.01785	0.01590
19000	0.01989	0.01919	0.01724	65000	0.01852	0.01782	0.01587
20000	0.01980	0.01910	0.01715	67500	0.01850	0.01780	0.01585
21000	0.01972	0.01902	0.01707	70000	0.01848	0.01778	0.01583
22000	0.01965	0.01895	0.01700	72500	0.01846	0.01776	0.01581
23000	0.01958	0.01888	0.01692	75000	0.01844	0.01774	0.01579
24000	0.01951	0.01881	0.01686	77500	0.01842	0.01772	0.01577
25000	0.01945	0.01875	0.01679	80000	0.01840	0.01770	0.01575
26000	0.01939	0.01869	0.01673	82500	0.01838	0.01768	0.01573
27000	0.01933	0.01863	0.01668	85000	0.01836	0.01766	0.01571
28000	0.01927	0.01857	0.01662	87500	0.01835	0.01765	0.01570
29000	0.01922	0.01852	0.01657	90000	0.01833	0.01763	0.01568
30000	0.01917	0.01847	0.01652	92500	0.01832	0.01762	0.01566
31000	0.01913	0.01843	0.01648	95000	0.01830	0.01760	0.01565
32000	0.01908	0.01838	0.01643	97500	0.01829	0.01759	0.01563
33000	0.01904	0.01834	0.01639	100000	0.01827	0.01757	0.01562
34000	0.01900	0.01830	0.01635				

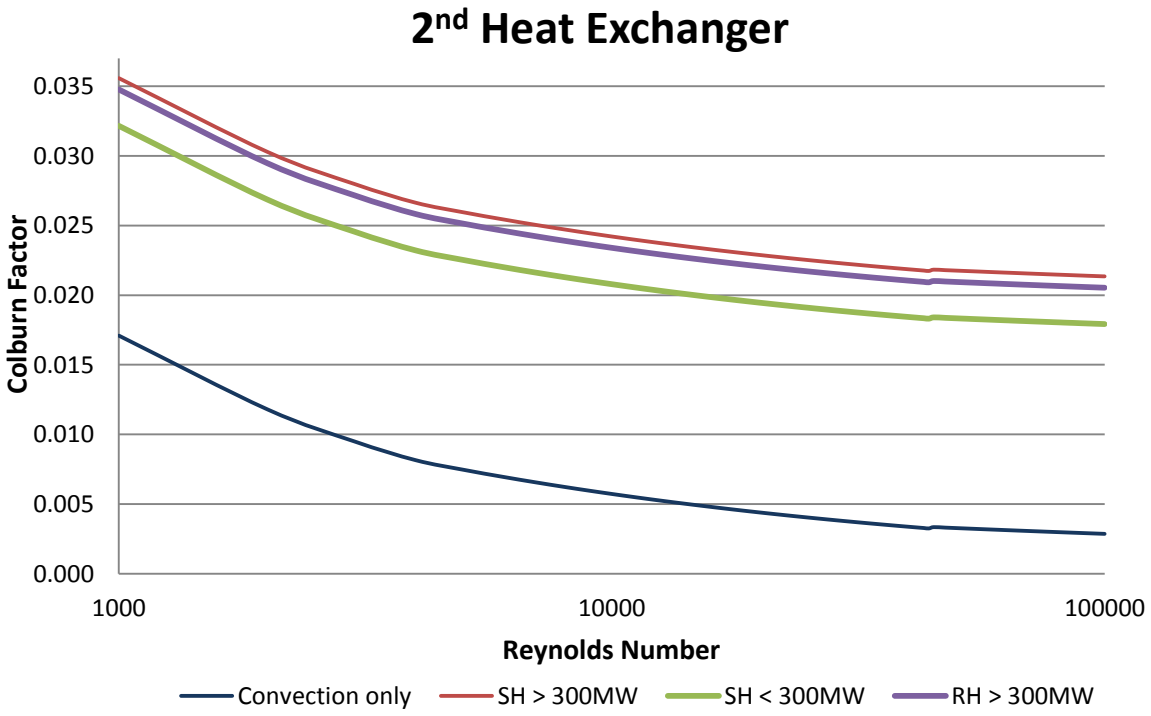

Figure B-3: Heat exchanger characteristic chart for the 2nd HX in all boiler groups.

3rd Heat exchanger in terms of flue gas flow

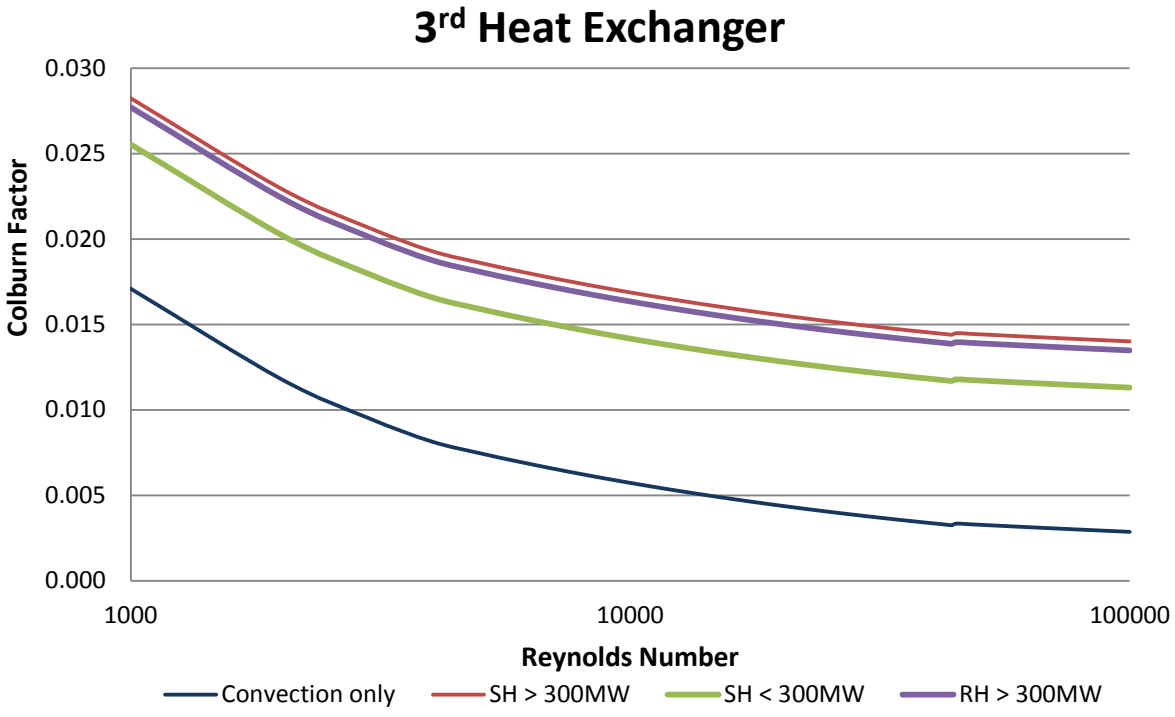

Figure B-4: Heat exchanger characteristic chart for the 3rd HX in all boiler groups.

Table B-4: Colburn factor data for 3rd heat exchanger characteristic chart.

Reynolds Number	SH Colburn: 300+ HX 3	RH Colburn: 300+ HX 3	SH Colburn: 300 HX 3	Reynolds Number	SH Colburn: 300+ HX 3	RH Colburn: 300+ HX 3	SH Colburn: 300 HX 3
1000	0.02824	0.02772	0.02554	35000	0.01470	0.01417	0.01199
2000	0.02296	0.02243	0.02025	36000	0.01466	0.01413	0.01196
3000	0.02066	0.02013	0.01795	37000	0.01462	0.01410	0.01192
4000	0.01930	0.01877	0.01660	38000	0.01459	0.01406	0.01188
5000	0.01861	0.01808	0.01591	39000	0.01456	0.01403	0.01185
6000	0.01811	0.01758	0.01541	40000	0.01452	0.01399	0.01182
7000	0.01771	0.01718	0.01501	41000	0.01449	0.01396	0.01179
8000	0.01739	0.01686	0.01468	42000	0.01446	0.01393	0.01175
9000	0.01711	0.01658	0.01441	43000	0.01443	0.01390	0.01173
10000	0.01688	0.01635	0.01417	44000	0.01440	0.01387	0.01170
11000	0.01667	0.01614	0.01397	45000	0.01449	0.01397	0.01179
12000	0.01649	0.01596	0.01379	47500	0.01446	0.01393	0.01175
13000	0.01633	0.01580	0.01363	50000	0.01443	0.01390	0.01172
14000	0.01619	0.01566	0.01348	52500	0.01440	0.01387	0.01169
15000	0.01606	0.01553	0.01335	55000	0.01437	0.01384	0.01166
16000	0.01594	0.01541	0.01323	57500	0.01434	0.01381	0.01163
17000	0.01583	0.01530	0.01312	60000	0.01431	0.01378	0.01161
18000	0.01573	0.01520	0.01302	62500	0.01429	0.01376	0.01158
19000	0.01563	0.01510	0.01293	65000	0.01426	0.01373	0.01156
20000	0.01555	0.01502	0.01284	67500	0.01424	0.01371	0.01154
21000	0.01546	0.01493	0.01276	70000	0.01422	0.01369	0.01151
22000	0.01539	0.01486	0.01268	72500	0.01420	0.01367	0.01149
23000	0.01532	0.01479	0.01261	75000	0.01418	0.01365	0.01147
24000	0.01525	0.01472	0.01254	77500	0.01416	0.01363	0.01145
25000	0.01519	0.01466	0.01248	80000	0.01414	0.01361	0.01143
26000	0.01513	0.01460	0.01242	82500	0.01412	0.01359	0.01142
27000	0.01507	0.01454	0.01236	85000	0.01410	0.01358	0.01140
28000	0.01502	0.01449	0.01231	87500	0.01409	0.01356	0.01138
29000	0.01496	0.01443	0.01226	90000	0.01407	0.01354	0.01137
30000	0.01491	0.01439	0.01221	92500	0.01406	0.01353	0.01135
31000	0.01487	0.01434	0.01216	95000	0.01404	0.01351	0.01134
32000	0.01482	0.01429	0.01212	97500	0.01403	0.01350	0.01132
33000	0.01478	0.01425	0.01207	100000	0.01401	0.01348	0.01131
34000	0.01474	0.01421	0.01203				

4th Heat exchanger in terms of flue gas flow

Table B-5: Colburn factor data for 4th heat exchanger characteristic chart.

Reynolds Number	SH Colburn: 300+ HX 4	RH Colburn: 300+ HX 4	SH Colburn: 300 HX 4	Reynolds Number	SH Colburn: 300+ HX 4	RH Colburn: 300+ HX 4	SH Colburn: 300 HX 4
1000	0.02394	0.02366	0.02200	35000	0.01040	0.01011	0.00845
2000	0.01866	0.01837	0.01671	36000	0.01036	0.01008	0.00841
3000	0.01636	0.01607	0.01441	37000	0.01032	0.01004	0.00838
4000	0.01500	0.01472	0.01306	38000	0.01029	0.01000	0.00834
5000	0.01431	0.01403	0.01237	39000	0.01026	0.00997	0.00831
6000	0.01381	0.01353	0.01187	40000	0.01022	0.00994	0.00828
7000	0.01341	0.01313	0.01147	41000	0.01019	0.00991	0.00824
8000	0.01309	0.01280	0.01114	42000	0.01016	0.00988	0.00821
9000	0.01281	0.01253	0.01087	43000	0.01013	0.00985	0.00818
10000	0.01258	0.01229	0.01063	44000	0.01010	0.00982	0.00816
11000	0.01237	0.01209	0.01043	45000	0.01019	0.00991	0.00825
12000	0.01219	0.01191	0.01025	47500	0.01016	0.00987	0.00821
13000	0.01203	0.01175	0.01008	50000	0.01013	0.00984	0.00818
14000	0.01189	0.01160	0.00994	52500	0.01010	0.00981	0.00815
15000	0.01176	0.01147	0.00981	55000	0.01007	0.00978	0.00812
16000	0.01164	0.01135	0.00969	57500	0.01004	0.00975	0.00809
17000	0.01153	0.01124	0.00958	60000	0.01001	0.00973	0.00807
18000	0.01143	0.01114	0.00948	62500	0.00999	0.00970	0.00804
19000	0.01133	0.01105	0.00939	65000	0.00996	0.00968	0.00802
20000	0.01124	0.01096	0.00930	67500	0.00994	0.00966	0.00799
21000	0.01116	0.01088	0.00922	70000	0.00992	0.00963	0.00797
22000	0.01109	0.01080	0.00914	72500	0.00990	0.00961	0.00795
23000	0.01102	0.01073	0.00907	75000	0.00988	0.00959	0.00793
24000	0.01095	0.01066	0.00900	77500	0.00986	0.00957	0.00791
25000	0.01089	0.01060	0.00894	80000	0.00984	0.00955	0.00789
26000	0.01083	0.01054	0.00888	82500	0.00982	0.00954	0.00788
27000	0.01077	0.01048	0.00882	85000	0.00980	0.00952	0.00786
28000	0.01071	0.01043	0.00877	87500	0.00979	0.00950	0.00784
29000	0.01066	0.01038	0.00872	90000	0.00977	0.00949	0.00783
30000	0.01061	0.01033	0.00867	92500	0.00976	0.00947	0.00781
31000	0.01057	0.01028	0.00862	95000	0.00974	0.00946	0.00779
32000	0.01052	0.01024	0.00858	97500	0.00973	0.00944	0.00778
33000	0.01048	0.01019	0.00853	100000	0.00971	0.00943	0.00777
34000	0.01044	0.01015	0.00849				

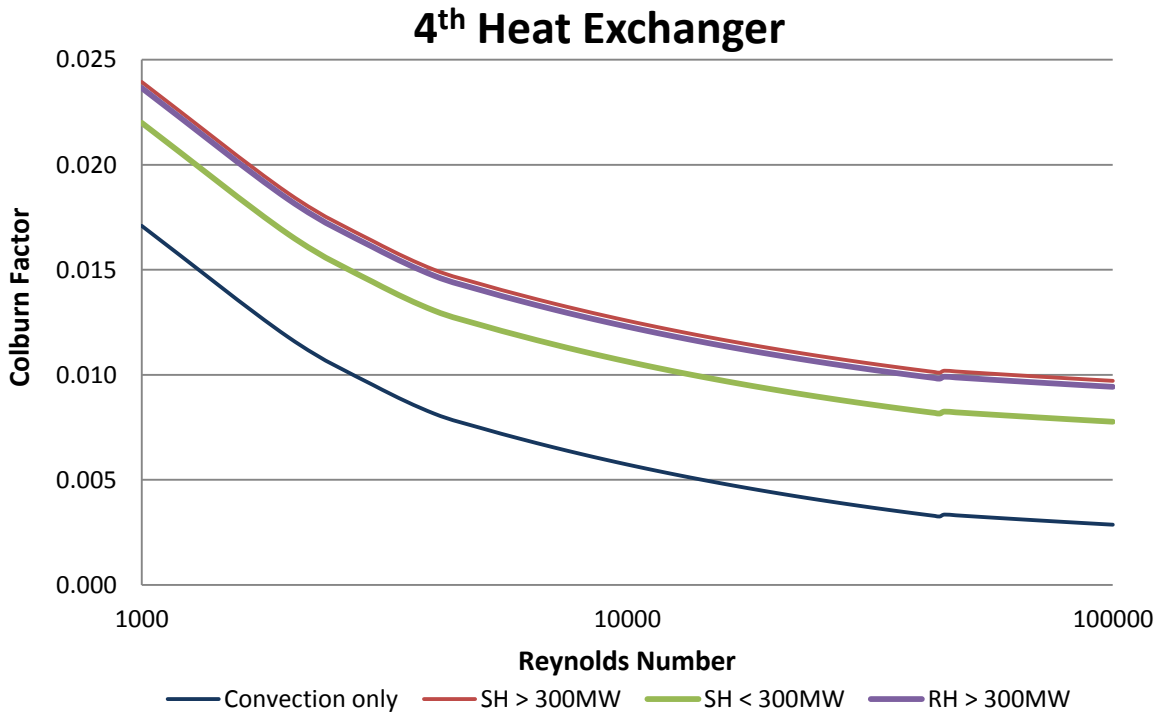

Figure B-5: Heat exchanger characteristic chart for the 4th HX in all boiler groups.

5th Heat exchanger in terms of flue gas flow

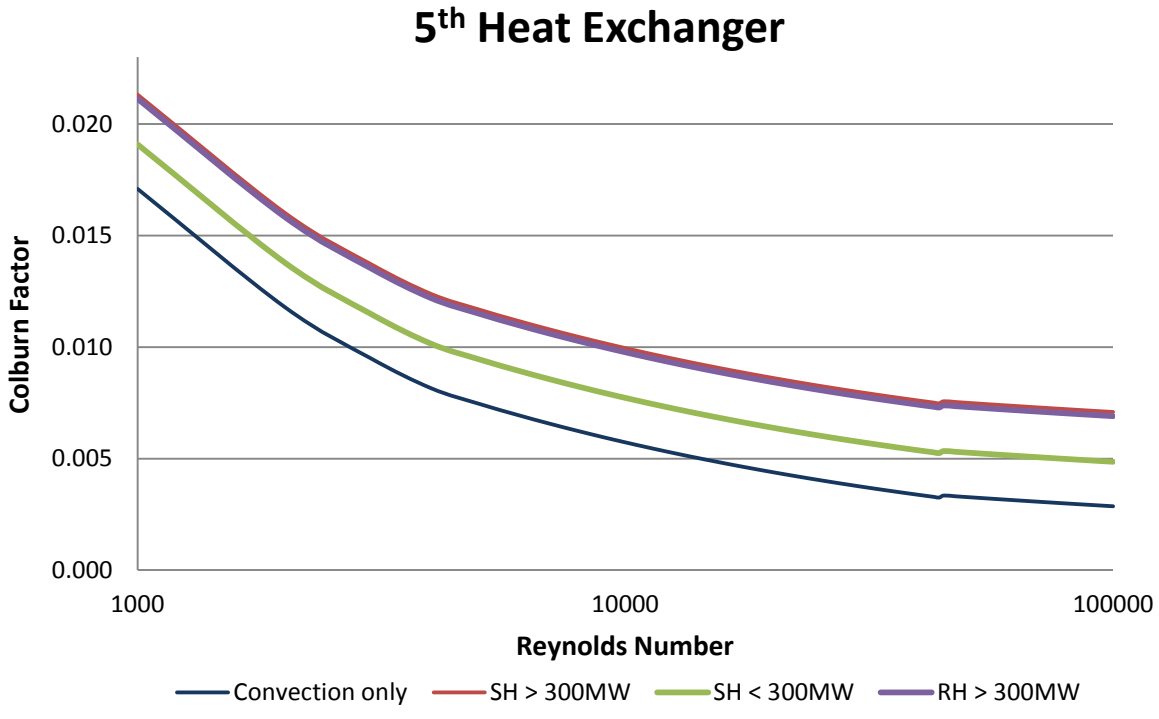

Figure B-6: Heat exchanger characteristic chart for the 5th HX in all boiler groups.

Table B-6: Colburn factor data for 5th heat exchanger characteristic chart.

Reynolds Number	SH Colburn: 300+ HX 5	RH Colburn: 300+ HX 5	SH Colburn: 300 HX 5	Reynolds Number	SH Colburn: 300+ HX 5	RH Colburn: 300+ HX 5	SH Colburn: 300 HX 5
1000	0.02132	0.02113	0.01909	35000	0.00778	0.00759	0.00554
2000	0.01603	0.01585	0.01380	36000	0.00774	0.00755	0.00551
3000	0.01373	0.01355	0.01150	37000	0.00770	0.00751	0.00547
4000	0.01238	0.01219	0.01015	38000	0.00767	0.00748	0.00543
5000	0.01169	0.01150	0.00946	39000	0.00763	0.00745	0.00540
6000	0.01119	0.01100	0.00896	40000	0.00760	0.00741	0.00537
7000	0.01079	0.01060	0.00856	41000	0.00757	0.00738	0.00534
8000	0.01046	0.01028	0.00823	42000	0.00754	0.00735	0.00531
9000	0.01019	0.01000	0.00796	43000	0.00751	0.00732	0.00528
10000	0.00995	0.00977	0.00772	44000	0.00748	0.00729	0.00525
11000	0.00975	0.00956	0.00752	45000	0.00757	0.00738	0.00534
12000	0.00957	0.00938	0.00734	47500	0.00754	0.00735	0.00530
13000	0.00941	0.00922	0.00718	50000	0.00750	0.00732	0.00527
14000	0.00926	0.00908	0.00703	52500	0.00747	0.00729	0.00524
15000	0.00913	0.00895	0.00690	55000	0.00744	0.00726	0.00521
16000	0.00901	0.00883	0.00678	57500	0.00742	0.00723	0.00518
17000	0.00890	0.00872	0.00667	60000	0.00739	0.00720	0.00516
18000	0.00880	0.00862	0.00657	62500	0.00736	0.00718	0.00513
19000	0.00871	0.00852	0.00648	65000	0.00734	0.00715	0.00511
20000	0.00862	0.00844	0.00639	67500	0.00732	0.00713	0.00509
21000	0.00854	0.00835	0.00631	70000	0.00730	0.00711	0.00506
22000	0.00847	0.00828	0.00623	72500	0.00728	0.00709	0.00504
23000	0.00839	0.00821	0.00616	75000	0.00726	0.00707	0.00502
24000	0.00833	0.00814	0.00609	77500	0.00724	0.00705	0.00500
25000	0.00826	0.00808	0.00603	80000	0.00722	0.00703	0.00498
26000	0.00820	0.00802	0.00597	82500	0.00720	0.00701	0.00497
27000	0.00815	0.00796	0.00591	85000	0.00718	0.00699	0.00495
28000	0.00809	0.00790	0.00586	87500	0.00717	0.00698	0.00493
29000	0.00804	0.00785	0.00581	90000	0.00715	0.00696	0.00492
30000	0.00799	0.00780	0.00576	92500	0.00713	0.00695	0.00490
31000	0.00794	0.00776	0.00571	95000	0.00712	0.00693	0.00489
32000	0.00790	0.00771	0.00567	97500	0.00710	0.00692	0.00487
33000	0.00786	0.00767	0.00562	100000	0.00709	0.00690	0.00486
34000	0.00782	0.00763	0.00558				

6th Heat exchanger in terms of flue gas flow

Table B-7: Colburn factor data for 6th heat exchanger characteristic chart.

Reynolds Number	SH Colburn: 300+ HX 6	SH Colburn: 300 HX 6	Reynolds Number	SH Colburn: 300+ HX 6	SH Colburn: 300 HX 6
1000	0.01903	0.01894	35000	0.00549	0.00540
2000	0.01374	0.01366	36000	0.00545	0.00536
3000	0.01145	0.01136	37000	0.00541	0.00532
4000	0.01009	0.01000	38000	0.00538	0.00529
5000	0.00940	0.00931	39000	0.00534	0.00525
6000	0.00890	0.00881	40000	0.00531	0.00522
7000	0.00850	0.00841	41000	0.00528	0.00519
8000	0.00818	0.00809	42000	0.00525	0.00516
9000	0.00790	0.00781	43000	0.00522	0.00513
10000	0.00767	0.00758	44000	0.00519	0.00510
11000	0.00746	0.00737	45000	0.00528	0.00519
12000	0.00728	0.00719	47500	0.00525	0.00516
13000	0.00712	0.00703	50000	0.00522	0.00513
14000	0.00698	0.00689	52500	0.00518	0.00509
15000	0.00684	0.00675	55000	0.00516	0.00507
16000	0.00672	0.00664	57500	0.00513	0.00504
17000	0.00662	0.00653	60000	0.00510	0.00501
18000	0.00651	0.00642	62500	0.00508	0.00499
19000	0.00642	0.00633	65000	0.00505	0.00496
20000	0.00633	0.00624	67500	0.00503	0.00494
21000	0.00625	0.00616	70000	0.00501	0.00492
22000	0.00618	0.00609	72500	0.00499	0.00490
23000	0.00611	0.00602	75000	0.00497	0.00488
24000	0.00604	0.00595	77500	0.00495	0.00486
25000	0.00597	0.00589	80000	0.00493	0.00484
26000	0.00591	0.00583	82500	0.00491	0.00482
27000	0.00586	0.00577	85000	0.00489	0.00480
28000	0.00580	0.00571	87500	0.00488	0.00479
29000	0.00575	0.00566	90000	0.00486	0.00477
30000	0.00570	0.00561	92500	0.00485	0.00476
31000	0.00566	0.00557	95000	0.00483	0.00474
32000	0.00561	0.00552	97500	0.00482	0.00473
33000	0.00557	0.00548	100000	0.00480	0.00471
34000	0.00553	0.00544			

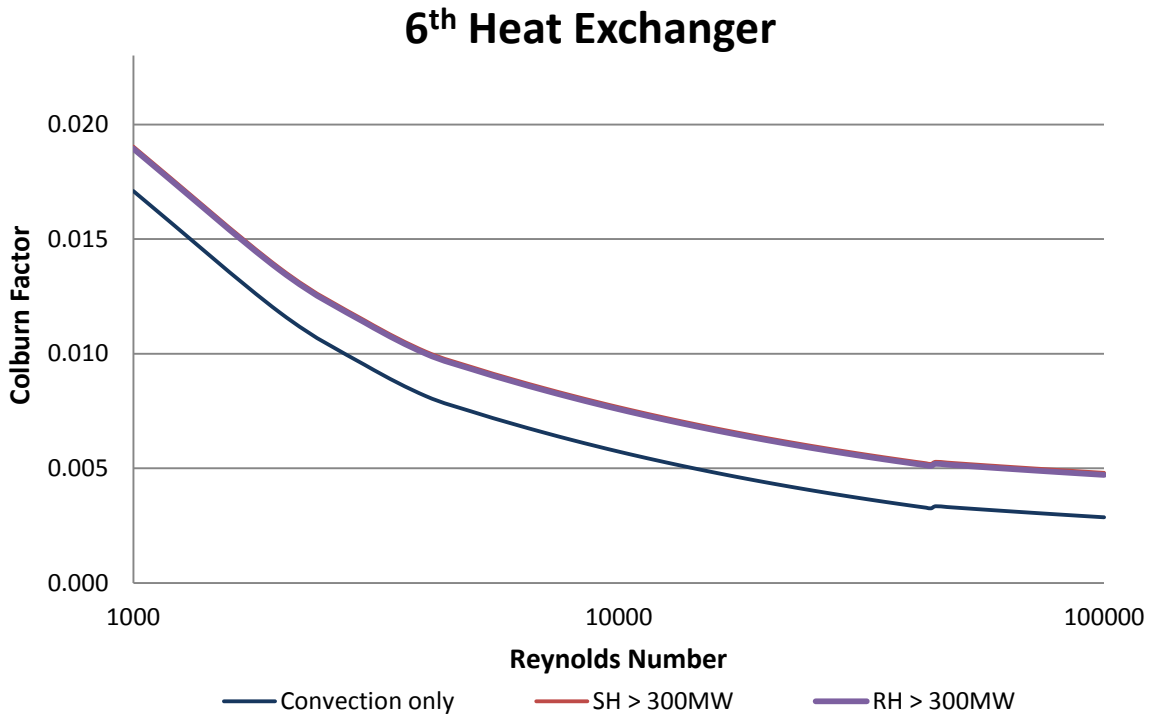

Figure B-7: Heat exchanger characteristic chart for the 6th HX in all boiler groups.

Appendix C. Additional calculations

Radiation from gas mixtures

Additional graphs for calculating high detail radiative heat transfer with all gas constituents added are illustrated below:

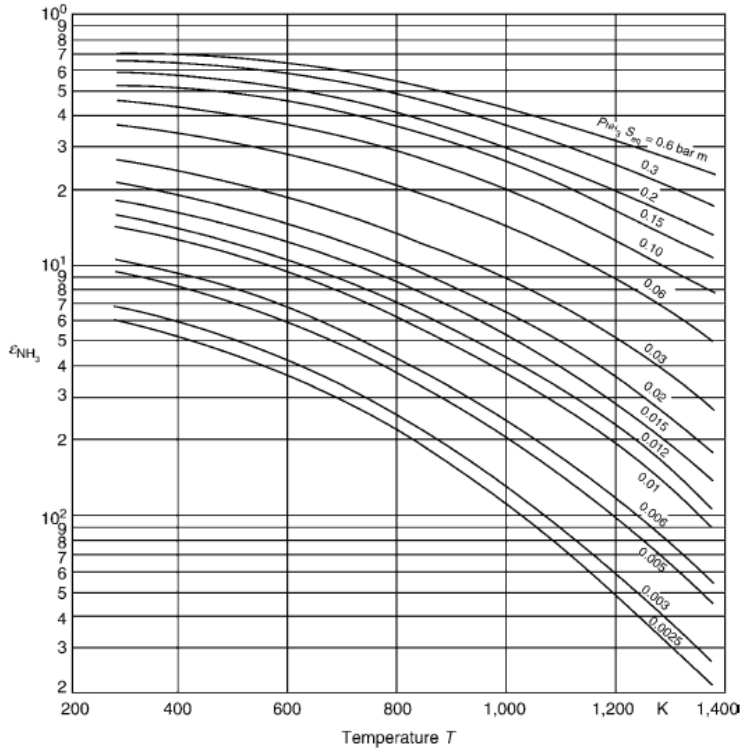

Figure C-1: Graph for calculating emissivity of ammonia (NH_3). [18]

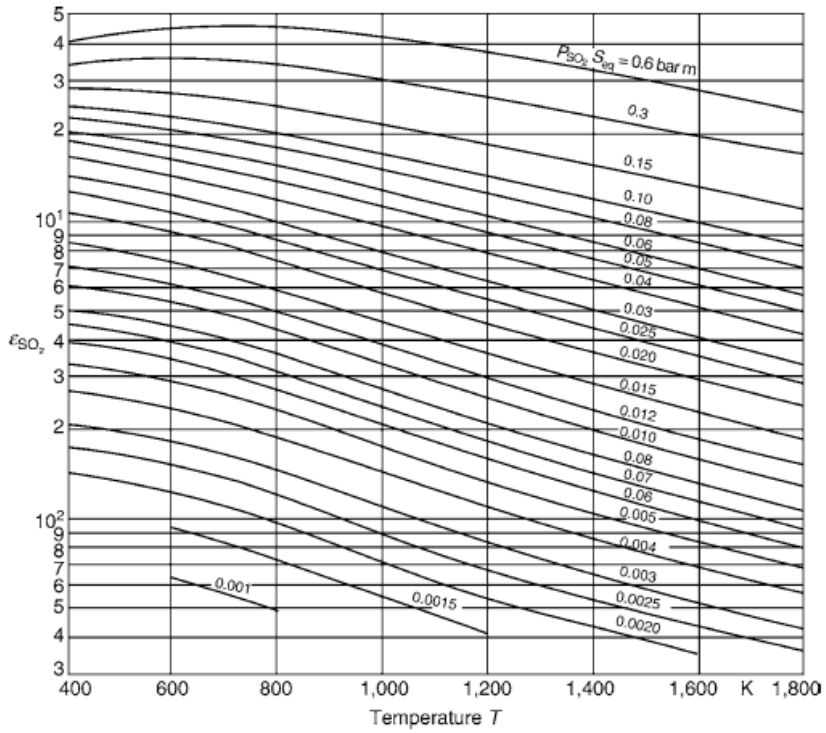

Figure C-2: Graph for calculating emissivity of sulphur dioxide (SO_2). [18]

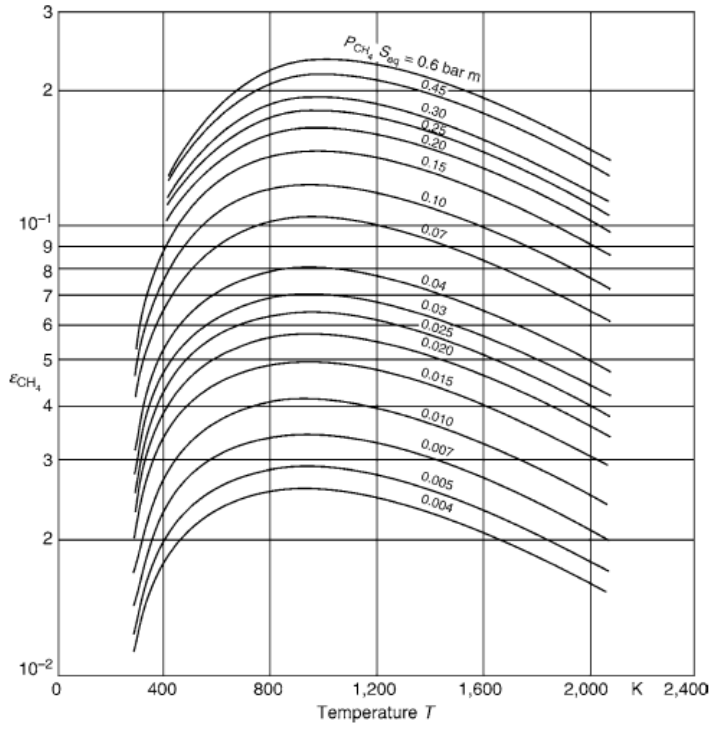

Figure C-3: Graph for calculating emissivity of methane (CH_4). [18]

Correction factors for gas mixtures

Correction factors, for water vapour and carbon dioxide, which are not used in this project can be calculated using the following graphs.

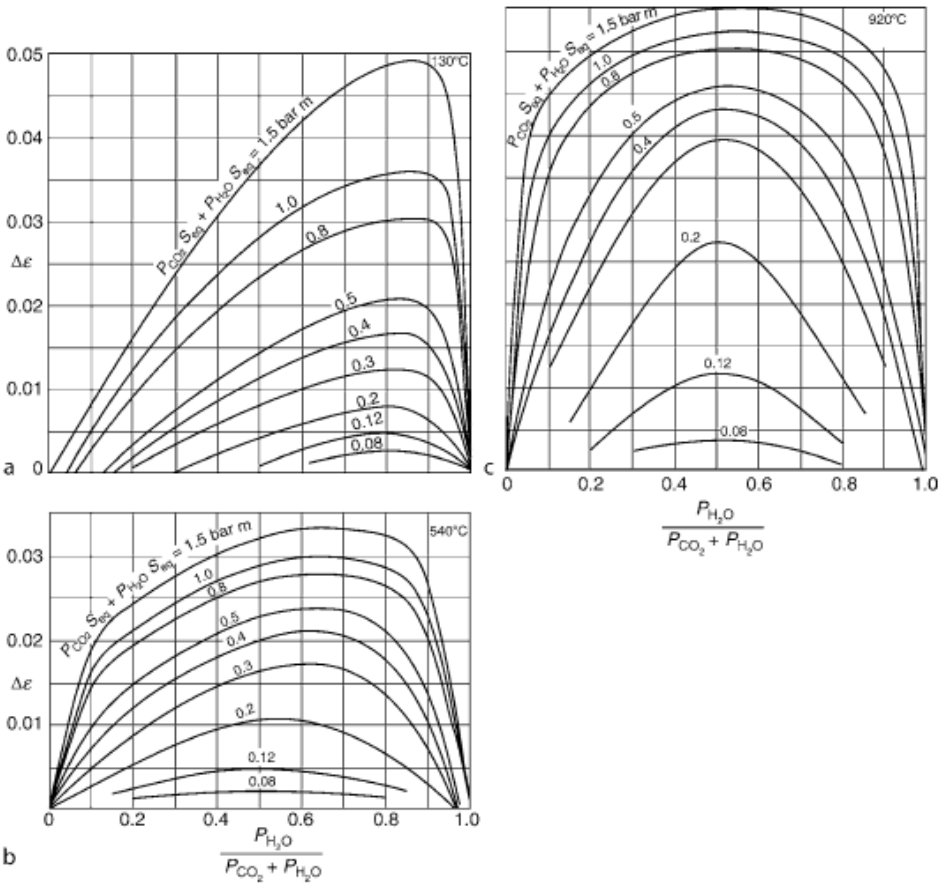

Figure C-4: Correction factors for water vapour and carbon dioxide. [18]